Aspects of Cosmological Inflation

Anders Basbøll

PhD Dissertation

Department of Physics and Astronomy
University of Aarhus
Denmark

Aspects of Cosmological Inflation

A Dissertation
Presented to the Faculty of Science
of the University of Aarhus
in Partial Fulfilment of the Requirements for the
PhD Degree

by
Anders Basbøll
October 13, 2008

ACKNOWLEDGEMENTS

I'm very grateful to my supervisor Steen Hannestad for both teaching, inspiration, collaboration and supervision – and proofreading/input to talks – often at short notice. It has been a privilege to be supervised by you.

Many thanks to Ole Bjælde for friendship, help with various technical problems, collaboration, proofreading and last, but not least, sharing my interest for strange things as American football, snooker and bookmaking. Coffee breaks won't be the same without you.

Thanks to Philip Jarnhus for the many trainrides – I will miss your company, if not the trains! I'm thankful to the whole group – Martin, Troels, Alessandro, Anna, Tina, Jacob and Katrine – for a great time. And thanks to Marianne and Danijela for pleasant office cohabitation.

I owe thanks to Subir Sarkar for the chance to go to Oxford in 2006. It was a great experience. I am especially grateful to David Maybury, with whom I shared an office. You took the time to teach me about supersymmetry and let me join your next working project. That project changed my line of work completely – Thank you!

Thanks to Georg Raffelt, Francesco Riva and Stephen West for collaboration on different projects.

A very special thanks goes to my family. My Mother, Father and Brother for many, many years of love, support and an ever ready helping hand (from child care to rigorous proofreading).

I'm very thankful to my daughter Amanda. For (nearly) always looking happily at me, for showing trust towards me and towards the world – and for countless dental check-ups...

I don't know how to thank my wife, Katrine. Thank you for your endless love, support, belief in me, for your patience with all the insecurity about where I will work next – and your strong belief (shared!) that we can be happy anywhere! You are my safe haven.

OUTLINE AND LIST OF PUBLICATIONS

This dissertation concludes my 3 years at Aarhus University as a Ph.D. student. The subject of inflation is very broad – with hundreds, if not thousands of papers published every year. Therefore the overview cannot contain all aspects of this fascinating theory. Focusing on aspects relevant for my publications has been unavoidable. Chapter 1 is a short overview of inflation – including reheating and preheating. Chapter 2 introduces various non standard model physics – violation of baryon number and lepton number, neutrino masses and the see-saw mechanism for providing these masses. Chapter 3 introduces supersymmetry and the minimal version hereof (MSSM) and its flat directions. Also the ideas of the influence of the flat directions on preheating and of a flat direction being the inflaton are introduced, as is our contribution to the field and the latest developments and my opinions on these. In chapter 4 the idea of neutrinos being coupled to a pseudo-scalar is introduced. The influence of this idea on the Cosmic Microwave Background radiation and the slowness of establishing kinetic equilibrium is discussed. Our contributions to the field are introduced.

The second part consists of the papers I have (co-)authored – ordered after their mentioning above. Below is a list of my publications and the chapter in which they are printed. Only some typos have been corrected. The manuscript in chapter 9 is unfinished. However, the calculations and the numerical work are finished. Therefore the paper has been included.

A. Basbøll og S. Hannestad: Decay of heavy Majorana neutrinos using the full Boltzmann equation including its implications for leptogenesis, JCAP01(2007)003. Chapter 5.

A. Basbøll, D. Maybury, F. Riva and S. M. West: Nonperturbative flat direction decay, Phys. Rev. D **76**, 065005 (2007). Chapter 6.

A. Basbøll: SUSY Flat Direction Decay - the prospect of particle production and preheating investigated in the unitary gauge , Phys. Rev. D **78**, 023528 (2008). Chapter 7.

A. Basbøll, O. E. Bjælde, S. Hannestad and G. Raffelt: Are cosmological neutrinos free–streaming?, arXiv:stro-ph/0806.1735. Chapter 8.

A. Basbøll, O. E. Bjælde, S. Hannestad and G. Raffelt: Thermalisation of a neutrino gas by decays and inverse decays, in preparation. Chapter 9.

SUMMARY – IN ENGLISH

This dissertation concludes my 3 years at Aarhus University as a Ph.D. student. It contains an introduction and 5 papers. In one (chapter 5), we showed that using the full Boltzmann equation rather than its integrated version makes a 15-30% difference when calculating leptogenesis. In a second (chapter 8) we found that if neutrinos have become strongly interacting, it happened no earlier than at redshift $z = 1500$ and we restricted the neutrino-majoron coupling constants accordingly. In a third (chapter 9) we confirmed that kinetic equilibrium in a neutrino gas system is delayed by 2 Lorentz-Gamma-factors – one for time dilation of the neutrino lifetime and one for the effect of the opening angle. In a fourth (chapter 6) we investigated the effect of MSSM flat directions in cosmological (p)reheating – investigated in the unitary gauge where unphysical Goldstone bosons have been removed. In addition we found that different phases (those that cannot be gauged away) in general have nontrivial dynamical equations. In the fifth (chapter 7), I found that there is no preheating in flat directions $U^cD^cD^c, LLE^c, UD^cD^c + LLE^c$ but there is particle production in $QLQLQLE^c$ and $QLD^c + LLE^c$.

RESUMÉ – PÅ DANSK

Denne afhandling afslutter 3 års ph.d.-studier ved Aarhus Universitet. Den indeholder en introduktion og 5 artikler. I den ene (kapitel 5) viste vi, at det at bruge den fulde Boltzmannligning i stedet for den integrerede version, giver 15-30% forskel på udregninger af leptogenese. I en anden (kapitel 8) viste vi at hvis neutrinoer er blevet stærkt vekselvirkende, er det ikke sket før rødforskydning $z = 1500$, og vi satte begrænsninger på neutrino-majoron-koblingerne i henhold hertil. I en tredje (kapitel 9) bekræftede vi at kinetisk ligevægt i et neutrinogassystem forsinkes af 2 Lorentz gammafaktorer – én for tidsforlængelse af neutrinoens levetid og én for effekten af åbningsvinklen. I en fjerde (kapitel 6) undersøgte vi effekten af MSSM flade retninger på kosmologisk genopvarmning af Universet. Vi brugte "unitary gauge", hvor de ufysiske Goldstonebosoner er fjernet. Derudover fandt vi at forskellige faser (blandt dem der ikke kan fjernes ved valg af gauge) generelt har forskellige dynamiske ligninger. I den femte (kapitel 7) viste jeg at der ikke er nogen genopvarmning via parametrisk resonans i de flade retninger $U^cD^cD^c, LLE^c, U^cD^cD^c + LLE^c$, men der er partikelproduktion i $QLQLQLE^c$ og $QLD^c + LLE^c$.

CONTENTS

Part I

OVERVIEW

1

Introduction to Inflation

Inflation is as violent as a mugger, as frightening as an armed robber and as deadly as a hit man.
— Ronald Reagan, President of The United States

1.1 Inflation

This is a very short presentation of inflation, based on Perkins [1] – values are taken from this book also, even though there might be better data available now. It is from 2003, but the values have not changed significantly.

1.2 The problems inflation shall solve

If you take a first look at the outside world, the first thing that will strike you is hardly neither the homogeneity nor the isotropy of the (visible) world. After all, we live at the surface of a very dense object, in a very big solar system. This dense object also gives us a very distinct feeling of one direction, down. But when we look at bigger distances, not only outside the solar system, but outside our galaxy and The Local Group, everything looks very homogenous and isotropic. The best indication for this is probably the temperature of the Cosmic Microwave Background (CMB) that varies only about 1 part in 100.000 around the mean temperature of 2.725K.

The CMB is obviously a very strong indication of the Big Bang, but even in that context it is very strange, because our visible universe contains areas that were not in thermal contact at the time the CMB was created. How did they end up at exactly the same temperature? In fact, the CMB was created at matter-radiation decoupling, which took place at redshift $z = 1100$. It is easy to calculate that an area in causal contact at that time, will only cover an angle of 2° today.

If one is a fan of different Grand Unified Theories (GUTs), one might also ask why we don't see any magnetic monopoles, domain walls (that is walls between domains of different particle physics, for instance, different "choices" between degenerated vacua) and other possible very high energy phenomena.

Also, there is the puzzling fact that there is just about the right amount of energy in the universe to give us spacial flatness, that is on large scales our universe doesn't have neither positive nor negative curvature. This is a very well defined energy density, and even though uncertainty today is huge, the Friedmann equation suggests that going back in time, the energy density has been equal to the critical density to an extreme degree.

Starting with the Friedmann equation, with a being the scale factor of the universe and defining the Hubble Parameter, the critical density and the closeness parameter on the way, we find

$$H^2 \equiv \left(\frac{\dot{a}}{a}\right)^2 \equiv \frac{8\pi G\rho_{tot}}{3} - \frac{K}{a^2} \equiv H_0^2\left(\frac{\rho_{tot}}{\rho_{crit}} - \frac{K}{H_0 a^2}\right) \equiv H_0^2\left(\Omega - \frac{K}{H_0 a^2}\right) \quad (1.1)$$

where K is the Curvature parameter, that is $K > 0, K = 0, K < 0$ for a closed, a flat and an open universe, respectively.

By just taking the very mild demand that Ω being of order unity today (in fact it is 1 with percentage order uncertainty), one can scale back and find that at GUT temperature of $10^{14}GeV$, $|\Omega - 1|$ would be of order 10^{-52}. Is that just a coincidence?

1.3 The basic idea

In 1981 Guth suggested inflation, a period of exponential growth of the universe. Imagine vacuum energy (here I just mean an energy density that is constant even as the size of the universe changes) once dominated the energy density. Ignoring curvature the Friedmann equation becomes

$$H^2 = \left(\frac{\dot{a}}{a}\right)^2 = \frac{8\pi G\rho_{vac}}{3} \quad (1.2)$$

that has the solution

$$a_2 = a_1 e^{H(t_2 - t_1)} \quad (1.3)$$

where H is the constant Hubble parameter. For all the visible universe to have been in causal contact before inflation, the expansion shall be at least of about 60 e-foldings, that is a shall have grown by a factor of e^{60}. The curvature term in the Friedmann equation is proportional to a^{-2}, such that

$$\frac{\Omega_{c,end}}{\Omega_{a,begin}} = \left(\frac{a_{end}}{a_{begin}}\right)^{-2} = e^{-2H(t_2 - t_1)} = e^{-120} \sim 10^{-52} \quad (1.4)$$

or more. Now the argument before is reversed. If, before inflation, Ω is just of order unity, it will after inflation be $\Omega = 1 \pm 10^{-52}$ and we have an explanation of the observed flatness.

This can easily be done by a scalar field, where the energy density and pressure is given by:

$$\rho = \dot{\phi}^2/2 + V(\phi) \qquad P = \dot{\phi}^2/2 - V(\phi)$$

As can be seen, if the ϕ develops very slowly, ρ will be almost constant. (Incidently, this gives $P = -E$, just the relation that we want for the cosmological constant, ie. the vacuum energy.)

Let us take an inflation field ϕ and write a Lagrangian

$$\mathcal{L} = T - V = a^3(\dot{\phi}^2/2 - V(\phi)) \tag{1.5}$$

Making the Euler-Lagrange equation gives

$$\ddot{\phi} + 3H\dot{\phi} + \frac{dV}{d\phi} = 0 \qquad \textbf{for a real field} \tag{1.6}$$

This looks like a pendulum with a Hubble friction term.

As mentioned, what we need is a potential that is almost constant as a function of time. There are many ways to construct such a field. We also need to make inflation end again. One can either make a field that rolls slowly on a very high potential with a very shallow slope and end inflation by the flat potential going over to a steeper harmonic potential, or by simply making the potential an extremely flat harmonic oscillator.

1.4 Reheating

Regardless of whether the inflaton is in a harmonic oscillator all the time, or only in the end, inflation ends when the oscillating field transfers its energy by decaying to fundamental particles. These particles will be very light and get a large fraction of their energy as kinetic energy. These created particles will reach thermal equilibrium at some temperature, which we call the reheating temperature T_{reh}. Reheating is a rather unfortunate name, since the kinetic energy of the inflaton is very small, and therefore reheating is the first (known[1]) heating of the universe. After the inflaton has gone, the universe develops in the normal Big Bang way. However, Big Bang is no longer a real singularity, this has been removed by inflation.

1.5 Preheating

The standard approach would be to assume that the inflaton field decayed perturbatively.

[1] What happened before inflation is effectively out of reach. All traces have been removed. It might be all the universe that inflated, or maybe just a tiny bit where the right conditions incidentally occurred.

[2] found that if the initial amplitude of the oscillation is large enough, there can be a parametric resonance. This they called preheating. It happens in a stochastic way, since the universe expands during the oscillation. Despite the stochastic nature, the result is exponential growth of occupation numbers of the created particles. This happens for bosons, because as soon as the occupation number becomes high, the Bose enhancement will be proportional to the occupation number. The project reported in the article of chapter 5 is independent of the question of how the heat got into the universe, but it is at the core of the articles of chapters 6 and 7.

This follows [2] and the shorter introducing article by the same authors [3].

They look at a simple potential for a scalar inflaton

$$V(\varphi) = \pm\frac{1}{2}m_\phi^2\phi^2 + \frac{1}{4}\phi^4 \tag{1.7}$$

where the minus sign gives spontaneous symmetry breaking which gives a classical field $\sigma = \frac{m_\phi}{\sqrt{\lambda}}$ and a redefinition of the inflaton field around this classical value $\phi \to \phi + \sigma$. Bosons (ξ) and fermions (χ) behave quite differently so we include both with interaction terms $-g^2\phi^2\chi^2$ and $-h\bar{\psi}\psi\varphi$ respectively. Assuming that the bare masses are negligible, the induced masses are proportional to the inflaton field $m_\chi(\phi) = g\phi$ and $m_\psi(\phi) = |h\phi|$.

Reheating (without resonance) considers ϕ to be particles at rest, and the decay rates are $\Gamma(\phi \leftarrow \chi\chi) = \frac{g^4\sigma^2}{8\pi m_\phi}$ and $\Gamma(\phi \leftarrow \bar{\psi}\psi) = \frac{h^2 m_\phi}{8\pi}$. Reheating ends when the system couples $\Gamma_{tot} > H$ and the corresponding temperature is of order $T_r = 0.2\sqrt{\Gamma M_p}$.

However, at the beginning of inflation and when boson production is possible, both the nonzero momentum and quantum effects of χ must be included. The point can be made with only a classical inflaton field with quadratic (positive) potential and quantum scalars.

A quantum scalar field looks like this in the Heissenberg picture

$$\hat{\chi}(t,\vec{x}) = \frac{1}{(2\pi)^{3/2}}\int d^3k \left(\hat{a}_{\vec{k}}\chi_{\vec{k}}(t)\exp\left(-i\vec{k}\cdot\vec{x}\right) + \hat{a}^\dagger_{\vec{k}}\chi^*_{\vec{k}}(t)\exp\left(i\vec{k}\cdot\vec{x}\right)\right) \tag{1.8}$$

where $\vec{k}$ is the comoving momentum and the a's are annihilation and creation operators respectively.

For a fluctuation with physical momentum $\vec{k}/a(t)$, the equation of motion (with Hubble friction term) is

$$\ddot{\chi_k} + 3H\dot{\chi_k} + \left(\frac{k^2}{a(t)^2} + g^2\phi\right)\chi_k = 0 \tag{1.9}$$

– with curvature ignored. It turns out that the important momenta are much larger than the Hubble rate, so we can consider the scale factor to be a constant which makes the Hubble term vanish as well. Now we just have a harmonic oscillator with a variable frequency (the square root of the larger bracket above)

$$\ddot{\chi_k} + \left(k^2 + 2g^2\sigma\Phi\right)\chi_k = 0 \tag{1.10}$$

and Φ is the amplitude of the oscillation. If one changes the time coordinate to the dimensionless variable $z = m_\phi t/2 + \pi/4$ and further defines $q = \frac{4g^2\sigma\Phi}{m_\phi^2}$ and $A(k) = 4\frac{k^2+g^2\sigma^2}{m_\phi^2}$ the equation of motion is transformed to the Mathieu equation

$$\chi_k'' + (A(k) - 2q\cos(2z))\,\chi_k = 0 \tag{1.11}$$

This equation has a (index n) number of frequency bands $\Delta k^{(n)}$ with exponential growth $\chi_k \propto \exp(\mu_k^{(n)} z)$ corresponding to exponential occupation numbers $n_{\vec{k}} \propto \exp(2\mu_k^{(n)} m_\phi t)$ – that is explosive particle production. μ_k takes its maximum ($\frac{q}{2}$)at $k = \frac{m}{2}$ – corresponding to an inflaton at rest decaying into 2 bosons – each carrying away half the energy. The effect only shows up when the equation is solved nonperturbatively and is caused by Bose enhancement – when $n_k >> 1$, its derivative is proportional to the occupation number itself.

1.6 Particle production – coupled bosons

In chapters 6 and 7 particle production is the core issue. In those cases there are many boson fields. This changes things. Particle production for several fields – including the case of several bosons – were investigated in [4]. I will here sketch how the apparently "magic" formulas for the generalised Bogolyubov come about.

Using conformal time (η), comoving fields ($\varphi_i = a\phi_i$) a system of coupled bosons will have action

$$S = \frac{1}{2}\int d^4x \left(\dot{\varphi}_i\dot{\varphi}_i - \varphi_i\Omega_{ij}^2\varphi_j\right) \tag{1.12}$$

giving equations of motion (summation over j)

$$\ddot{\varphi}_i + \Omega_{ij}\varphi_j = 0. \tag{1.13}$$

Defining conjugate momenta,

$$\Pi_i \equiv \frac{\partial\mathcal{L}}{\partial\dot{\varphi}_i} = \dot{\varphi}_i \tag{1.14}$$

the Hamiltonian becomes

$$H = \frac{1}{2}\int d^3x \left(\Pi_i\Pi_i - \varphi_i\Omega_{ij}^2\varphi_j\right). \tag{1.15}$$

At any (conformal) time, Ω^2 can be diagonalised

$$C^T(\eta)\Omega^2(\eta)C(\eta) = \omega(\eta) \tag{1.16}$$

and we define ω_i^2 to be the i'th entry of the diagonal matrix. Decomposing the variables in creation and annihilation operators

$$\begin{aligned}
\varphi_i &= C_{ij}\frac{1}{(2\pi)^{3/2}}\int d^3k \left(\exp(i\vec{k}\cdot\vec{x})h_{jk}(\eta)a_k(\vec{k}) + \exp(-i\vec{k}\cdot\vec{x})h_{jk}^*(\eta)a_k^\dagger(\vec{k})\right)\\
\Pi_i &= C_{ij}\frac{1}{(2\pi)^{3/2}}\int d^3k \left(\exp(i\vec{k}\cdot\vec{x})\tilde{h}_{jk}(\eta)a_k(\vec{k}) + \exp(-i\vec{k}\cdot\vec{x})\tilde{h}_{jk}^*(\eta)a_k^\dagger(\vec{k})\right)
\end{aligned}$$

and demanding the following quantisation rules

$$[\varphi_i(\vec{x}), \Pi_j(\vec{y})] = i\delta^3(\vec{x}-\vec{y})\delta_{ij} \quad (1.17)$$

$$\left[a_i(\vec{k}), a_j^\dagger(\vec{p})\right] = \delta^3(\vec{k}-\vec{p})\delta_{ij} \quad (1.18)$$

will work out if

$$\left[h, \tilde{h}^\dagger - h^*\tilde{h}^T\right]_{ij} = i\delta_{ij}. \quad (1.19)$$

Changing to the basis where Ω is diagonal ($\hat{\varphi} \equiv C^T\varphi$ and likewise for Π), the Hamiltonian becomes

$$H = \frac{1}{2}\int d^3x \left(\hat{\Pi}_i\hat{\Pi}_i - \omega_i^2\hat{\varphi}_i\hat{\varphi}_i\right). \quad (1.20)$$

Imposing

$$h = \frac{\exp\left(-i\int^\eta \omega d\eta'\right)}{\sqrt{2\omega}}A + \frac{\exp\left(i\int^\eta \omega d\eta'\right)}{\sqrt{2\omega}}B \quad (1.21)$$

$$\tilde{h} = \frac{-i\omega\exp\left(-i\int^\eta \omega d\eta'\right)}{\sqrt{2\omega}}A + \frac{i\omega\exp\left(i\int^\eta \omega d\eta'\right)}{\sqrt{2\omega}}B \quad (1.22)$$

A and B emerges as the multi-field generalisation of the Bogolyubov coefficients of the one field case.

Further defining

$$\alpha = \exp\left(-i\int^\eta \omega d\eta'\right)A \quad (1.23)$$

$$\beta = \exp\left(i\int^\eta \omega d\eta'\right)B \quad (1.24)$$

the differential equations given by the equations of motion and the definition of conjugate momenta, 1.13 and 1.14 translate into the equations quoted in the articles of chapters 6 and 7:

$$\begin{aligned}\dot{\alpha} &= -i\omega\alpha + \frac{\dot{\omega}}{2\omega}\beta - I\alpha - J\beta \\ \dot{\beta} &= \frac{\dot{\omega}}{2\omega}\alpha + i\omega\beta - J\alpha - I\beta\end{aligned} \quad (1.25)$$

with the definitions

$$I = \frac{1}{2}\left(\sqrt{\omega}\,C^T\dot{C}\frac{1}{\sqrt{\omega}} + \frac{1}{\sqrt{\omega}}\,C^T\dot{C}\sqrt{\omega}\right) \quad (1.26)$$

$$J = \frac{1}{2}\left(\sqrt{\omega}\,C^T\dot{C}\frac{1}{\sqrt{\omega}} - \frac{1}{\sqrt{\omega}}\,C^T\dot{C}\sqrt{\omega}\right). \quad (1.27)$$

.

1.7 Why more matter than anti-matter?

Why is there more matter than anti-matter? When we look around in the world, in every possible meaning of the word, we see a lot of matter, and very little anti-matter. That is contrary to the natural assumption that due to symmetry, equal amounts of matter and anti-matter should be created. It is rather fortunate that there is a matter surplus, since we are made out of baryons, and equal amounts of baryons and anti-baryons would annihilate. This phenomenon seems not to be local. At least we know from cosmic rays that all matter/anti-matter "near" to us is matter. Could the global baryon number be $B = 0$? In that case there would be large domains containing matter and large domains containing anti-matter. That would give dramatic radiation from domain walls. We do not observe such radiation, even though, looking more and more backwards in time, domains must have been ever closer.
Also, data from the Cosmic Microwave Background and Big Bang Nucleosynthesis corresponds perfectly to our model of cosmology [5] that has

$$\eta_B \equiv -\frac{n_b - n_{\bar{b}}}{n_\gamma} \sim 6 \cdot 10^{-10} \tag{1.28}$$

One can, of course, imagine that all anti-matter is clumped in very dense regions. But in that case, explaining why matter and anti-matter spread so differently would be arguably more difficult than to find explanations why the baryon number is not zero globally.
In short, it is most likely that B is non-zero today.

1.8 Inflation destroys initial Baryon Number

The reason why there can be no Baryon Number (at least not enough to account for the asymmetry observed today) at the end of Inflation is the following [6]:

To give the necessary homogeneity and isotropy, inflation must have lasted at least 70 e-foldings (such that distances grew by a factor of e^{70})[2], such that any number density must have been diluted by a factor of e^{-210}.

This is bad enough for initial Baryon Number to survive, but it is worse. If we take the energy density in the excess of baryons today, we know that it scales with $\rho_{baryon,excess} \propto R^{-3}$ (when matter) and $\rho_{baryon,excess} \propto R^{-4}$, (when radiation) as a function of time. This means that we can calculate (or rather estimate) the energy density of excess baryons at the end of inflation. During inflation this energy will develop as radiation $\rho_{baryon,excess} \propto R^{-4}$ thus further increasing backwards in time. Just 6 e-foldings before the end of inflation, $\rho_{baryon,excess}$ will be the dominant part of the energy density in the universe. This, however, is a complete contradiction to the concept of inflation, since ρ_{tot} must be constant in time during inflation to give the exponential solution to the Friedmann equation.

Thus the Baryon density today must have been created after the end of inflation.

[2] Yes, it is in contrast to the 60 I stated earlier. These numbers are taken from different sources. However, it is not important for this argument.

2

Particle Physics beyond the Standard Model

Both now and for always, I intend to hold fast my belief in the hidden strength of the human spirit
— Andrei Sakharov, Nuclear Physicist

2.1 Changing Baryon Number: Sakharov criteria

If B is nonzero today, and if it has been zero earlier (after inflation), then B must have changed! In 1967 Sakharov [7] found 3 criteria for this to happen.

1. **B violation in some processes** (2.1)
2. **C and CP violation in some processes** (2.2)
3. **Non equilibrium dynamics.** (2.3)

1 is rather self evident; 2 is necessary in order to allow rates for particle/anti-particle to be different so B-changing rates are not canceled by the charge conjugated process; 3 is necessary to allow deviations from equilibrium, since equilibrium will always mean equal numbers of particle/antiparticles regardless of how they are created.

2.2 Sphalerons

Sphalerons are particles corresponding to a saddle point in the electro-weak potential energy [8]. This makes transformations of baryons to anti-leptons possible, breaking $B + L$ but leaving $B - L$ as a strictly conserved quantum number. This is immensely important. It means that any nonzeroness in either B or L can be transferred to the other. In short, we only need to find either baryogenesis or leptogenesis.

Leptogenesis have some important advantages. First of all, we already know that the otherwise ridiculously[1] successful standard model of particle physics

[1] What seems to be a low energy approximation to a larger theory holds extremely well over many, many orders of magnitude.

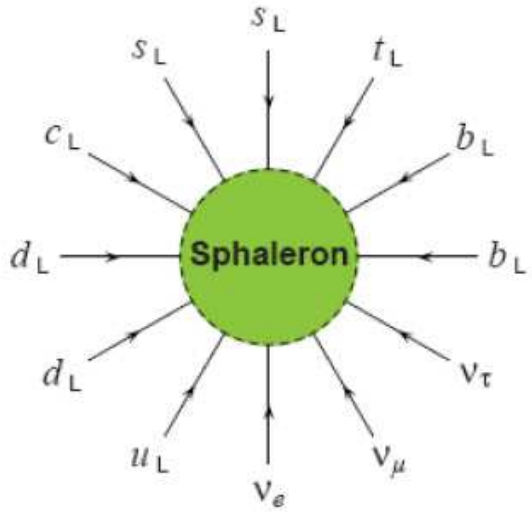

Fig. 2.1: Sphaleron process. Figure from M. Plümacher .

(SM) is not all the story for neutrinos. We know that there are neutrino flavor oscillations. This demands neutrino masses, and this means that either a righthanded neutrino exists, or the neutrino is a Majorana particle. This is the subject of the next session. The point is: if we need to do strange things in the lepton sector, it would be nice if these strange things could explain the observed strange thing in the baryon sector, i.e. the asymmetry.

2.3 Neutrinos and their masses

There is clear evidence that neutrinos have masses. They can be Dirac-particles and have mass terms corresponding to the charged leptons:

$$\mathcal{L}_D = -m_D \overline{\nu_R} \nu_L + h.c. \tag{2.4}$$

Notice, however, that this means that the righthanded field ν_R exists. This is not the same as the anti-neutrino $\overline{\nu_L}$. In fact, this righthanded particle will be most difficult to detect, since it has no electromagnetical, weak or strong nuclear reactions.

This means that a Dirac-neutrino will demand physics beyond the SM. It is also a question why the mass is so much smaller than other fermion masses.

However, the neutrino could also be a Majorana particle, ie. a particle that is identical to its own anti-particle. This could have a mass term

$$\mathcal{L}_{M_L} = -\frac{m_L}{2} \overline{\nu_L^c} \nu_L \tag{2.5}$$

This does not contradict the experimentally found difference between anti-neutrinos and neutrinos, it just means that the "anti-neutrino" is just the same

particle, but with opposite chirality. The lefthanded neutrino will react in the weak interaction on equal footing with charged leptons, whereas the "anti-neutrino" would be the neutrino reacting on an equal footing with the charged anti-leptons.

If there is such a particle, ν_R is not necessary in the theory.

However, we know that if the neutrino has a Dirac mass term, righthanded leptons do exist. So why not have ν_R a Majorana particle with

$$\mathcal{L}_{M_R} = -\frac{m_R}{2}\overline{\nu_R^c}\nu_R \tag{2.6}$$

2.4 The see-saw mechanism

Let us assume that the neutrino does have a Dirac mass term. That does not preclude the possibility that it could also have a righthanded Majorana mass term. In fact, a Dirac mass term would guarantee that the righthanded field exists. Nothing we know suggests that not both mass terms would be present. With a Dirac-mass there is no need for a left-left mass.

$$\mathcal{L}_{\nu_m} = -m_D\overline{\nu_R}\nu_L - \frac{m_R}{2}\overline{\nu_R^c}\nu_R + h.c. = -\frac{1}{2}\begin{pmatrix} \overline{\nu_L^c} & \overline{\nu_R} \end{pmatrix}\begin{pmatrix} 0 & m_D \\ m_D & m_R \end{pmatrix}\begin{pmatrix} \nu_L \\ \nu_R^c \end{pmatrix} \tag{2.7}$$

Since ν_R has no weak interactions, there is no reason why it should have a mass comparable to the weak mass scale. In fact, the GUT-scale seems more natural. Anyway, let us just assume that

$$m_R \gg m_D \tag{2.8}$$

and then we find the eigenvalues to be

$$m_1 \simeq m_R \qquad \textbf{and} \qquad m_2 \simeq m_D^2/m_R. \tag{2.9}$$

This result shows a way to explain the low neutrino mass. Assume that the neutrino has a Dirac mass comparable to other lepton Dirac masses – let us even take the heaviest, $m_D = m_{top} = 175GeV$ and let $m_R = 10^{15}GeV$ then one find $m_2 \simeq 3 \cdot 10^{-2}eV$ which could be around the observed neutrino mass. One can choose a smaller Dirac mass and get the mass m_2 even smaller. In that case, in a sense, the neutrino mass is not small at all, it just appears to be so, due to its much, much heavier partner. It has been put down, like by a see-saw[2].

Not only is this a beautiful mechanism in itself, it also predicts the existence of m_1, a super heavy sterile neutrino. That is exactly what we need in leptogenesis.

It is also worth mentioning that the eigenstates are in fact Majorana. Boris Kayser said [3]"Either the neutrino is Dirac or it is Majorana. And if it is Dirac, it is probably Majorana anyway!"

[2] up towards zero from positive - strange see-saw!

[3] ISAPP Summer School 2006, München.

3

Supersymmetry

The mathematical sciences particularly exhibit order, symmetry, and limitation; and these are the greatest forms of the beautiful.
— Aristotélēs, Philosopher

3.1 Fast introduction to Supersymmetry

The main idea of supersymmetry (SUSY) is that each field we know get a "partner" field with essentially the same interactions, with a spin quantum number that differs by 1/2 (the partner particle with less spin than the particle we know – where possible), such that each fermion we know, has a boson partner (squarks and sleptons), and the bosons we know have fermions partners (gauginos and Higgsinos). This stabilises Quantum Field Theory dramatically from radiative instabilities, since each fermion loop gives a factor of -1 to action calculations compared to boson loops. The number of loops in a Feynmann diagram is essentially the order of perturbation theory used. Supersymmetry thus means, that a fermion loop diagram cancels the known boson loop diagram – at least in the high energy limit, where masses and other symmetry breaking effects are negligible – and vice versa. Also, postulating a new quantum number, R-parity, defined by the conservation of $R = (-1)^{3B+L+2S}$, all known particles have $R = 1$ while their superpartners have $R = -1$. This means that the number of superpartners can only change by units of 2. In other words, annihilations of, but not decays of, the lightest superpartner is possible – making it a(n odds-on?) favorite dark matter candidate. The rest of this section follows [9]. Instead of space just having 4 coordinates, we add Grassmann variables θ^α and $\overline{\theta}^{\dot{\alpha}}$[1]. In a sense these variables are associated with left- and righthanded particles, since with covariant derivatives defined to be

$$D_\alpha = \frac{\partial}{\partial\theta^\alpha} + i\sigma^\mu_{\alpha\dot{\beta}}\overline{\theta}^{\dot{\beta}}\partial_\mu \tag{3.1}$$

$$\overline{D}_{\dot{\alpha}} = -\frac{\partial}{\partial\overline{\theta}^{\dot{\alpha}}} - i\sigma^\mu_{\beta\dot{\alpha}}\theta^\beta\partial_\mu \tag{3.2}$$

[1] Notice: Bars and dots always follow each other – dot does not mean derivative.

we define the chiral superfields to abide to

$$\overline{D}_{\dot{\alpha}}\Phi_L = 0 \qquad \textbf{and} \qquad D_\alpha \Phi_R = 0$$

With $y^\mu = x^\mu + i\theta\sigma^\mu\overline{\theta}$ the lefthanded superfield can be written

$$\Phi_L(y,\theta) = \phi(y) + \theta\psi(y) + \theta\theta F(y)$$

This contains one spin-1/2 fermion (ψ), and two spin-zero bosons (ϕ and F – both complex scalar fields). Notice that $\overline{\theta}$ is not present. There is also a vector superfield that in the clever Wess-Zumino gauge is given by

$$V(x,\theta,\bar{\theta}) = -\theta\sigma^\mu\bar{\theta}V_\mu + i\theta\theta\bar{\theta}\bar{\lambda} - i\bar{\theta}\bar{\theta}\theta\lambda + \frac{1}{2}\theta\theta\bar{\theta}\bar{\theta}D$$

where V_μ is a real vector (spin 1 boson), D is a real scalar (spin 0 boson) and λ is a Weyl spinor.

3.2 MSSM

The MSSM (Minimal Supersymmetric Standard Model) is exactly what the name suggests. The only chiral superfields are those that contain the known quarks and Higgses, the only vector superfields are those that contain the known vector force particles. (Augmenting this by the metric superfield one gets supergravity). The only chiral superfields are (with small Greek indices for SU(2), capital Latin indices for SU(3), and Latin indices for family) quark doublets $Q_i^{\alpha A}$, quark singlets U_{iA} and D_{iA}, lepton doublets L_i^α, lepton singlets E_i and Higgs doublets H_u^α and H_d^α. The vector superfields are g, W, B (B^A, A^i, A^0 in the notation of the articles in chapters 6 and 7) corresponding to $SU(3)_c, SU(2)_L, U(1)_Y$.

The two tables list all the superfields (same names as we have used in the articles, except that we have used capital letters for all the superfields) of MSSM, including their field content and their transformation rules under the Gauge symmetries. These tables are taken from the excellent introduction to SUSY and MSSM [10] – which the next observations are taken from also.

It is worth mentioning that the fields in the table are the ones of the unbroken symmetries. Just as W^0 and B combine to form the photon (γ) and Z^0, the neutral Wino ($\tilde{W}^0$) and Bino ($\tilde{B}^0$) combine to form Zino ($\tilde{Z}^0$)and the photino ($\tilde{\gamma}$). The introduction of two Higgs doublets is the price to pay for the following superpotential

$$W = y_{\mathrm{u}}^{ij}\bar{u}_i Q_j \cdot H_{\mathrm{u}} - y_{\mathrm{d}}^{ij}\bar{d}_i Q_j \cdot H_{\mathrm{d}} - -y_{\mathrm{e}}^{ij}\bar{e}_i L_j \cdot H_{\mathrm{d}} + \mu H_{\mathrm{u}} \cdot H_{\mathrm{d}}. \tag{3.3}$$

where we continue to use the notation of [10]. The fantastic thing about this is that the Yukawa couplings (the y's) are exactly the same as for the standard model! This demands that H_u and H_d (that is the 2 superfields giving mass to

Names		spin 0	spin 1/2	$SU(3)_c$, $SU(2)_L$, $U(1)_y$
squarks, quarks	Q	$(\tilde{u}_L, \tilde{d}_L)$	(u_L, d_L)	**3**, **2**, 1/3
($\times$ 3 families)	$\bar{u}$	$\bar{\tilde{u}}_L(\tilde{u}_R)$	$\bar{u}_L \sim (u_R)^c$	$\bar{\mathbf{3}}$, **1**, -4/3
	$\bar{d}$	$\bar{\tilde{d}}_L(\tilde{d}_R)$	$\bar{d}_L \sim (d_R)^c$	$\bar{\mathbf{3}}$, **1**, 2/3
sleptons, leptons	L	$(\tilde{\nu}_{eL}, \tilde{e}_L)$	(ν_{eL}, e_L)	**1**, **2**, -1
($\times$ 3 families)	$\bar{e}$	$\bar{\tilde{e}}_L(\tilde{e}_R)$	$\bar{e}_L \sim (e_R)^c$	**1**, **1**, 2
higgs, higgsinos	H_u	(H_u^+, H_u^0)	$(\tilde{H}_u^+, \tilde{H}_u^0)$	**1**, **2**, 1
	H_d	(H_d^0, H_d^-)	$(\tilde{H}_d^0, \tilde{H}_d^-)$	**1**, **2**, -1

Tab. 3.1: Chiral supermultiplet fields in the MSSM.

Names	spin 1/2	spin 1	$SU(3)_c$, $SU(2)_L$, $U(1)_y$
gluinos, gluons	$\tilde{g}$	g	**8**, **1**, 0
winos, W bosons	$\widetilde{W}^{\pm}, \widetilde{W}^0$	$W^{\pm}$, W^0	**1**, **3**, 0
bino, B boson	$\tilde{B}$	B	**1**, **1**, 0

Tab. 3.2: Gauge supermultiplet fields in the MSSM.

up-quarks and d-quarks respectively) are independent superfields – since 2 fields that are charge conjugate of each other, are not allowed in the superpotential. μ is the only parameter that is not in the standard model. That is extraordinary given all the new fields introduced. It seems to good too be true – and it is. Supersymmetry is in fact broken – and once it is broken a forest of new parameters is possible.

3.3 The scalar sector and flatness

The scalar part of the potential is given by the so called F-terms and D-terms, $V = \sum_A \frac{g_A^2}{2} D^A D^A + \sum_I |F_{\chi I}|^2$ where

$$D^A \equiv \chi^\dagger T^A \chi_i \tag{3.4}$$

$$F_{\chi_I} \equiv \frac{\partial W}{\partial \chi_i} \tag{3.5}$$

where χ_I is the scalar part of a superfield, and T^A is a generator of the Lie gauge algebra. One thing to note is that one can get a flat potential in some directions – that is $V = 0$ for nonzero field values. One simply needs to get all the individual D-terms and F-terms to be zero.

Total flatness is, however, only possible when supersymmetry is exact. In the real world, we will expect other terms in the potential than the renormalisable terms given by 3.3. We expect soft terms (mass terms) given by $V_{soft} = m^2|\phi|^2$ with masses probably at the electroweak scale and non-renormalisable terms given by $W_{nonren} = \sum_{n>3} \frac{\lambda \Phi^n}{M^{n-3}}$ where Φ is some monomial and M is some cut-off scale (perhaps the Planck scale).

Gherghetta, Kolda and Martin [11], which is followed in this section, categorised all roughly 300 flat directions, and divided them according to whether they are lifted by renormalisable terms or non-renormalisable terms.

[11] found that all flat directions are lifted by terms of order between $n = 4$ and $n = 9$. There is only one flat direction that is not lifted until $n = 9$. All flat directions involving Higgs fields are lifted by the μ-term in the renormalisable potential. However, this might not be that important since μ is expected to be of the order of the weak scale.

3.4 Flat direction evolution

The evolution of a flat direction during inflation was studied by Dine, Randall and Thomas [12], which is followed here. Consider a flat direction QLD^c. For instance

$$Q_1^\alpha = \frac{1}{\sqrt{3}} \begin{pmatrix} \phi \\ 0 \end{pmatrix} \qquad L_1 = \frac{1}{\sqrt{3}} \begin{pmatrix} 0 \\ \phi \end{pmatrix} \qquad \bar{d}_2^\alpha = \frac{1}{\sqrt{3}}\phi \tag{3.6}$$

where Greek letters are color indices and Latin letters are family indices. Here we consider the vacuum expectation values (VEVs) to have equal phases, even though, as will be very important in chapters 6 and 7, flatness is independent of phase. Also, in this case where the fields have equal magnitude, flatness is very easy to check. We have a field with color, and one with the same (or opposite, if you like) color. We have one $SU(2)$ up-charge, and one down-charge. The sum of the hypercharges is also zero. That means it all balances, we have flatness.

It is worth noticing that the flat direction carry $B - L = -1$.

We may write down a monomial to characterise the flat direction $X = Q_1 L_1 D_2^c$. The scalar part of this will be $X = c\phi^m$ where $m = 3$ has not been inserted – in order to have a general case rather than this specific flat direction.

The zero mode (the only relevant mode) is governed by a Hubble damped oscillator

$$\ddot{\phi} + 3H\dot{\phi} + V'(\varphi) = 0 \tag{3.7}$$

Let us look at the potential. The superpotential can contain the invariant X to some power k giving (with $n = k * m$)

$$W = \frac{\lambda}{nM^{n-3}} X^k = \frac{\lambda}{nM^{n-3}} \phi^n \tag{3.8}$$

Some derivative with respect to one of the participating fields (F-term) will take away one power of ϕ, and this term will then be (absolutely) squared $V = \frac{|\lambda|^2}{nM^{2n-6}}|\phi|^{2n-2}$. There might also be self-couplings leading to an A-term $V = \frac{Am_{3/2}\lambda}{nM^{n-3}}\phi^n$, and finally there are SUSY breaking mass terms $V = m^2|\phi|^2$. However, the finite energy density of the vacuum means that supersymmetry is not exact. Instead there will be induced masses of order $m_{induced} = H(t)$ which will dominate the "real" mass terms during inflation.

Thus we have a potential (with $H \propto t^{-1}$)

$$V(\varphi) = m_\varphi^2|\varphi|^2 - \frac{c'}{t^2}|\varphi|^2 + \left(\frac{Am_{3/2} + aH}{nM^{n-3}}\lambda\phi^n + h.c\right) + \frac{|\lambda|^2}{nM^{2n-6}}|\phi|^{2n-2} \tag{3.9}$$

c' can have either sign, and if it is negative (50% fine tuning?), the minimum is displaced from zero. During inflation the "real" mass terms are overwhelmingly suppressed, and the minimum will be

$$|\phi_0| = \left(\frac{\beta H_I M^{n-3}}{\lambda}\right)^{\frac{1}{n-2}} \tag{3.10}$$

where β is a numerical constant depending of the constants a,c,n and $|\phi_0|$ could easily be of order $10^{16}GeV$. Thus the flat direction can get an almost arbitrarily large VEV since, due to flatness, large field values do not "cost" any energy. Flat directions with extremely high VEVs are the starting point of the articles in chapters 6 and 7.

When inflation ends, the "real" masses will first be on equal footing with the induced ones, and later they will dominate and the flat direction will rotate around the new minimum at $\varphi = 0$. The phase dependence of the potential (middle term) means that when the phase changes, B-L is produced. Due to the sphaleron processes mentioned in 2.2 this can eventually lead to any combination of baryon and lepton number.

3.5 The possible cosmological role of flat directions

Allahverdi and Mazumdar [13] realised that the flat directions with high VEVs can have other cosmological consequences than the creation of baryon number. They will give large masses to inflaton decay products (MSSM scalars) of order $g\langle\phi\rangle > H_I$ for a scalar χ coupled by $g^2\phi^2\chi^2$. This means that there are no light scalars for the inflaton to couple to, and therefore no instability in the Mathieu equation. This means that the inflaton cannot decay explosively at large temperatures, but will only decay after the VEVs have redshifted. This means that preheating is avoided, and that the reheating temperature will be small ($10^3 - 10^7 GeV$). This solves the gravitino problem (why we don't see them) and also gets rid of WIMPs.

For this to work, nonperturbative particle production must be avoided. This is the classic adiabicity condition $\frac{d\omega}{dt} < \omega^2$. This translates to a conservative bound of an initial VEV that has to be larger than something around $10^{13}GeV - M_{pl}$ depending on the couplings g and λ.

In other words: that is very likely to be the case.

On the other hand, Olive and Peloso [14] claim that in most cases 2 flat directions will give preheating. The mechanism for that is the one described in section 1.6. In the only numerical example they give, however, they preheat to Goldstones. They claim that it works in physical situations also. In the first edition they didn't point out that their example was preheating to Goldstones. This has been added in a later edition. This had been pointed out in [15] that was put on arxiv.org in the meantime.

In the same article they put forward the formula

$$N_{light} = N_{total} - 2 \cdot N_{broken}$$

where N_{light} is the number of light degrees of freedom, N_{total} is the number of real fields involved and N_{broken} is the number of broken generators of the SM $SU(3)_c \times SU(2)_L \times U(1)_Y$. Take LLE^c as example, $N_{total} = 4 + 4 + 2 = 10$, $N_{broken} = 3 + 1 = 4$ (breaks $SU(2) \times U(1)$ to nothing) so $N_{light} = 2$. These

2 directions are simply the direction of the VEVs and what I shall call its superorthogonal field – the field that is orthogonal in each plane made of the real and imaginary part of each field. However, with hindsight after the article in chapter 7 one needs to be careful since in some cases also light degrees of freedom parameterising the flat direction and its superorthogonal field might be able to rotate with the Higgses. Furthermore, Higgses of different mass might in theory also be able to rotate with each other.

3.6 The flat direction as the inflaton itself

While the articles just mentioned described the reactions of the unknown inflaton with the flat directions which we know are there - presuming that SUSY is correct – Allahverdi, Enquist, Garcia-Bellido and Mazumdar came up with the idea that the flat direction, being a scalar, could be the inflaton itself [16]. They followed up, with Jokinen, with a more detailed paper [17] which we follow here.

Using a slightly different notation than in earlier sections, the flat direction is now parameterised by real fields $\Phi = \phi e^{i\theta}$, and likewise the coupling (known before as A) is now $Ae^{i\theta_A}$.The potential is (with no induced term since there is no (other) inflaton to create them and assuming the breaking scale is the Planck scale)

$$V = m_\varphi^2\varphi^2 + A\cos(n\theta + \theta_A)\frac{\lambda_n\phi^n}{nM_{pl}^{n-3}} + \frac{\lambda_n^2}{nM^{2n-6}}\phi^{2n-2} \tag{3.11}$$

Here (as is also possible but not necessary when there are induced masses) the cosine factor can make the A-term negative and displace the minimum away from zero.

Choosing a θ that makes the cosine -1, V has a local minimum at $\phi = \phi_0 = (m_\phi M_{pl}^{n-3})^{\frac{1}{n-2}} << M_{pl}$ if

$$A^2 \geq 8(n-1)m_\phi^2 \tag{3.12}$$

Inflation needs flatness, and the way to get maximal flatness is to make the minimum become extremely shallow, or simply let it become a saddle point (demanding V'' to be zero, not just V') instead.

This happens if 3.6 is changed to become an equation. This is obviously infinitely fine tuned (to be relaxed), but it serves as an example – and at least when it is gravity that breaks SUSY both the m_ϕ and A will be of order of the gravitino mass.

Two flat directions come into play: LLE^c and $U^cD^cD^c$. The reason is that these 2 directions both are lifted by $n = 6$ monomials

$$W = \frac{(LLE^c)(LLE^c)}{M_{pl}^3} \qquad W = \frac{(U^cD^cD^c)(U^cD^cD^c)}{M_{pl}^3} \tag{3.13}$$

This gives an A-term of order $n = 6$ as the lowest order, and they can get the correct COBE normalisation and CMB spectrum.

Assuming λ_6 is of order 1, which is claimed to be the most natural case, the parameters needed are

$$m_\phi = 1 - 10TeV, \qquad n = 6, \qquad A = \sqrt{40}m_\phi. \tag{3.14}$$

This gives around a thousand e-foldings, a Hubble parameter during inflation of $1 - 10GeV$ and $\phi_0 = 1 - 3 \times 10^{14} GeV$. These are great values and free of speculative physics beyond the Planck scale.

This leads to predictions of the mass of the flat direction (a combination of the MSSM masses involved in the flat direction) of

$$m_\phi \simeq \frac{100GeV}{\lambda} \left(\frac{50}{\mathcal{N}_{COBE}} \right)^4 \tag{3.15}$$

and spectral index and tilt

$$n_s \sim 0,92, \qquad \frac{dn_s}{d\ln k} \sim -0.002. \tag{3.16}$$

The authors have investigated the fine tuning, and found this mechanism to work and give reasonable predictions if the equation holds to one part to 10^{8-9}.

They find also that the mechanism is safe from supergravity and radiative corrections. However, due to unknown couplings and running thereof and other uncertainties, the only prediction of MSSM inflation for the LHC is that TeV scale supersymmetry should be found.

Even though the reheating temperature apparently will be of order $10^9 GeV$ or higher, this mechanism also solves the gravitino albeit in a slightly different way. First of all, direct production of the gravitino from the decay of the inflaton is very much suppressed by the decay of the inflaton's coupling into MSSM fields – since the inflaton is not a gauge singlet. If LLE^c is the inflaton Gravitinos could still be produced by scattering of gluons/gluinos, but this can be avoided if these particles can be made heavy. W's, Z's, Winos and Zinos are already made heavy since LLE^c breaks $SU(2)_L \times U(1)$ completely.

While LLE^c is the inflaton, $U^c D^c D^c$ can still exist – with a smaller VEV than LLE^c. In that case, since $U^c D^c D^c$ breaks $SU(3)_c$ the gluons and gluinos become heavy as well. In fact, if the VEV of $U^c D^c D^c$ is larger than $10^{10} GeV$, the reheating temperature is pushed down to $T_R \leq 10^7 GeV$ and the gravitino problem is solved.

This is very appealing since the point of a flat direction getting a large VEV is not restricted to 1 flat direction. On the contrary, one would assume that many flat directions – perhaps as many as are permitted to "live" at the same time, would get large values. This second flat direction rather than spoiling the mechanism, solves some problems.

While the fine tuning is enormous, one should not forget the advantage. Normally the inflaton is an arbitrarily scalar field - "invented" for the sole purpose of inflation. Here the scalar field is known to exist – again under the presumption that SUSY is correct. That is a huge advantage. Normally also other inflatons must have their behaviour fine tuned to get inflation right anyway.

3.7 What we found

In the article in chapter 6 our most important achievement was the developement of the formalism that parameterises the problem correctly. That is making sure that we work in the unitary gauge, such that there are no unphysical

Goldstone bosons that the Higgses can rotate into and making sure that all the excitation fields are correctly normalised such that they have the kinetic terms of real physical fields. We also concluded that all phases that cannot be gauged away generically will have independent dynamical evolution equations because they are part of different SUSY breaking monomials. In addition we found that it was possible to have preheating with only one flat direction. However, this was for a toy model where 2 fields had the same gauge charges – not necessarily a result that can be transferred to the MSSM.

In the article in 7 we found that there is no particle production from changing eigenstates neither in LLE^c, $U^cD^cD^c$ or the 2 combined. This is, of course, very important since these are the 2 directions at the centre of the MSSM inflation scenario 3.6. However, we found preheating with just one flat direction $QLQLQLE^c$. Also, we found preheating in a case with 2 directions having a common field $QLE^c + LLE^c$ with an L-field in common.

Finally, a couple of technical remarks. In the article in chapter 7 all gauge fields components have Lorentz index zero - even though the index is omitted. This is because we assume that only the time derivative of the phases are significant. Also in chapter 7 the definition of the U-matrix has been corrected compared to chapter 6.

3.8 Latest developements

In [18] it was claimed that nonperturbative particle production was impossible due to some charge conservation. This was answered to in [19] where it is stated that though these charges are indeed conserved, they can be distributed among the produced particles as well. Therefore this charge conservation does not exclude particle production. I agree, and I find any analysis that only include the excitation in the direction of the VEV (and its superorthogonal field) incomplete.

A few other things from [19] are worth mentioning. The authors write, correctly, that I (in the article of chapter 7) found that no particle production takes place in one flat direction (LLE^c or $U^cD^cD^c$). However, it seems that they have not seen the later editions of my paper, where I find particle production in $QLQLQLE^c$. In line with their statement that our article in chapter 6 had 2 flat directions because there were 2 independent phases, they might say that $QLQLQLE^c$ are 3 flat directions. This disagreement is about the definition of how one counts flat directions – it is not a disagreement of substance. However, with $QLQLQLE^c$ I think it is clear that saying it is 3 directions shows that a bad choice of counting definition is being applied, because $QLQLQLE^c$ cannot be divided into 3 (sub)directions. Also, in the article in chapter 6 we showed that generally one would expect different phases to get different dynamical equations of motion. This is due to the fact that each participating field is part of different SUSY breaking monomials.

Further [19] claims that the results I found (at least for $LLE^c + U^cD^cD^c$) are predictable from just counting the fields. Their point is, briefly stated, that there are 28 relevant fields, 12 Higgses and 12 Goldstones (SM completely broken), and the 4 remaining fields are the real and imaginary parts (the latter is

the one I call the superorthogonal field) of the excitations of the flat directions. This is to some degree true. However, as I write in the article in chapter 7, these excitations can in some cases rotate with the Higgses – as in $QLD^c + LLE^c$ – and the Higgses might also rotate with each other.

Furthermore [19] points out that the longitudinal part of the gauge boson is coupled to the Higgs at the linearised level, and therefore excitations of the gauge boson should be included. It is indeed correct to include the gauge excitations too.

They find, in a $U(1)$-case with 2 fields, that the action can be split into 3 subsystems. One contains the excitation in the flat direction and its superorthogonal field. The second is the transverse part of the gauge field. The third contains the Higgs and the zeroth and longitudinal part of the gauge boson. The zeroth component is non-dynamical and can be integrated out. But the Higgs and the longitudinal part remain coupled.

However, in what I call the U-matrix (their K-matrix), the term mixing the Higgs and the longitudinal boson is proportional to φ^{-1} and therefore suppressed. I have only included terms of zeroth order in the VEV. In the M-matrix (their Ω-matrix) the diagonal terms are of order of φ^2 whereas the off-diagonal term is of order of φ^1. All M-matrices I have calculated have been to order φ^2 only.

Very interestingly, when they calculate a $SU(2)$-case they find 3 copies of the U(1) case – one for each generator. Therefore the conclusions concerning the order of the terms we did not include, are still valid.

They also have a case of 2 $U(1)$ flat directions. Two fields with the same U(1)-charge and different VEVs – and 2 partner fields with same VEVs but opposite charges. The conclusion still holds for the mass matrix (in fact, mixing terms between Higgses and longitudinal fields are only of order of φ^0). However, there are terms of order φ^0, that is of leading order, in the U-matrix.

However, having 2 fields with exactly the same gauge charges seems artificial to me – there is no parallel of this in the standard model. Indeed this is quite similar to our toy model in chapter 6 – and we found preheating in that case as well. It is hard to compare terms from the gauge boson for two reasons. First [19] for some reason demand that the phases of 2 fields with the same (magnitude of) VEV should be the same; secondly in chapters 6 and 7 we demanded that the VEV had a slow development of magnitude compared to phase, that is a VEV that is primarily rotating, $\dot{\varphi} << \varphi\dot{\sigma}$, whereas [19], assumed that both the mentioned terms are suppressed to the same order compared to φ^2.

This difference on assumptions is also behind the fact that [19] also get particle production from the changing eigenvalues, that is they break the adiabaticity condition $\frac{\omega'}{\omega^2} << 1$ – whereas our particle production is always due to the changing eigenstates.

4

Neutrinos and majorons

Neutrinos they are very small
They have no charge and have no mass
And do not interact at all.
The earth is just a silly ball
To them, through which they simply pass,
Like dustmaids down a drafty hall
Or photons through a sheet of glas
— John Updike, poet

The subject of the article in chapter 8 and the draft article in chapter 9 is the possible coupling between the SM neutrinos and a pseudoscalar – the majoron (ϕ). We imagine a term in the Lagrangian

$$\mathcal{L} = -i \sum_{j,k} g_{jk} \phi \bar{\nu}_j \nu_k \tag{4.1}$$

This means that the off-diagonal elements of g correspond to decay terms (or inverse decay), whereas the diagonal elements are scattering terms. Since scattering has 4 g-factors in the rate (1 diagonal for each neutrino involved in the matrix element) and decays only 2 (1 off-diagonal element in the matrix element), it is very possible for the off-diagonal elements to be much smaller than the diagonal ones while decays still dominate over scatterings! This means that we can have a gas, where only decays and inverse decays play a role, whereas scattering can be ignored! A very special gas indeed.

The effect of such a term in the Lagrangian is that if the interaction is sufficiently strong, neutrinos and majorons will form a perfect fluid and neutrinos will loose their free-streaming properties.

The effect of strongly interacting neutrinos was investigated in [20] which is followed here.

Defining the conformal time, comoving momentum (and splitting this in size and direction), comoving energy and the perturbation in the distribution

function:

$$d\tau \equiv dt/a(t) \tag{4.2}$$

$$q_j = ap_j, \qquad q_j = qn_j \tag{4.3}$$

$$\epsilon = \sqrt{q^2 + a^2 m^2} \tag{4.4}$$

$$f(x^i, q, n_j, \tau) = f_0(q)\Big(1 + \Psi(x^i, q, n_j, \tau)\Big) \tag{4.5}$$

and defining the metric perturbations by

$$ds^2 = a^2(\tau)\Big(- d\tau^2 + (\delta_{ij} + h_{ij})dx^i dx^j\Big) \tag{4.6}$$

$$h_{ij} = \int d^3k e^{i\vec{k}\cdot\vec{x}}\Big(\hat{k}_i\hat{k}_j h(\vec{k},\tau) + \Big(\hat{k}_i\hat{k}_j - \frac{1}{3}\delta_{ij}\Big)6\eta(\vec{k},\tau)\Big) \tag{4.7}$$

and finally introducing a cosine parameter $\mu = n^j\hat{k}_j$, the Boltzmann equation becomes:

$$\frac{1}{f_0}L[f] = \frac{\partial\Psi}{\partial\tau} + i\frac{q}{\epsilon}\mu\Psi + \frac{d\ln f_0}{d\ln q}\Big(\dot{\eta} - \frac{\dot{h} + 6\dot{\eta}}{2}\mu^2\Big) = \frac{1}{f_0}C[f] \tag{4.8}$$

First, if there are no collisions, the collision operator on the right hand side is zero.

Expanding the perturbation $\Psi = \sum_{l=0}^{\infty}(-i)^l(2l+1)\Psi_l P_l(\mu)$, the Boltzmann equation turns into a hierarchy:

$$\dot{\Psi}_0 = -k\frac{q}{\epsilon}\Psi_1 + \frac{1}{6}\dot{h}\frac{d\ln f_0}{d\ln q} \qquad \textbf{energy conservation} \tag{4.9}$$

$$\dot{\Psi}_1 = -k\frac{q}{3\epsilon}(\Psi_0 - 2\Psi_2) \qquad \textbf{momentum conservation} \tag{4.10}$$

$$\dot{\Psi}_2 = k\frac{q}{5\epsilon}(2\Psi_1 - 3\Psi_3) - \left(\frac{\dot{h}}{15} + \frac{2\dot{\eta}}{5}\right)\frac{d\ln f_0}{d\ln q} \qquad \textbf{shear} \tag{4.11}$$

$$\dot{\Psi}_l = k\frac{q}{(2l+1)\epsilon}(l\Psi_{l-1} - (l+1)\Psi_{l+1}) \qquad \textbf{higher order terms} \tag{4.12}$$

On the contrary, in a strongly interacting gas, apart from the zeroth and first terms of the collision operator which automatically sum to zero due to energy and momentum conservation, all other terms in the collision operator can be approximated by

$$\frac{1}{f_0}C[f] = -\frac{\Psi}{\tau} \tag{4.13}$$

where τ is the mean time between collisions. Making the interaction sufficiently strong, τ will become sufficiently small for the collision operator to dominate all other terms in the Boltzmann equation, unless $\Psi_{i>1} = 0$. This means no shear, no viscosity and no anisotropic stress. This holds for both the neutrinos and the majorons.

This means that the neutrinos will have acoustic oscillations rather than free-streaming. Just the effect of "no shear" will change the CMB significantly as shown in [21]. In general it is very attractive to study neutrinos from the

CMB – both because neutrinos carry a large fraction of the energy density of the Universe at that time, but also because they are semi-relativistic - in contrast to the relativistic solar and Supernovae neutrinos.

One should note the perhaps counterintuitive fact that the the majorons and neutrinos become more and more strongly coupled in the sense that Γ/H is increasing during radiation domination. For scatterings $(ij \to ij)$ $\Gamma/H \propto T^{-1/2}$ since $\Gamma \propto g_{ii}^2 g_{jj}^2 T, \quad H \propto T^{3/2}$. For decays $(i \to j)$ $\Gamma/H \propto T^{-3/2}$ since $\Gamma \propto g_{ij}^2 m_i$. This means that instead of the usual decoupling when the fraction drops below unity, we have recoupling [1] when the fraction increases above unity.

For simplicity one can imagine that at a certain redshift z_i, the majorons and neutrinos become strongly coupled after having been not coupled at all. For the purpose here, this is a fine approximation.

Hannestad and Raffelt argued in [22] that since the neutrinos have no cosmological imprint after recombination[2], this would mean that $z_i \lesssim 1088$.

In translating this to a limit on the coupling, the authors also noted that in the decay case, kinetic equilibrium is delayed by a factor of $\gamma^2 = \left(\frac{E}{m_0}\right)^2$ (where m_0 is the mass of the heavier neutrino involved, and where the lighter is approximated to be massless). One γ-factor comes from the well known decrease of decay rate (time dilation of the characteristic life time). The other factor comes from the opening angle. The decay products are created isotropically in the rest frame of the decaying particle – this transforms into a preferred direction in the laboratory frame – aligned with the momentum of the decaying particle.

For the largest coupling [22] found $g \lesssim 1.1 \times 10^{-7}$ and for the limit for the off-diagonal couplings it found (translated to the more intuitive life time of the heavier neutrino involved) $\tau \gtrsim 2 \times 10^{10} s \left(\frac{m_0}{50meV}\right)^3$.

4.1 What we found

In the article in chapter 8 we made a Bayesian analysis of a broad range of cosmological data in the ΛCDM-model – with the extra parameter z_i mentioned in the prior section. This assures that we use a better limit than the one obtained from just taking the time of recoupling. We found, using both linear and logarithmic priors, that we could only be sure that $z_i < 1500$. This translates into bounds $g < 1.05 \times 10^{-7}$ and $\tau > 1.0 \times 10^{10} s \left(\frac{m_0}{50meV}\right)^3$.

In the draft article in chapter 9 we confirmed the γ^2 dependence of momentum transfer – both calculating analytical expressions for thermalising a perturbation of momentum of the heavier neutrino – with or without a thermal background of the lighter neutrino – and by making numerical simulations.

[1] this is the first (known) coupling – the name is a misnomer of the same kind as mentioning the first known heating of the universe as reheating.

[2] indeed, another misnomer of the same type.

Part II

PAPERS

5

Decay of heavy Majorana neutrinos using the full Boltzmann eqn. – leptogenesis

The paper *Decay of heavy Majorana neutrinos using the full Boltzmann equation including its implications for leptogenesis* presented in this chapter has been published by Journal of Cosmology and Astroparticle Physics (JCAP) [23].

[23] A . Basbøll og S. Hannestad: Decay of heavy Majorana neutrinos using the full Boltzmann equation including its implications for leptogenesis, JCAP01(2007)003.

Except for minor typographical changes, this version is identical to the arXiv version 3. Compared to the printed version, typos have been corrected and parameters have been defined more explicitly.

Decay of heavy Majorana neutrinos using the full Boltzmann equation including its implications for leptogenesis

Anders Basbøll* Steen Hannestad†

Abstract

We have studied the two-body production and decay of a heavy, right-handed neutrino to two light states using the full Boltzmann equation instead of the usual integrated Boltzmann equation which assumes kinetic equilibrium of all species. Decays and inverse decays are inefficient for thermalising the distribution function of the heavy neutrino and in some parameter ranges there can be very large deviations from kinetic equilibrium. This leads to substantial numerical differences between the two approaches. Furthermore we study the impact of this difference on the lepton asymmetry production during leptogenesis and find that in the strong washout regime the final asymmetry is changed by 15-30% when the full Boltzmann equation is used.

5.1 Introduction

Leptogenesis is perhaps the most attractive model for generating the matter-antimatter asymmetry in our Universe [1] after inflation. The process generates a lepton asymmetry via the production and subsequent decay of a heavy Majorana neutrino. This lepton asymmetry is partially converted to a baryon asymmetry via sphaleron processes [2] which break both B and L, but conserve $B-L$.

The fraction of $B-L$ that ends up in B by instantaneous sphaleron processes is given by $a_{sph} = 28/79$ giving $n_B = a_{sph} n_{B-L} = -a_{sph} n_L$ where the non-zero n_{B-L} is created by leptogenesis (see for instance [3]).

In its simplest form (within the context of the see-saw model) leptogenesis consists of adding three heavy right-handed neutrinos to the standard model. In the hierarchical limit one of these right handed neutrinos, ν_{R_1}, is much lighter than the other two and the leptogenesis mechanism consists essentially of the process

$$\nu_{R_1} \rightarrow \begin{cases} \nu_L + \phi \\ \overline{\nu_L} + \phi \end{cases} , \tag{5.1}$$

* Department of Physics and Astronomy, University of Aarhus, Ny Munkegade, DK-8000 Aarhus C, Denmark. E-mail: andersb@phys.au.dk.

† Department of Physics and Astronomy, University of Aarhus, Ny Munkegade, DK-8000 Aarhus C, Denmark, Max-Planck-Institut für Physik (Werner-Heisenberg-Institut), Föhringer Ring 6, D-80805 München, Germany. E-mail: sth@phys.dk.

where ν_L is a light, left-handed neutrino and ϕ the Higgs doublet. All light flavours behave identically, so one can think of the other light flavours as included as a factor of 3 in the decay rate. Because of loop corrections there can be CP violation in the decay, usually quantified by the asymmetry parameter ϵ. In the following we denote the heavy neutrino by R, the light by L, and the Higgs by H.

This model has been studied extensively in the literature, including deviations from the hierarchical limit, thermal corrections etc [3–19]. However, all studies have used the integrated Boltzmann equation to follow the evolution of the heavy neutrino number density and the lepton asymmetry. This approach assumes Maxwell-Boltzmann statistics for all particles as well as kinetic equilibrium for the heavy species. This assumption is normally justified in freeze-out calculations where elastic scattering is assumed to be much faster than inelastic reactions. However, in the present context kinetic equilibrium in the heavy species would have to be maintained by the decays and inverse decays alone. Therefore it is not obvious that the integrated Boltzmann equation is always a good approximation. Furthermore $1 \leftrightarrow 2$ processes are generally inefficient for thermalization compared with $2 \leftrightarrow 2$ processes. For $2 \leftrightarrow 2$ deviations from kinetic equilibrium are always of order 20% or less [20], but for $1 \leftrightarrow 2$ processes they can be very large (see for instance Refs. [21–24] for a case where deviation from equilibrium is extremely large).

In this paper we investigate how the use of the full Boltzmann equation affects the final lepton asymmetry in a simplified model with only decays and inverse decays and resonant scattering. We will return to the point of resonant scattering in due course. We find that when $T \sim m_R$ the difference can be very large. However, at small temperature where the inverse decay dominates the difference decreases in magnitude to about 20%.

5.2 The Boltzmann equation

Here we study only the two-body decay of a heavy right-handed neutrino to a light neutrino plus a Higgs. We do not include thermal corrections to the particle masses, so that for instance the process $H \to LR$ is not kinematically possible. We assume that the asymmetry, represented by

$$\epsilon = -\frac{\Gamma - \bar{\Gamma}}{\Gamma + \bar{\Gamma}} \tag{5.2}$$

is small, so that when we calculate anything with R, we can assume identical distributions of L and $\bar{L}$. $\Gamma, \bar{\Gamma}$ are the decay rates from R to particles and antiparticles, respectively. We consider only initial zero abundance of R. We use only single particle distribution functions, in which case the Boltzmann equation for the heavy species can be written as [4, 25]

$$\frac{\partial f_R}{\partial t} - pH\frac{\partial f_R}{\partial p} = \frac{1}{2E_R}\int \frac{d^3p_L}{2E_L(2\pi)^3}\frac{d^3p_H}{2E_H(2\pi)^3}(2\pi)^4\delta^4(p_R - p_L - p_H) \times \left[f_H f_L(1-f_R)(|M_{HL\to R}|^2 + |M_{H\bar{L}\to R}|^2) - f_R(1-f_L)(1+f_H)(|M_{R\to HL}|^2 + |M_{R\to H\bar{L}}|^2)\right], \quad (5.3)$$

and for the light neutrino it is

$$\frac{\partial f_L}{\partial t} - pH\frac{\partial f_L}{\partial p} = \frac{1}{2E_L}\int \frac{d^3p_R}{2E_R(2\pi)^3}\frac{d^3p_H}{2E_H(2\pi)^3}(2\pi)^4\delta^4(p_R - p_L - p_H) \times \left[-f_H f_L(1-f_R)|M_{HL\to R}|^2 + f_R(1-f_L)(1+f_H)|M_{R\to HL}|^2\right], \quad (5.4)$$

with a similar equation for $\bar{L}$. The interesting Boltzmann equations for the present purpose are those for R and for $B-L$. H and $L, \bar{L}$ have gauge interactions which are very fast. This means that H can be described by a distribution in chemical equilibrium, and that $L, \bar{L}$ can be described as distributions in kinetic equilibrium,

$$f_H = (-1 + e^{p_R/T})^{-1} \quad (5.5)$$
$$f_L = (1 + e^{(p_L-\mu)/T})^{-1} \quad (5.6)$$
$$f_{\bar{L}} = (1 + e^{(p_{\bar{L}}+\mu)/T})^{-1}, \quad (5.7)$$

with $\mu/T = 3(n_L - n_{\bar{L}})/T^3 + \mathcal{O}((\mu/T)^3)$.

Using CPT-invariance, following the idea of [25], we find

$$|M_{R\to HL}|^2 = |M_{H\bar{L}\to R}|^2 = M_0(1-\epsilon)$$
$$|M_{R\to H\bar{L}}|^2 = |M_{HL\to R}|^2 = M_0(1+\epsilon) \quad (5.8)$$

where M_0 is the average of the 2 (absolute matrix squared) elements. This simplifies the Boltzmann equations.

For the heavy neutrino the Boltzmann equation can be simplified to [22]

$$\frac{\partial f_R}{\partial t} - pH\frac{\partial f_R}{\partial p} = \frac{m_R\Gamma_{\rm tot}}{E_R p_R}\int_{(E_R-p_R)/2}^{(E_R+p_R)/2} dp_H\left[f_H f_L(1-f_R) - f_R(1-f_L)(1+f_H)\right], \quad (5.9)$$

where $\Gamma_{\rm tot} = \Gamma_{R\to LH} + \Gamma_{R\to\bar{L}H} = \Gamma + \bar{\Gamma}$ is the total rest frame decay rate. The corresponding equation for $L - \bar{L}$ [1] is

$$\frac{\partial(f_L - f_{\bar{L}})}{\partial t} - pH\frac{\partial(f_L - f_{\bar{L}})}{\partial p} = -\frac{m_R\Gamma}{E_L p_L}\int_{\frac{m_R^2}{4p_L}+p_L}^{\infty} dE_R\left[(f_H + f_R)F^- + \epsilon\Big(-2(1+f_H)f_R + (f_R - f_H(1-2f_R))F^+\Big)\right], \quad (5.10)\ (5.11)$$

[1] Note that we ignore the sphaleron L to B conversion during the decay process because we track only $L - \bar{L}$. Including it would have only a modest effect on our numerical results.

to first order in ϵ and with

$$F^+ = f_L + f_{\bar{L}} = \frac{2}{1+e^{p/T}} + \mathcal{O}((\mu/T)^2) \tag{5.12}$$

$$F^- = f_L - f_{\bar{L}} = \frac{2e^{p/T}}{(1+e^{p/T})^2}\frac{\mu}{T} + \mathcal{O}((\mu/T)^3) \tag{5.13}$$

$$\tag{5.14}$$

Since we have so far only included $2 \leftrightarrow 1$ processes, Eq. 5.11 suffers from the well-known problem of lepton asymmetry generation even in equilibrium [25]. To remedy this problem the resonant part of the $LH \leftrightarrow \bar{L}H$ must be included. To lowest order in ϵ this amounts to adding the term $2\epsilon(1-f_R)f_H F^+$ in Eq. 5.11 [10], so that the final form of the equation for the lepton asymmetry is

$$\begin{aligned} \frac{\partial(f_L - f_{\bar{L}})}{\partial t} &- pH\frac{\partial(f_L - f_{\bar{L}})}{\partial p} \\ &= -\frac{m_R\Gamma}{E_L p_L}\int_{\frac{m_R^2}{4p_L}+p_L}^{\infty} dE_R \left[(f_H+f_R)(F^- + \epsilon F^+) - 2\epsilon f_R(1+f_H)\right], \end{aligned} \tag{5.15}$$

This equation does not exhibit any lepton asymmetry generating behaviour in thermal equilibrium because $[(f_H+f_R)(F^-+\epsilon F^+) - 2\epsilon f_R(1+f_H)] = 0$ explicitly.

To first order in μ/T equations Eq. 5.10 and 5.16 can be easily integrated numerically for given values of m_R and Γ. If Maxwell-Boltzmann statistics and kinetic equilibrium for R are assumed the equations can be further simplified. The integrated Boltzmann equations are then

$$\dot{n}_R + 3Hn_R = -\langle\Gamma\rangle(n_R - n_{R,\mathrm{eq}}) \tag{5.16}$$

$$\dot{n}_{L-\bar{L}} + 3Hn_{L-\bar{L}} = \epsilon\langle\Gamma\rangle(n_R - n_{R,\mathrm{eq}}) + n_{L-\bar{L}}\frac{\Gamma}{4}\mathcal{K}_1(m_R/T)\frac{m_R^2}{T^2}, \tag{5.17}$$

where $z \equiv \frac{m_R}{T}$ and $\langle\Gamma\rangle = (\Gamma+\bar{\Gamma})\mathcal{K}_1(z)/\mathcal{K}_2(z)$ is the thermally averaged total decay rate.

These equations are the ones normally used in leptogenesis calculations for the simplest case of one massive and one light neutrino. However, compared with Eqs. (5.10-5.16) they involve the approximation of assuming Maxwell-Boltzmann statistics and kinetic equilibrium. Particularly for the case where $\Gamma/H(T=m_R) \sim 1$ this approximation is not necessarily good.

When decays and inverse decays are included (as well as gauge interactions of L and H which establish kinetic equilibrium for $L, \bar{L}$, and H individually, but which conserve $L-\bar{L}$) there are essentially only two interesting parameters. All terms that contribute to the development of densities are proportional to either H or Γ. This competition can be parameterised by the single parameter $K = \Gamma/H(T=m_R)$, the decay parameter. The other important parameter is the net decay asymmetry ϵ.

In the present study we assume that the heavy neutrinos start with zero abundance, i.e. that they are not equilibrated at high temperatures through

other interactions. We refer the reader to [10] for a thorough discussion of the various possibilities for initial R abundance.

When solving the Boltzmann equations we make a number of standard assumptions. While these assumptions are generic to almost all studies of leptogenesis they can in principle have an impact on our numerical results.

We assume instantaneous conversion by sphaleron processes. Relaxing this assumption could be done by including a further set of Boltzmann equations to track these processes directly. However, the approximation does not affect our main result result, i.e. the difference between using the full and the integrated Boltzmann equations.

We also assume zero chemical potential for all other particles than the leptons. This can have some influence on the results (see e.g. [7]).

Finally, we neglect elastic scattering processes apart from the resonant part of the $2 \leftrightarrow 2$ process. In the simplest thermal leptogenesis scenario this is justified for $K \gtrsim 1$, but not for $K \ll 1$. In more realistic models the approximation is not necessarily valid (see e.g. [9]).

In Figs. 1-3 we show a calculation of n_R and the net asymmetry for different values of K. At high temperatures the equilibration rate of R is much higher when the full Boltzmann equation is used. The main reason for this can be seen in Fig. 4. When $z < 1$ the low momentum states of R are populated very efficiently, while there is little population of high momentum modes. This in turn means that the inverse decay $HL \to R$ is suppressed relative to the decay process $R \to HL$.

To quantify this, we want to define a momentum dependant inverse decay rate,

$$\Gamma(p_R) \equiv \frac{1}{f_{R,eq}(p_R)} \frac{df_R}{dt}|_{p=p_R} \tag{5.18}$$

The efficiency with which R states with momentum p_R are produced from the background (ignoring decays and Pauli Blocking) is then given by

$$\begin{aligned} \frac{\Gamma(p_R)}{H} &= \frac{1}{f_{R,eq} H} \frac{df_R}{dt} = \frac{m_R \Gamma}{f_{R,eq} H E_R p_R} \int_{(E_R - p_R)/2}^{(E_R + p_R)/2} dp_H f_H f_L. \\ &= \frac{m_R T \Gamma}{H p_R E_R} \log \left[\sinh\left((E_R + p_R)/2T\right) / \sinh\left((E_R - p_R)/2T\right) \right]. \end{aligned} \tag{5.19}$$

This function is sharply peaked at low momentum with the following limiting behaviour

$$\frac{\Gamma(p_R)}{H} \to \begin{cases} \frac{\Gamma}{H} \coth(m_R/2T) \propto z^2 \coth(z/2) & p_R \to 0 \\ \frac{\Gamma m_R}{H p_R^2} \left(p_R + T \log\left(\frac{2 p_R T}{m_R^2} \right) \right) & p_R \to \infty \end{cases}. \tag{5.20}$$

This is a steeply increasing function of z and at low temperatures when $T << m_R$ the distribution of R is in complete equilibrium and $f_R << 1$ so that the Boltzmann approximation is valid. Therefore the curves for $n_R/n_{\rm eq}$ approach each other in Figs. 1-3. Note, however, that the highest p_R modes are always out of equilibrium because of the asymptotic $1/p_R$ term. In fact for given values of z and K there will be a limiting value of p_R above which the distribution

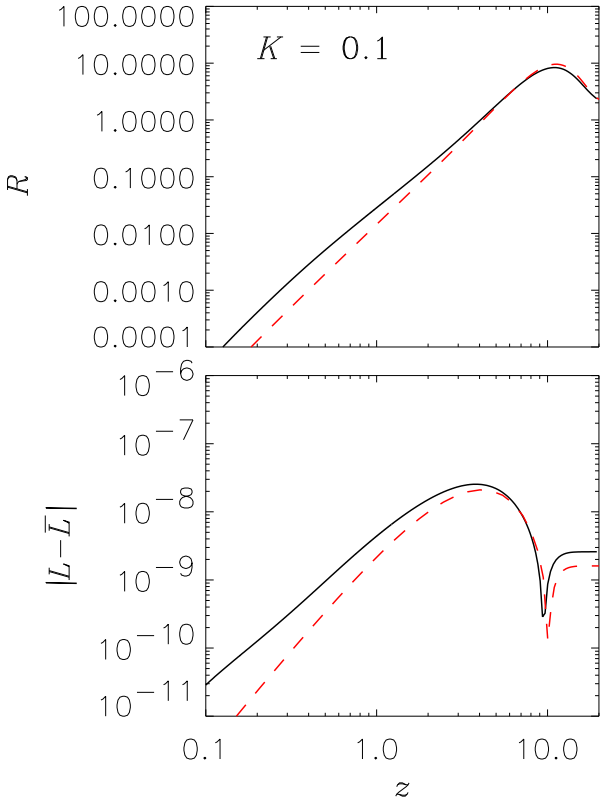

Fig. 5.1: Upper panel: The evolution of $n_R/n_{\rm eq}$ for the full (solid line) and integrated (dotted line) Boltzmann equations. Bottom panel: The evolution of $|n_{L-\bar{L}}|/T^3$ for the same cases. The calculation is for $K = 0.1$ and $\epsilon = 10^{-6}$.

will be out of equilibrium. In Fig. 5 we show the value of p_R/T for which $\Gamma(p_R)/H = 1$ as a function of z, for the specific case of $K = 1$. At high temperatures no momentum states are in equilibrium, whereas at low temperatures only progressively higher momentum states are out of equilibrium. This figure corresponds well to what is shown in Fig. 4. For $z = 0.2$ no states are in equilibrium, for $z = 1$ states above $p_R/T \sim 1$ are not yet in equilibrium, and for $z = 5$ almost all states have been populated to their equilibrium value.

As can be seen in Figs. 1-3 the net asymmetry also grows much more rapidly initially when the full Boltzmann equation is used, and the change of sign occurs at higher temperature. However, at low temperatures the differences are smaller.

In Fig. 6 we show the ratio of the final asymmetry in the two cases

$$\frac{\eta_{\rm full}}{\eta_{\rm int}} = \frac{(n_L - n_{\bar{L}})/n_\gamma|_{\rm full}}{(n_L - n_{\bar{L}})/n_\gamma|_{\rm int}} \tag{5.21}$$

As can be seen from Fig. 6 there can be a significant difference in the asymmetry between the two approaches. For very high values of K the difference is small because the distribution is kept very close to kinetic equilibrium (for a Fermi-Dirac distribution) throughout the decay. Note, however, that the

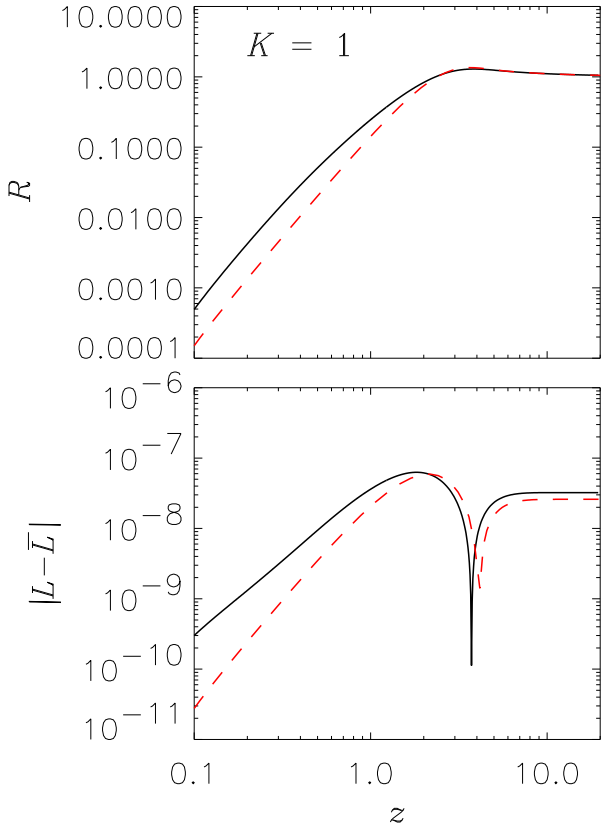

Fig. 5.2: Upper panel: The evolution of $n_R/n_{\rm eq}$ for the full (solid line) and integrated (dotted line) Boltzmann equations. Bottom panel: The evolution of $|n_{L-\bar{L}}|/T^3$ for the same cases. The calculation is for $K = 1$ and $\epsilon = 10^{-6}$.

difference never goes to zero. The reason is that the thermal decay width is changed relative to the Maxwell-Boltzmann approximation when Pauli blocking and stimulated emission factors are included (as also noted by [10]). For smaller values of K the difference increases and can be as large as 50%. However, it should be noted that our framework will break down for small values of K because we have not included scattering.

Another important point to note is that $\eta_{\rm full}/\eta_{\rm int}$ does not depend on ϵ because the deviation from kinetic equilibrium is governed completely by the total decay rate (i.e. by K), not by the asymmetry, as long as $\epsilon << 1$.

We are only interested in the final value of the asymmetry since, in order to maximise the baryon asymmetry for any given value of ϵ, we want leptogenesis to end before the conversion through sphalerons end.

5.3 Discussion

We have solved the full Boltzmann equation for decays and inverse decays to follow the generation of lepton asymmetry during leptogenesis. When decays are semi-relativistic the difference between using the full Boltzmann equation

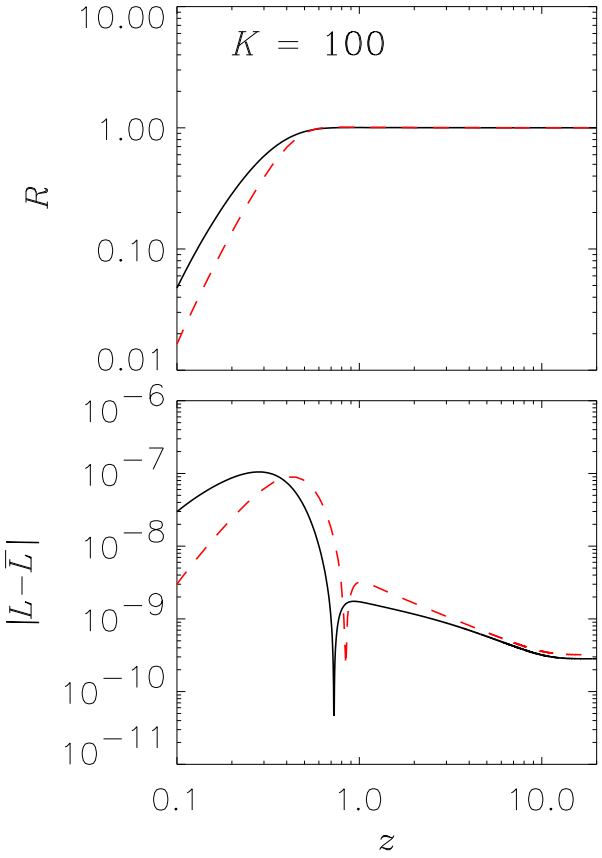

Fig. 5.3: Upper panel: The evolution of $n_R/n_{\rm eq}$ for the full (solid line) and integrated (dotted line) Boltzmann equations. Bottom panel: The evolution of $|n_{L-\bar{L}}/T^3|$ for the same cases. The calculation is for $K = 100$ and $\epsilon = 10^{-6}$.

and the standard integrated Boltzmann equation can be very large. However, at low temperature where washout dominates the difference is relatively modest.

The difference at $K \gtrsim 1$ is less than about 30% between the two approaches. For smaller K the difference can be larger. However, this is the regime where $1 \leftrightarrow 2$ processes do not dominate, i.e. outside the regime in which our framework is valid.

The conclusion is that the Boltzmann approximation yields results in the strong washout regime which are accurate to at least 30%. For $K > 5$ the difference is not larger than 15%.

Acknowledgments

SH acknowledges support from the Alexander von Humboldt Foundation through a Friedrich Wilhelm Bessel Award. We thank Pasquale Di Bari and Alessandro

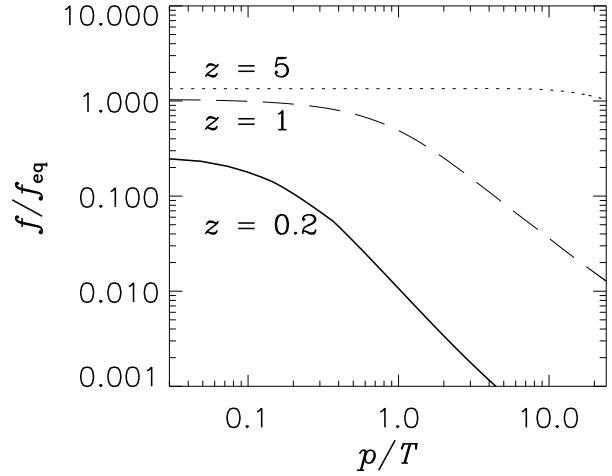

Fig. 5.4: The distribution function of R relative to a chemical equilibrium Fermi-Dirac distribution with the same temperature for different values of z. The calculation is for $K = 1$.

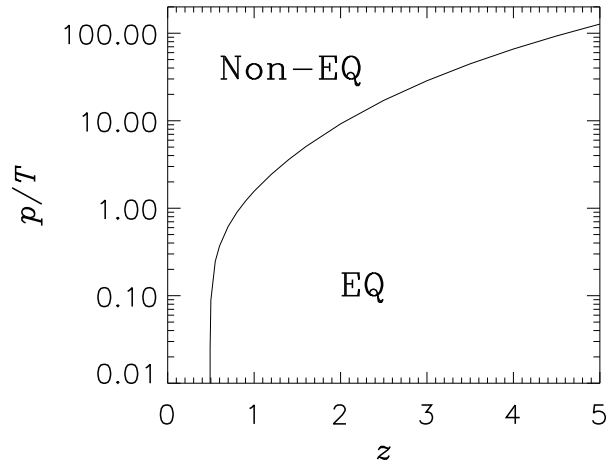

Fig. 5.5: The dividing line between equilibrium and non-equilibrium for $K = 1$. All momentum states above the line are out of equilibrium.

Strumia for valuable comments.

References

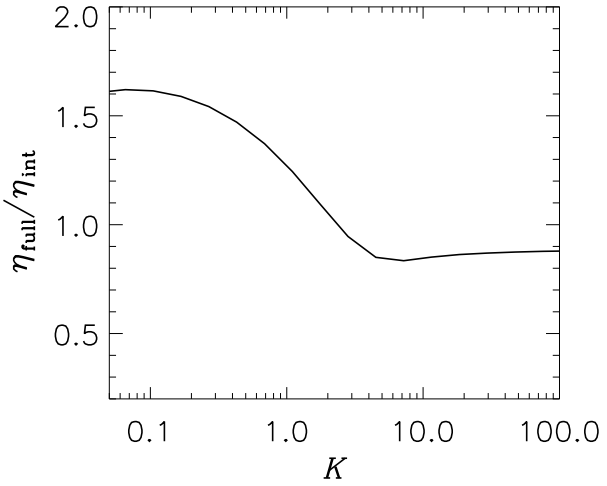

Fig. 5.6: The difference between the asymmetry in the full case and the integrated case as a function of K.

BIBLIOGRAPHY

[1] M. Fukugita and T. Yanagida, "Baryogenesis Without Grand Unification," Phys. Lett. B **174**, 45 (1986).

[2] V. Kuzmin, V.A. Rubakov and M.E. Shaposhnikov, "On anomalous electroweak baryon-number non-conservation in the early uiniverse," Phys. Lett. **155B**, 36-42 (1985).

[3] W. Buchmuller, P. Di Bari and M. Plumacher, "Leptogenesis for pedestrians," Annals Phys. **315**, 305 (2005) [arXiv:hep-ph/0401240].

[4] M. A. Luty, "Baryogenesis Via Leptogenesis," Phys. Rev. D **45**, 455 (1992).

[5] T. Hambye, Y. Lin, A. Notari, M. Papucci and A. Strumia, "Constraints on neutrino masses from leptogenesis models," Nucl. Phys. B **695**, 169 (2004) [arXiv:hep-ph/0312203].

[6] W. Buchmuller, P. Di Bari and M. Plumacher, "The neutrino mass window for baryogenesis," Nucl. Phys. B **665**, 445 (2003) [arXiv:hep-ph/0302092].

[7] W. Buchmuller and M. Plumacher, Phys. Lett. B **511**, 74 (2001) [arXiv:hep-ph/0104189].

[8] W. Buchmuller and M. Plumacher, "Neutrino masses and the baryon asymmetry," Int. J. Mod. Phys. A **15**, 5047 (2000) [arXiv:hep-ph/0007176].

[9] M. Plumacher, Z. Phys. C **74**, 549 (1997) [arXiv:hep-ph/9604229].

[10] G. F. Giudice, A. Notari, M. Raidal, A. Riotto and A. Strumia, "Towards a complete theory of thermal leptogenesis in the SM and MSSM," Nucl. Phys. B **685**, 89 (2004) [arXiv:hep-ph/0310123].

[11] G. F. Giudice, M. Peloso, A. Riotto and I. Tkachev, "Production of massive fermions at preheating and leptogenesis," JHEP **9908**, 014 (1999) [arXiv:hep-ph/9905242].

[12] M. Hirsch, M. Malinsky, J. C. Romao, U. Sarkar and J. W. F. Valle, "Thermal leptogenesis in extended supersymmetric seesaw," arXiv:hep-ph/0608006.

[13] S. Blanchet and P. Di Bari, "Leptogenesis beyond the limit of hierarchical heavy neutrino masses," JCAP **0606**, 023 (2006) [arXiv:hep-ph/0603107].

[14] S. Blanchet and P. Di Bari, "Flavor effects on leptogenesis predictions," arXiv:hep-ph/0607330.

[15] A. Abada, S. Davidson, A. Ibarra, F. X. Josse-Michaux, M. Losada and A. Riotto, "Flavour matters in leptogenesis," arXiv:hep-ph/0605281.

[16] T. Ota and W. Rodejohann, "Breaking of L(mu) - L(tau) flavor symmetry, lepton flavor violation and leptogenesis," Phys. Lett. B **639**, 322 (2006) [arXiv:hep-ph/0605231].

[17] E. Nardi, Y. Nir, E. Roulet and J. Racker, "The importance of flavor in leptogenesis," JHEP **0601**, 164 (2006) [arXiv:hep-ph/0601084].

[18] A. Abada, S. Davidson, F. X. Josse-Michaux, M. Losada and A. Riotto, "Flavour issues in leptogenesis," JCAP **0604**, 004 (2006) [arXiv:hep-ph/0601083].

[19] T. Hambye, M. Raidal and A. Strumia, "Efficiency and maximal CP-asymmetry of scalar triplet leptogenesis," Phys. Lett. B **632**, 667 (2006) [arXiv:hep-ph/0510008].

[20] S. Hannestad, "Non-equilibrium effects on particle freeze-out in the early universe," New Astron. **4**, 207 (1999) [arXiv:astro-ph/9903034].

[21] J. Madsen, "Bose Condensates, Big Bang Nucleosynthesis, And Cosmological Decay Of A Phys. Rev. Lett. **69**, 571 (1992).

[22] G. D. Starkman, N. Kaiser and R. A. Malaney, "Mixed dark matter from neutrino lasing," Astrophys. J. **434**, 12 (1994) [arXiv:astro-ph/9312020].

[23] N. Kaiser, R. A. Malaney and G. D. Starkman, "Neutrino lasing in the early universe," Phys. Rev. Lett. **71**, 1128 (1993) [arXiv:hep-ph/9302261].

[24] S. Hannestad and J. Madsen, "A cosmological three level neutrino laser," Phys. Rev. D **55**, 4571 (1997) [arXiv:astro-ph/9702125].

[25] E. W. Kolb and S. Wolfram, "Baryon Number Generation In The Early Universe," Nucl. Phys. B **172**, 224 (1980) [Erratum-ibid. B **195**, 542 (1982)].

6

Nonperturbative flat direction decay

The paper *Nonperturbative flat direction decay* presented in this chapter has been published by Physical Review D [24].

[24] A. Basbøll, D. Maybury, F. Riva and S. M. West: Nonperturbative flat direction decay, Phys. Rev. D **76**, 065005 (2007).

This is the latest version from arXiv.org. References have been added compared to the printed version.

Non-Perturbative Flat Direction Decay

Anders Basbøll* David Maybury† Francesco Riva‡
Stephen M West§

Abstract

We argue that supersymmetric flat direction vacuum expectation values can decay non-perturbatively via preheating. Considering a toy $U(1)$ gauge theory, we explicitly calculate the scalar potential, in the unitary gauge, for excitations around several flat directions. We show that the mass matrix for the excitations has non-diagonal entries which vary with the phase of the flat direction vacuum expectation value. Furthermore, this mass matrix has zero eigenvalues whose eigenstates change with time. We show that these light degrees of freedom are produced copiously in the non-perturbative decay of the flat direction vacuum expectation value.

6.1 Introduction

The scalar potential of the Minimal Supersymmetric Standard Model (MSSM) possesses a large number of F- and D-flat directions along which the scalar potential nearly vanishes [1, 2]. These flat directions can have important cosmological consequences, including the generation of the baryon asymmetry of the Universe through the out-of-equilibrium CP violating decay of coherent field oscillations along the flat directions themselves [3–7].

Recently, much interest has focused on the cosmological fate of flat direction vacuum expectation values (vev)s. In particular, it has been argued [8] that in realistic supersymmetric models, large flat direction vevs can persist long enough to delay thermalization after inflation and therefore lead to low reheat temperatures. Furthermore, it has also been asserted [9] that large flat direction vevs can prevent non-perturbative parametric resonant decay (preheating) of the inflaton since the inflaton decay products become sufficiently massive preventing preheating from ever becoming efficient. These arguments hold so long as the flat direction vevs do not rapidly decay – they must persist long enough so that they can delay thermalization and block inflaton preheating. In [10] it

* Department of Physics and Astronomy, University of Aarhus, Ny Munkegade, DK-8000 Aarhus C, Denmark. E-mail: andersb@phys.au.dk.

† Rudolf Peierls Centre for Theoretical Physics, University of Oxford, 1 Keble Rd., Oxford OX1 3NP, UK. E-mail: d.maybury1@physics.ox.ac.uk.

‡ Rudolf Peierls Centre for Theoretical Physics, University of Oxford, 1 Keble Rd., Oxford OX1 3NP, UK. E-mail: f.riva1@physics.ox.ac.uk.

§ Rudolf Peierls Centre for Theoretical Physics, University of Oxford, 1 Keble Rd., Oxford OX1 3NP, UK. E-mail: s.west1@physics.ox.ac.uk.

was claimed that non-perturbative decay can lead to a rapid depletion of the flat direction condensate and thus precludes the delay of thermalization after inflation. It was also concluded that in order for the flat direction to decay non-perturbatively the system requires more than one flat direction [10,11]. Finally, in [11] it was pointed out that even in the presence of multiple flat directions, some degree of fine-tuning was necessary to achieve flat direction decay.

An important aspect of this discussion centers on the issue of Nambu-Goldstone (NG) bosons. In general, supersymmetric flat directions are charged under the gauge group of the MSSM. Consequently, the flat direction vev will break some or all of the gauge symmetries of the theory and thus we expect the presence of the associated NG bosons. In calculating non-perturbative flat direction decays, [10] considers a gauged $U(1)$ model and constructs the mixing matrix for the excitations around the flat direction vev. The results in [10] show that in the single flat direction case, non-perturbative decay proceeds solely via a massless NG mode as only the NG mode mixes with the Higgs and all other massless moduli remain decoupled. Since the NG boson represents an unphysical gauge degree of freedom, it was concluded [10,11] that no preheating occurs in the single flat direction case. As the appearance of a massless NG boson in the spectrum is a gauge dependent artifact, it remains unclear if the conclusions drawn about the system hold in the unitary gauge. In order to determine if flat direction vevs decay non-perturbatively into scalar degrees of freedom, the effect of the NG boson mixing in the scalar potential must first be removed. The process of removing the NG modes by switching to the unitary gauge changes the form of the mixing matrix among the left over scalar degrees of freedom.

In this letter we consider toy models to demonstrate that, in the unitary gauge, the mixing matrix of the excitations around a flat direction vev permits preheating. Moreover, we find that flat direction decay depends on the *number of dynamical, physical phases* appearing in the flat direction vev. Specifically, a physical phase difference between two of the individual field vevs making up the flat direction is needed.

The outline of the rest of this letter proceeds as follows: first we explicitly construct – in the unitary gauge – the mass squared matrix arising from the D-terms of a toy gauged $U(1)$ model with three charged chiral superfields. We then present the formalism of preheating with multi-component fields and show that preheating occurs for the light moduli associated with the flat direction. We then analyze the specific dynamics of the background field equations for the toy models examined. Finally we evolve the background field equations for one of the toy models to obtain quantitative results.

6.2 Toy Model with a gauged $U(1)$ Symmetry.

As an example, we examine a toy model which demonstrates the important features of supersymmetric flat direction vev decay. We introduce three complex superfields[1] , Φ_1, Φ_2 and Φ_3 charged under a $U(1)$ gauge group with charges

[1] We use Φ to denote both superfields and scalar components of superfields.

$q_1 = +1/2$, $q_2 = -1$ and $q_3 = +1/2$ respectively. The Lagrangian reads

$$\mathcal{L} = \sum_{i=1}^{3} \frac{1}{2}|D_\mu \Phi_i|^2 - V - \frac{1}{4}F_{\mu\nu}^2, \tag{6.1}$$

where $D_\mu = \partial_\mu - iq_i A_\mu$ denotes the covariant derivative. The potential we consider arises from the supersymmetric D-terms and has the form

$$V = \frac{g^2}{2}(q_1 |\Phi_1|^2 + q_2 |\Phi_2|^2 + q_3 |\Phi_3|^2)^2, \tag{6.2}$$

where g is the gauge coupling of the $U(1)$ gauge symmetry. In the above, we have neglected contributions from supersymmetry (SUSY) breaking and from any non-renormalisable terms arising from the superpotential. These contributions are highly model-dependent and cloud the analysis we wish to present. A fully realistic model must include these additional contributions which can significantly affect the resulting particle production. The effects we investigate here do not depend on their inclusion in the quadratic part of the potential and so for clarity we neglect them[2].

The potential in eq.6.2 admits several flat directions. Choosing one particular direction and including excitations around the vev we can write

$$\begin{aligned} \Phi_1 &= (\varphi + \xi_1)e^{i(\sigma_1 + \frac{\theta_1}{\varphi})}, \\ \Phi_2 &= (\varphi + \xi_2)e^{i(\sigma_2 + \frac{\theta_2}{\varphi})}, \\ \Phi_3 &= (\varphi + \xi_3)e^{i(\sigma_3 + \frac{\theta_3}{\varphi})}, \end{aligned} \tag{6.3}$$

where $\sigma_{1,2,3}$ represent time dependent phases of the vevs, φ denotes the vev's time dependent amplitude[3] while $\xi_{1,2,3}$ and $\theta_{1,2,3}$ parameterize the six real scalar degrees of freedom corresponding to the excitations around the vevs. Note that the flat direction vev breaks the $U(1)$ gauge symmetry. Thus, out of the six real scalar degrees of freedom we expect one massive Higgs field and one massless NG boson, leaving four massless scalar degrees of freedom.

The kinetic terms for the scalar fields play an important role in this analysis. Their expansion in eq.6.1 includes the term

$$\mathcal{L} \supset -\varphi^2 A_0(\dot{\sigma_1} - 2\dot{\sigma_2} + \dot{\sigma_3}) \tag{6.4}$$

which has the form of a coupling between the gauge field and the background condensate. Terms of this type will feed into the equations of motion for the gauge field which, in turn, will have an effect on the equations of motion for the scalar excitations. By making a $U(1)$ gauge transformation on the vev of the form

$$\langle \Phi_i \rangle \to \langle \Phi_i' \rangle = e^{iq_i\lambda} \langle \Phi_i \rangle \tag{6.5}$$

[2] SUSY breaking terms are needed for the computation of the evolution of the flat direction vev.

[3] Throughout this analysis we assume $\dot{\varphi} \ll \varphi\dot{\sigma}$.

with

$$\lambda = \frac{2\sigma_2 - \sigma_1 - \sigma_3}{3}, \tag{6.6}$$

we can gauge this term away and avoid a complicated analysis of the kinetic terms. The resulting form of the vev reads

$$\begin{aligned} \langle \Phi_1 \rangle &= \varphi e^{i(\sigma+\gamma)}, \\ \langle \Phi_2 \rangle &= \varphi e^{i\sigma}, \\ \langle \Phi_3 \rangle &= \varphi e^{i(\sigma-\gamma)}, \end{aligned} \tag{6.7}$$

where $\gamma = (\sigma_1 - \sigma_3)/2$ and $\sigma = (\sigma_1 + \sigma_2 + \sigma_3)/3$ represent the two remaining independent physical phases. Following Kibble [12], we can write the fields in the unitary gauge as

$$\begin{aligned} \Phi_1 &= (\varphi + \xi_1) e^{i(\sigma+\gamma+\frac{\theta}{\varphi\sqrt{2}}+\frac{\theta'}{\varphi\sqrt{3}})}, \\ \Phi_2 &= (\varphi + \xi_2) e^{i(\sigma+\frac{\theta'}{\varphi\sqrt{3}})}, \\ \Phi_3 &= (\varphi + \xi_3) e^{i(\sigma-\gamma-\frac{\theta}{\varphi\sqrt{2}}+\frac{\theta'}{\varphi\sqrt{3}})}, \end{aligned} \tag{6.8}$$

where $\xi_{1,2,3}$, θ and θ' denote the physical excitations – the NG boson has been removed[4]. We choose the particular combination of field excitations appearing in eq.6.8 (the exponent in particular) in order to retain canonically normalised kinetic terms.

On substituting the fields of eq.6.8 into the Lagrangian given in eq.6.1 and defining the vector $\Xi \equiv (\xi_1, \xi_2, \xi_3, \theta, \theta')^T$, we find the quadratic terms

$$\mathcal{L} \supset \frac{1}{2}|\partial_\mu \Xi|^2 - \frac{1}{2}\Xi^T \mathcal{M}^2 \Xi + \frac{1}{2}\dot{\Xi}^T U \Xi + ... \tag{6.9}$$

where the ellipses denote higher order terms and interactions. The matrix U given in the last term in eq.6.9 reads

$$U = \begin{pmatrix} 0 & 0 & 0 & \frac{\dot\sigma+\dot\gamma}{\sqrt{2}} & \frac{\dot\sigma+\dot\gamma}{\sqrt{3}} \\ 0 & 0 & 0 & 0 & \frac{\dot\sigma}{\sqrt{3}} \\ 0 & 0 & 0 & \frac{-\dot\sigma+\dot\gamma}{\sqrt{2}} & \frac{\dot\sigma-\dot\gamma}{\sqrt{3}} \\ -\frac{\dot\sigma+\dot\gamma}{\sqrt{2}} & 0 & \frac{\dot\sigma-\dot\gamma}{\sqrt{2}} & 0 & 0 \\ -\frac{\dot\sigma+\dot\gamma}{\sqrt{3}} & -\frac{\dot\sigma}{\sqrt{3}} & \frac{-\dot\sigma+\dot\gamma}{\sqrt{2}} & 0 & 0 \end{pmatrix} \tag{6.10}$$

while the mass matrix for the physical excitations appears as

$$\mathcal{M}^2 = (g\varphi)^2 \begin{pmatrix} 1 & -2 & 1 & 0 & 0 \\ -2 & 4 & -2 & 0 & 0 \\ 1 & -2 & 1 & 0 & 0 \\ 0 & 0 & 0 & 0 & 0 \\ 0 & 0 & 0 & 0 & 0 \end{pmatrix} = B\mathcal{M}_d^2 B^T \tag{6.11}$$

[4] This can be verified by expanding out the scalar kinetic terms which reveals the absence of terms of the form $A_\mu \partial^\mu(...)$.

with eigenvalues $M_1^2 = 6(g\varphi)^2$, $M_2^2 = M_3^2 = M_4^2 = M_5^2 = 0$ (the entries of the diagonal matrix $\mathcal{M}_d$). B is an orthogonal matrix which diagonalizes $\mathcal{M}^2$ and M_1 corresponds to the mass of the physical Higgs field associated with the spontaneous breaking of the $U(1)$ symmetry. The four zero eigenvalues correspond to the massless excitations around the flat direction vev.

The last term in eq.6.9 appears as a consequence of the time-dependence of the background – it represents a mixing between the fields $\xi_{1,2,3}$, θ, θ' and their time-derivatives. The effect of these terms on the system becomes clear if we make field redefinitions that remove the mixed derivative terms. The resulting transformation leaves the system in an inertial frame in field space and leads to a time-dependent mass matrix. Defining $\Xi' = A\Xi$ (A is orthogonal), we find the condition that A must satisfy, in order for all the mixed derivative terms to cancel, to be

$$\dot{A}^T A = U. \tag{6.12}$$

The Lagrangian for the Ξ' system now reads

$$\mathcal{L} \supset \frac{1}{2}|\partial_\mu \Xi'|^2 - \frac{1}{2}\Xi'^T \mathcal{M}'^2 \Xi' \tag{6.13}$$

where $\mathcal{M}'^2 = A\mathcal{M}^2 A^T = AB\mathcal{M}_d^2 B^T A^T = C\mathcal{M}_d^2 C^T$ and $C = AB$. The matrix C is an orthogonal time-dependent matrix, with columns corresponding to the eigenvectors of $\mathcal{M}'^2$. We now have a system of scalar fields with canonically normalized kinetic terms and time dependent eigenvectors.

The central point of this discussion centers precisely on the appearance of the *time dependent* eigenvectors for the five scalar fields. This satisfies a necessary but not sufficient condition for preheating. In the next sections, we investigate the details of the non-perturbative production of the light scalar fields following the analysis of [13].

6.3 Non-perturbative production of particles

Including gravity, the dynamics of the re-scaled conformally coupled scalar fields, $\chi_i = a\Xi'_i$, where a denotes the scale factor and Ξ'_i the i-th component of the vector Ξ', are governed by the following equations of motion (sum over repeated indices is implied),

$$\ddot{\chi}_i + \Omega_{ij}^2(t)\chi_j = 0 \tag{6.14}$$

where dots represent derivatives with respect to conformal time t, and

$$\Omega_{ij}^2 = a^2 \mathcal{M}'^2_{ij} + k^2\delta_{ij}, \tag{6.15}$$

where k labels the comoving momentum. Using an orthogonal time-dependent matrix $C(t)$, we can diagonalize Ω_{ij} via $C^T(t)\Omega^2(t)C(t) = \omega^2(t)$, giving the diagonal entries $\omega_j^2(t)$. Terms of the form $\sim \varphi\dot{\sigma}\dot{\chi}$ arising from the kinetic terms do not affect the evolution of the non-zero k quantum modes [14].

Once we have identified the basis in which the Hamiltonian appears diagonal (via the orthogonal matrix $C(t)$), the study of particle creation by the

time-varying background proceeds as in [13, 15, 16], which extends the results of [17]. Following [13], we assume that Ω_{ij} initially evolves adiabatically by assuming that the initial angular motion of the flat-direction varies slowly. This assumption allows us to define adiabatically evolving mode functions with positive and negative frequency. We rewrite the quantum fields as mode expansions in terms of the mode functions and their associated creation/annihilation operators which allows us to define the initial vacuum. During the evolution, the entries of Ω_{ij} do not necessarily change adiabatically and consequently we must find new mode functions that satisfy eq.6.14. A new set of creation/annihilation operators required to define the new vacuum can be related to the initial set using a Bogolyubov transformation with Bogolyubov coefficients α and β (which denote matrices in the multi-field case).

Initially $\alpha = \mathbb{I}$ and $\beta = 0$ while the coupled differential equations (matrix multiplication implied)

$$\begin{aligned} \dot{\alpha} &= -i\omega\alpha + \frac{\dot{\omega}}{2\omega}\beta - I\alpha - J\beta \\ \dot{\beta} &= \frac{\dot{\omega}}{2\omega}\alpha + i\omega\beta - J\alpha - I\beta \end{aligned} \tag{6.16}$$

govern the system's time evolution with the matrices I and J given by

$$I = \frac{1}{2}\left(\sqrt{\omega}\, C^T \dot{C} \frac{1}{\sqrt{\omega}} + \frac{1}{\sqrt{\omega}}\, C^T \dot{C} \sqrt{\omega}\right), \tag{6.17}$$

$$J = \frac{1}{2}\left(\sqrt{\omega}\, C^T \dot{C} \frac{1}{\sqrt{\omega}} - \frac{1}{\sqrt{\omega}}\, C^T \dot{C} \sqrt{\omega}\right). \tag{6.18}$$

Similarly to the single-field case it can be shown [13] that at any generic time the occupation number of the ith bosonic eigenstate reads

$$n_i(t) = (\beta^* \beta^T)_{ii}. \tag{6.19}$$

As pointed out in [10, 13], there exists two sources of non-adiabaticity in the multi-field scenario. The first source arises from the individual frequency time dependence and appears as the only source of non-adiabaticity in the single field case. The second source appears from the time dependence of the frequency matrix Ω_{ij} giving rise to terms in eq.6.16 proportional to I and J. This second source provides the most important contribution in our analysis and gives rise to non-perturbative particle production.

Since initially $\alpha = \mathbb{I}$ and $\beta = 0$, eq.6.16 shows that a non-vanishing matrix J is a necessary condition to obtain $\dot{\beta} \neq 0$ and hence $n_i(t) \neq 0$. In general, we have

$$C^T \dot{C} = B^T A^T \dot{A} B = -B^T U B \tag{6.20}$$

where A, B and U were defined in the previous section. For the toy $U(1)$ example outlined above, J is a 5×5 matrix in the χ_i basis with non-vanishing components

$$J_{1,2} = J_{2,1} = \frac{k - \sqrt{k^2 + M_1^2}}{2\sqrt{3k}(k^2 + M_1^2)^{1/4}} \dot{\gamma}, \tag{6.21}$$

where M_1 denotes the mass of the heavy Higgs field. These entries in the matrix J link the eigenstate of the Higgs ($i = 1$) with one of the light eigenstates ($i = 2$). We see that in the toy $U(1)$ model, preheating can occur provided that $\dot{\gamma} \neq 0$. We address this point in a later section.

6.4 Multiple VEV Amplitudes

We can extend the analysis of the previous sections by allowing the magnitudes of the individual field vevs to differ from one another. As above, we consider the case with three complex superfields charged under a $U(1)$ gauge group with charges $q_1 = +1/2$, $q_2 = -1$ and $q_3 = +1/2$ respectively, and with the scalar potential given in eq.6.2. We can write the flat direction with the following vev

$$\begin{aligned} \langle \Phi_1 \rangle &= \varphi_1 e^{i\sigma_1}, \\ \langle \Phi_2 \rangle &= \frac{1}{\sqrt{2}}(\varphi_1^2 + \varphi_2^2)^{1/2} e^{i\sigma_2}, \\ \langle \Phi_3 \rangle &= \varphi_2 e^{i\sigma_3}. \end{aligned} \tag{6.22}$$

By substituting the above into the potential given in eq.6.2, it can readily be shown that the configuration satisfies D-flatness. Expanding around this vev we have

$$\begin{aligned} \Phi_1 &= (\varphi_1 + \xi_1) e^{i\left(\sigma_1 + \frac{\theta_1}{\varphi_1}\right)}, \\ \Phi_2 &= \left(\frac{1}{\sqrt{2}}(\varphi_1^2 + \varphi_2^2)^{1/2} + \xi_2\right) e^{i\left(\sigma_2 + \frac{\sqrt{2}\theta_2}{\left(\varphi_1^2+\varphi_2^2\right)^{1/2}}\right)}, \\ \Phi_3 &= (\varphi_2 + \xi_3) e^{i\left(\sigma_3 + \frac{\theta_3}{\varphi_2}\right)}, \end{aligned} \tag{6.23}$$

where the fields $\xi_{1,2,3}$ and $\theta_{1,2,3}$ represent the excitations around the vevs. As in the previous case, we can use a gauge transformation to remove a phase from the vev structure that ensures the absence of terms of the form appearing in eq.6.4. The form of the vev in this case becomes,

$$\begin{aligned} \langle \Phi_1 \rangle &= \varphi_1 e^{i\left(\sigma + \frac{\varphi_2}{\varphi_1}\gamma\right)}, \\ \langle \Phi_2 \rangle &= \frac{1}{\sqrt{2}}(\varphi_1^2 + \varphi_2^2)^{1/2} e^{i\sigma}, \\ \langle \Phi_3 \rangle &= \varphi_2 e^{i\left(\sigma - \frac{\varphi_1}{\varphi_2}\gamma\right)}, \end{aligned} \tag{6.24}$$

where σ and γ represent two independent phases[5].

[5] Again we have applied the limit $\dot{\varphi} \ll \varphi\dot{\sigma}, \varphi\dot{\gamma}$. If we do not apply this limit the gauge transformation parameter (λ) needed to remove the linear term in A_0 can be found by integrating the coefficient of the A_0 term with respect to time. This is in general complicated and we choose to assume that φ is varying very slowly with time.

In the unitary gauge, a form that preserves the canonically normalized kinetic terms reads,

$$\begin{aligned}
\Phi_1 &= (\varphi_1+\xi_1)e^{i\left(\sigma+\frac{\varphi_2}{\varphi_1}\gamma+\frac{\theta\varphi_2+\theta'\varphi_1(2/3)^{1/2}}{\varphi_1(\varphi_1^2+\varphi_2^2)^{1/2}}\right)},\\
\Phi_2 &= \left(\frac{1}{\sqrt{2}}(\varphi_1^2+\varphi_2^2)^{1/2}+\xi_2\right)e^{i\left(\sigma+\frac{\theta'(2/3)^{1/2}}{(\varphi_1^2+\varphi_2^2)^{1/2}}\right)},\\
\Phi_3 &= (\varphi_2+\xi_3)e^{i\left(\sigma-\frac{\varphi_1}{\varphi_2}\gamma-\frac{\theta\varphi_1-\theta'\varphi_2(2/3)^{1/2}}{\varphi_2(\varphi_1^2+\varphi_2^2)^{1/2}}\right)},
\end{aligned} \tag{6.25}$$

where $\xi_{1,2,3}$, θ and θ' label the physical excitations around the vev once the NG boson has been gauged away. The resulting spectrum consists of one Higgs field with mass $M_1^2 = 3g^2(\varphi_1^2+\varphi_2^2)$, and four massless scalar fields.

We proceed, as before, by diagonalizing the kinetic terms and evaluating the J matrix given in eq.6.18. The non-vanishing entries of the J-matrix are

$$J_{1,2} = J_{2,1} = \frac{k-\sqrt{k^2+M_1^2}}{2\sqrt{3k}(k^2+M_1^2)^{1/4}}\dot{\gamma}, \tag{6.26}$$

which demonstrates that in this case preheating can take place provided that $\dot{\gamma}\neq 0$.

It is instructive to compare the two cases considered thus far. The first flat direction contained a single vev amplitude, the second contained two independent vev amplitudes. The final result, however, is the same for both cases. This demonstrates a simple property of flat direction vev decay: the determining factor is not the *number of flat directions* present in the system, but the *number of fields* that have vevs. In particular, a necessary (but not sufficient) condition for non-perturbative production of particles is the existence of at least one relative physical and dynamical phase between the field vevs that constitute the flat direction.

6.5 Dynamics of the vev phases

We now demonstrate that both physical phases are in general dynamical. In our particular toy example the cancellation of $U(1)^3$ and mixed $U(1)$-gravitational anomalies requires that we extend the field content of our model by including three additional complex superfields, Φ_4, Φ_5 and Φ_6. We assign the $U(1)$ charges and R-Parity (R_p) as follows:

	Φ_1	Φ_2	Φ_3	Φ_4	Φ_5	Φ_6
$U(1)$	1/2	-1	1/2	-1/2	1	-1/2
R_p	+	-	+	-	+	-

This choice of R_p assignments forbids the superpotential term $\Phi_1\Phi_2\Phi_3$, thus preserving F-flatness. There exist several possible flat directions for this particular field content. We assume that vevs for only Φ_1, Φ_2 and Φ_3 are turned on, leaving Φ_4, Φ_5 and Φ_6 with no vevs. With this assumption, the lowest dimension gauge invariant operators which have vevs are

$$\mathcal{O}_1 = \Phi_1\Phi_2\Phi_3, \quad \mathcal{O}_2 = \Phi_1^2\Phi_2 \quad \text{and} \quad \mathcal{O}_3 = \Phi_2\Phi_3^2. \tag{6.27}$$

Note that the last two operators depend on both physical phases, σ and γ. Using these operators, the lowest dimension terms appearing in the scalar potential, which are R_p invariant and phase-dependent, arise as soft SUSY breaking A-terms and appear as

$$V \supset \sum_{i,j} \frac{A_{ij} m_s}{M^3} \mathcal{O}_i \mathcal{O}_j + h.c., \tag{6.28}$$

where M denotes the cut off scale of the theory (e.g. the Planck mass or GUT scale), m_s represents the scale of the SUSY breaking, and A_{ij} label dimensionless coefficients of order one. Lower order phase-independent interactions will also contribute to the lifting of the flat direction and have the generic forms

$$V \supset \sum_i \frac{m_i^2}{2} |\Phi_i|^2 + \sum_{i,j} \frac{\lambda_{ij}}{8} |\Phi_i|^2 |\Phi_j|^2, \tag{6.29}$$

where m_i^2 denote the soft SUSY breaking masses, and the second terms arise from loop corrections with $\lambda_{i,j} \sim g^4 m_s^2/\varphi^2$ (see for example [3] for similar loop induced terms). The potential for the single flat direction amplitude case considered in section 6.2, using the vev form shown in eq.6.7, becomes

$$\begin{aligned} V \supset \frac{m_1^2 + m_2^2 + m_3^2}{2}\varphi^2 + \frac{\lambda'}{4}\varphi^4 + \varphi^6 \big(& A'_{11} e^{i6\sigma} + \\ & A'_{12} e^{i(6\sigma + 2\gamma)} + A'_{13} e^{i(6\sigma - 2\gamma)} + A'_{22} e^{i(6\sigma + 4\gamma)} \\ & + A'_{33} e^{i(6\sigma - 4\gamma)} \big), \end{aligned} \tag{6.30}$$

where A'_{ij} and λ' denote combinations of the couplings discussed above. The potential for the multiple vev amplitude case will be very similar with the obvious changes of vev amplitudes. The phase-dependent terms in the potential provide non-trivial dynamics for the phases σ and γ and will in general lead to $\dot{\gamma} \neq 0$ and therefore a non-vanishing J matrix. As discussed above, the appearance of a non-vanishing J matrix can lead to the non-perturbative production of particles by the rotating flat direction: the condensate can decay via preheating.

6.6 Two independent flat directions

A further instructive toy model consists of two independent flat directions existing simultaneously. We consider four chiral superfields Φ_1, Φ_2, Φ_3, and Φ_4 charged under a gauged $U(1)$ symmetry with charges $\pm q_1$ and $\pm q_2$ respectively. The potential arising from the D-terms reads

$$V = \frac{g^2}{8} (q_1 |\Phi_1|^2 - q_1 |\Phi_2|^2 + q_2 |\Phi_3|^2 - q_2 |\Phi_4|^2)^2. \tag{6.31}$$

Although this toy model has been examined previously in [10], applying the methods outlined in the first sections of this letter helps establish the important properties of the model. The potential in eq.6.31 admits flat direction vevs of

the following forms

$$\begin{aligned}\langle\Phi_1\rangle &= \varphi_1 e^{i\tilde{\sigma}_1},\\ \langle\Phi_2\rangle &= \varphi_1 e^{i\tilde{\sigma}_2},\\ \langle\Phi_3\rangle &= \varphi_2 e^{i\tilde{\sigma}_3},\\ \langle\Phi_4\rangle &= \varphi_2 e^{i\tilde{\sigma}_4}.\end{aligned} \tag{6.32}$$

We can write the excitations around the vevs as

$$\begin{aligned}\Phi_1 &= (\varphi_1+\xi_1)e^{i(\tilde{\sigma}_1+\frac{\theta_1}{\varphi_1})},\\ \Phi_2 &= (\varphi_1+\xi_2)e^{i(\tilde{\sigma}_2+\frac{\theta_2}{\varphi_1})},\\ \Phi_3 &= (\varphi_2+\xi_3)e^{i(\tilde{\sigma}_3+\frac{\theta_3}{\varphi_2})},\\ \Phi_4 &= (\varphi_2+\xi_4)e^{i(\tilde{\sigma}_4+\frac{\theta_4}{\varphi_2})}.\end{aligned} \tag{6.33}$$

As before we can make a gauge transformation and remove one phase in such a way that terms of the form shown in eq.6.4 vanish. The final form appears as

$$\begin{aligned}\langle\Phi_1\rangle &= \varphi_1 e^{i(\sigma_1+\gamma\frac{\varphi_2}{q_1\varphi_1})},\\ \langle\Phi_2\rangle &= \varphi_1 e^{i(\sigma_1-\gamma\frac{\varphi_2}{q_1\varphi_1})},\\ \langle\Phi_3\rangle &= \varphi_2 e^{i(\sigma_2+\gamma\frac{\varphi_1}{q_2\varphi_2})},\\ \langle\Phi_4\rangle &= \varphi_2 e^{i(\sigma_2-\gamma\frac{\varphi_1}{q_2\varphi_2})},\end{aligned} \tag{6.34}$$

demonstrating the existence of three physical phases. Transforming in to the unitary gauge, we can write the excitations around the vevs as

$$\begin{aligned}\Phi_1 &= (\varphi_1+\xi_1)e^{i(\sigma_1+\gamma\frac{\varphi_2}{q_1\varphi_1}+\theta\frac{1}{\sqrt{2}\varphi_1}+\theta''\frac{q_2\varphi_2}{\varphi'\varphi_1})},\\ \Phi_2 &= (\varphi_1+\xi_2)e^{i(\sigma_1-\gamma\frac{\varphi_2}{q_1\varphi_1}+\theta\frac{1}{\sqrt{2}\varphi_1}-\theta''\frac{q_2\varphi_2}{\varphi'\varphi_1})},\\ \Phi_3 &= (\varphi_2+\xi_3)e^{i(\sigma_2-\gamma\frac{\varphi_1}{q_2\varphi_2}+\theta'\frac{1}{\sqrt{2}\varphi_2}-\theta''\frac{q_1\varphi_1}{\varphi'\varphi_2})},\\ \Phi_4 &= (\varphi_2+\xi_4)e^{i(\sigma_2+\gamma\frac{\varphi_1}{q_2\varphi_2}+\theta'\frac{1}{\sqrt{2}\varphi_2}+\theta''\frac{q_1\varphi_1}{\varphi'\varphi_2})},\end{aligned} \tag{6.35}$$

where $\varphi' = \sqrt{2}(q_1\varphi_1^2 + q_2\varphi_2^2)^{1/2}$. The spectrum in this case consists of one massive Higgs particle and six massless scalar fields (the NG has been gauged away). Again, we must diagonalize the kinetic terms. Applying the necessary field redefinitions we are able to evaluate the J matrix. The non-vanishing J matrix elements read

$$\begin{aligned}J_{1,2} = J_{2,1} &= \frac{k-\sqrt{k^2+M_1^2}}{\sqrt{k}(k^2+M_1^2)^{1/4}}\frac{q_1q_2}{\varphi'^2}(\dot{\sigma}_1-\dot{\sigma}_2)\varphi_1\varphi_2\\ J_{1,3} = J_{3,1} &= \frac{k-\sqrt{k^2+M_1^2}}{\sqrt{2k}(k^2+M_1^2)^{1/4}}\frac{\dot{\gamma}\varphi_2}{\varphi'}\\ J_{1,4} = J_{4,1} &= \frac{k-\sqrt{k^2+M_1^2}}{\sqrt{2k}(k^2+M_1^2)^{1/4}}\frac{\dot{\gamma}\varphi_1}{\varphi'},\end{aligned} \tag{6.36}$$

which depend on the relative phases between the field vevs. We should point out that only the Higgs eigenstate ($i = 1$) is distinguishable. The other indices label the light fields which at this level are all massless. Preheating is again possible provided two of the phases have non-zero time derivatives. Using the particular case with $q_1 = q_2$, we can write the scalar potential (see Appendix for details) yielding the terms

$$V = \frac{1}{2}(m_1^2 + m_2^2)\varphi_1^2 + \frac{1}{2}(m_3^2 + m_4^2)\varphi_2^2 + \frac{A_1}{8}\frac{m_s}{M}\varphi_1^4 e^{i4\sigma_1} + \frac{A_2}{8}\frac{m_s}{M}\varphi_2^4 e^{i4\sigma_2} + \frac{A_3}{8}\frac{m_s}{M}\varphi_1^2\varphi_2^2 e^{i2(\sigma_1+\sigma_2+\gamma\frac{\varphi_2^2-\varphi_1^2}{\varphi_2\varphi_1})} + \frac{A_4}{8}\frac{m_s}{M}\varphi_1^2\varphi_2^2 e^{2i(\sigma_1+\sigma_2-\gamma\frac{\varphi_2^2-\varphi_1^2}{\varphi_2\varphi_1})} + ... \quad (6.37)$$

Clearly, non-trivial dynamics exist for the phases γ, σ_1 and σ_2.

6.7 Numerical analysis

As a proof-of-principle that achieves quantitative results, we numerically analyse the model described in section 6.6. We use a simplified version of the potential appearing in eq.6.37, confining ourselves to the potential

$$V = \frac{1}{2}m_{\varphi_1}^2\varphi_1^2 + \frac{1}{2}m_{\varphi_2}^2\varphi_2^2 + \frac{A_1}{8}\frac{m_s}{M}\varphi_1^4 e^{i4\sigma_1} + \frac{A_2}{8}\frac{m_s}{M}\varphi_2^4 e^{i4\sigma_2} + \text{h.c} \quad (6.38)$$

where $m_{\varphi_1}^2 = m_1^2 + m_2^2$, $m_{\varphi_2}^2 = m_3^2 + m_4^2$. This potential decouples the equations of motion for γ, σ_1 and σ_2. The equation of motion for γ reduce to $\ddot{\gamma} = 0$, and with the choice of initial conditions, $\dot{\gamma} = 0$, the effects of γ on preheating are removed. Our simplified potential allows us to numerically evolve the classical evolution of the flat direction vevs and analyze particle production in a self-consistent background. We also make the simplifying assumption setting $A_1 = A_2 = \lambda\frac{M}{m_s}$ in eq.6.37. Again, we stress that we use this grossly simplified potential simply to demonstrate the quantitative behaviour of the toy model class.

Measuring the conformal time in units of $\tau \to ft$ with $f = g\varphi_{1_0}$ and using the re-scaled flat-direction vev amplitudes

$$\begin{aligned} \varphi_1 &= \frac{\varphi_{1_0}}{a}F_1 \\ \varphi_2 &= \frac{\varphi_{2_0}}{a}F_2 \end{aligned} \quad (6.39)$$

we find the background equations,

$$F_1'' + \left[\frac{\mu_1^2 a^2}{2} - \sigma_1'^2 - \frac{a''}{a}\right]F_1 + \frac{\lambda F_1^3}{2g^2}\cos(4\sigma_1) = 0$$
$$F_2'' + \left[\frac{\mu_2^2 a^2}{2} - \sigma_2'^2 - \frac{a''}{a}\right]F_2 + \frac{\lambda F_2^3}{2g^2}\left(\frac{\varphi_{2_0}}{\varphi_{1_0}}\right)^2\cos(4\sigma_2) = 0 \quad (6.40)$$

where a prime represents a derivative with respect to τ and

$$\sigma_1'' + 2\sigma_1' \frac{F_1'}{F_1} - \frac{\lambda}{2g^2} F_1^2 \sin(4\sigma_1) = 0$$
$$\sigma_2'' + 2\sigma_2' \frac{F_2'}{F_2} - \frac{\lambda}{2g^2} \left(\frac{\varphi_{2_0}}{\varphi_{1_0}}\right)^2 F_2^2 \sin(4\sigma_2) = 0 \qquad (6.41)$$

describes the motion of the flat direction vevs; $\mu_1 = m_{\varphi_1}/f, \mu_2 = m_{\varphi_2}/f$. The scale factor evolves as,

$$\frac{a''}{a} = -\frac{a'^2}{a^2} + \frac{1}{2}\left[f_p^2 \left\{\mu_1^2 F_1^2 + \frac{\lambda}{2g^2}\frac{F_1^4}{a^2}\cos(4\sigma_1) + \mu_2^2 \left(\frac{\varphi_{2_0}}{\varphi_{1_0}}\right)^2 F_2^2 + \frac{\lambda}{2g^2}\left(\frac{\varphi_{2_0}}{\varphi_{1_0}}\right)^4 \frac{F_2^4}{a^2}\cos(4\sigma_2)\right\} + \frac{a^2\rho_\psi}{M_{pl}^2 f^2}\right] \qquad (6.42)$$

where ρ_ψ is the energy density of the inflaton field and $f_p = \varphi_{1_0}/M_{pl}$ is set to $f_p = 0.1$ in our numerics. We also take $\mu_1 = 10^{-2}, \mu_2 = 10^{-2}/2$, and $\lambda = \mu_1^2$ for computational ease. As initial conditions, we start the flat direction at rest, such that $(\varphi_{1,2}\exp(i\sigma_{1,2}))' = 0$. We choose to set initially $F_{1,2} = 1$, $\sigma_{1,2} = 0.05$, $\sigma_{1,2}' = 0$, $a = 1$ and $a' = \mu_1$, which implies $F_{1,2}' = a' = \mu_1$. While these initial conditions do not present a realistic case (where $\mu \sim 10^{-14}$ and $F_{1,2}' \gg \mu_1$), they do provide a numerical proof-of-principle similar to [10].

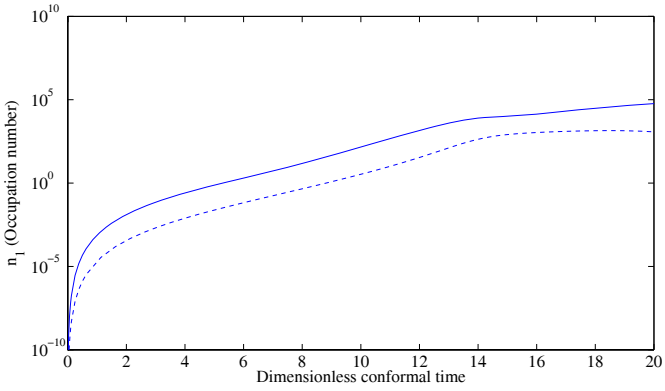

Fig. 6.1: Occupation number for one of the excited fields as a function of dimensionless conformal time, obtained using eq.6.19 after numerically integrating the background field equations and Bogolyubov matrices; $k = \mu_1/3 \times 10^5$, other parameters as explained in the text. The solid lines represents preheated fields with $\varphi_{2_0}/\varphi_{1_0} = 1$ while the dashed lines indicate the preheated fields with $\varphi_{2_0}/\varphi_{1_0} = 0.1$

Initially the flat direction vevs correspond to a condensate of coherent particles with vanishing momentum. The motion of these vevs, described by eq.6.40 and eq.6.41, and the interactions described in the previous section, cause the rapid decay of this condensate into a decoherent state of particles. FIG. 1 shows the occupation numbers, $n_i(t)$, of these light particles as a function of conformal time: the exponential growth of these functions signals the exponentially fast

decay of the flat-direction vev. The two line types, solid and dashed, represent the ratios $\varphi_{2_0}/\varphi_{1_0} = 1, 0.1$ respectively. We see that preheating occurs over a wide range of the ratio $\varphi_{2_0}/\varphi_{1_0}$. In this numerical example, preheating effects do not vanish until $\varphi_{2_0}/\varphi_{1_0} \lesssim 10^{-2}$. FIG 2 displays the resulting spectrum for one of the light fields, we see that production of higher momentum modes becomes kinematically suppressed.

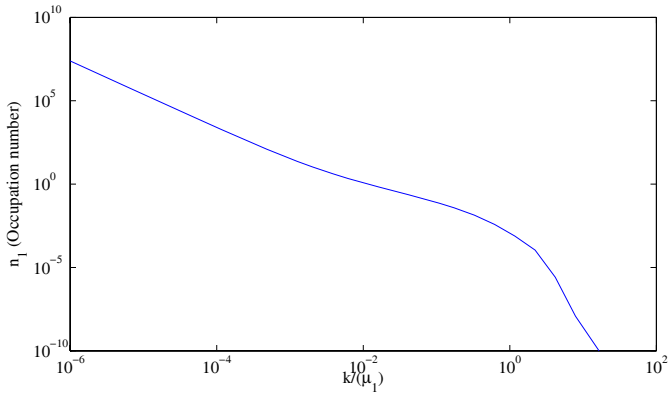

Fig. 6.2: Occupation number as a function of comoving momentum obtained as for FIG. 1, with $\varphi_{2_0}/\varphi_{1_0} = 0.5$ at time $t = 20$.

We must stress that effects of SUSY breaking terms in the Lagrangian eq.6.1 will significantly affect the amount of particle production produced by the rotating condensate. A mass term for the light fields translates into a momentum shift in eq.6.15 and this corresponds to a kinematic suppression of the modes [10]. A realistic model involving MSSM flat directions will in general contain many SUSY breaking terms and non-renormalisable operators, creating large model dependencies in the precise determination of the momentum shift. Consequently, we leave such a study to future work.

6.8 Conclusions

The cosmological fate of flat directions provides a major ingredient for the history of the early Universe. Flat directions can provide mechanisms for generating the baryon asymmetry of the Universe and can play an important role in reheating after inflation. Our analysis stresses the use of the unitary gauge in which the physical content of the theory becomes manifest. By transforming to the unitary gauge, complications arising from massless NG modes in the mixing of the excitations around the flat direction vev are removed. The mixing matrix in this gauge defines the mass eigenstates of the physical scalar fields and determines if non-perturbative decay is possible. Since the mass matrix in the unitary gauge can contain time dependent mixing among all fields, one of the necessary conditions for preheating can be satisfied.

Two further crucial conditions for preheating in our analysis center on the existence of physical relative phases between the field vevs that make up the flat direction(s) and that these phases possess non-trivial dynamics during the

early universe. The first of these conditions generally becomes satisfied if the difference between the number fields that acquire a vev and the number of broken diagonal generators is larger than one – every diagonal generator removes one unphysical phase. The second condition generally becomes satisfied if terms which explicitly depend on the phase differences appear in the scalar potential. The existence of gauge invariant products of background fields exhibiting this phase dependence represents the crucial ingredient and determines the phase dependence in the scalar potential. Once these conditions are satisfied, the flat direction condensate can decay non-perturbatively via preheating.

6.9 Appendix

In this appendix we specify a simple model to justify the form of the potential given in eq.6.37. We have the following field content with $U(1)$ charges and R_p assignments,

	Φ_1	Φ_2	Φ_3	Φ_4
$U(1)$	1	-1	1	-1
R_p	-	+	-	+

The lowest dimension gauge invariant operators are

$$\begin{aligned} \mathcal{O}_1 &= \Phi_1\Phi_2, \quad \mathcal{O}_2 = \Phi_3\Phi_4, \\ \mathcal{O}_3 &= \Phi_1\Phi_4, \quad \mathcal{O}_4 = \Phi_2\Phi_3. \end{aligned} \tag{6.43}$$

The lowest dimension terms which are R_p invariant and phase-dependent arise as soft SUSY breaking A-terms and appear in the scalar potential as

$$V = \sum_{i=1}^{4} \frac{m_i^2}{2}|\Phi_i|^2 + \frac{A_1}{8}\frac{m_s}{M}\mathcal{O}_1^2 + \frac{A_2}{8}\frac{m_s}{M}\mathcal{O}_2^2 + \frac{A_3}{8}\frac{m_s}{M}\mathcal{O}_3^2 + \frac{A_4}{8}\frac{m_s}{M}\mathcal{O}_4^2 + \ldots \tag{6.44}$$

where the ellipses stand for other terms of the same order with different products of the gauge invariant operators, loop induced contributions and higher order terms in the $(1/M)$ expansion. Substituting the vevs given in eq.6.34 we generate the potential terms given in eq.6.37.

6.10 Acknowledgements

We thank R. Allahverdi and J. March-Russell for many useful discussions. We are also grateful to I. Aitchison, S. Hannestad, P. Iafelice, G. Ross, S. Sarkar, D. Ghilencea, M. Schvellinger and M. Sloth for helpful discussions. AB wishes to thank Oxford University for hospitality during the course of this work, DM is supported by the NSERC Canada, FR by the Greendale scholarship. This work was partially supported by the EU 6th Framework Marie Curie Research and Training network "UniverseNet" (MRTN-CT-2006-035863).

BIBLIOGRAPHY

[1] T. Gherghetta, C. F. Kolda and S. P. Martin, Nucl. Phys. B **468**, 37 (1996).

[2] For a review, see K. Enqvist and A. Mazumdar, Phys. Rept. **380**, 99 (2003).

[3] I. Affleck and M. Dine, Nucl. Phys. B **249**, 361 (1985).

[4] A. D. Linde, Phys. Lett. B **160**, 243 (1985).

[5] M. Dine, L. Randall and S. D. Thomas, Phys. Rev. Lett. **75**, 398 (1995).

[6] M. Postma and A. Mazumdar, JCAP **0401**, 005 (2004).

[7] N. Shuhmaher and R. Brandenberger, Phys. Rev. D **73**, 043519 (2006)

[8] See eg., R. Allahverdi, K. Enqvist, J. Garcia-Bellido and A. Mazumdar, Phys. Rev. Lett. **97** (2006) 191304; J. C. Bueno Sanchez, K. Dimopoulos and D. H. Lyth, JCAP **0701** (2007) 015.

[9] R. Allahverdi, A. Mazumdar, [arXiv:hep-ph/0603244].

[10] K. A. Olive and M. Peloso, Phys. Rev. D **74**, 103514 (2006).

[11] R. Allahverdi, A. Mazumdar, [arXiv:hep-ph/0608296].

[12] T. W. B. Kibble Phys. Rev. **155** (1967) 1554.

[13] H. P. Nilles, M. Peloso and L. Sorbo, JHEP **0104**, 004 (2001)

[14] R. Casadio, P. L. Iafelice and G. P. Vacca, [arXiv:hep-th/0702175].

[15] J. H. Traschen and R. H. Brandenberger, Phys. Rev. D **42**, 2491 (1990).

[16] L. Kofman, A. D. Linde and A. A. Starobinsky, Phys. Rev. D **56** (1997) 3258.

[17] Y. B. Zeldovich and A. A. Starobinsky, Sov. Phys. JETP **34** (1972) 1159 [Zh. Eksp. Teor. Fiz. **61** (1971) 2161].

7

SUSY Flat Direction Decay - actual directions

The paper *SUSY Flat Direction Decay - the prospect of particle production and preheating investigated in the unitary gauge* presented in this chapter has been published by Physical Review D [25].

[25] A. Basbøll, SUSY Flat Direction Decay - the prospect of particle production and preheating investigated in the unitary gauge , Phys. Rev. D **78**, 023528 (2008).

Except for minor typographical changes the content of this chapter is equal to the published version. Typos in equation 7.43 and elsewhere have been corrected.

SUSY Flat Direction Decay - the prospect of particle production and preheating investigated in the unitary gauge

Anders Basbøll*

Abstract

We look at the possibility of non-perturbative particle production after inflation from SUSY flat directions produced by rotating eigenstates thereby avoiding the standard adiabaticity conditions. This might lead to preheating and prevent the delay of thermalisation of the universe. We investigate the flat directions LLE^c and $U^cD^cD^c$ and find no particle production. These 2 directions are very important, since they have been named as possible candidates for being the inflaton. We investigate $QLQLQLE^c$ and find particle production and therefore the possibility of preheating. We investigate the LLE^c and $U^cD^cD^c$ directions appearing simultaneously, and find no production. Finally, we investigate LLE^c and QLD^c simultaneously - with one L-field in common. Here we do find particle production and therefore the possibility of preheating. This means that if SUSY flat directions are to delay thermalisation and thus explain the (lack of) gravitino production, it is necessary to explain why complicated directions as $QLQLQLE^c$ are not exited, and why combinations like LLE^c and QLD^c are not both exited.

7.1 Introduction

The scalar potential of the Minimal Supersymmetric Standard Model (MSSM) possesses a large number of F- and D-flat directions [1, 2]. These flat directions might generate the baryon asymmetry of the Universe through the out-of-equilibrium CP violating decay of coherent field oscillations along the flat directions themselves [3–5].

Recently the cosmological importance of flat direction vacuum expectation values (VEV)s [Often we will use VEV meaning *nonzero* vacuum expectation value - this should not cause confusion] and the decay thereof has been investigated. In [6] it was asserted that large flat direction VEV's can persist long enough to delay thermalization after inflation and therefore lead to low reheat temperatures. This is of great importance. A lower reheating temperature would potentially solve the (lack of) gravitino problem [7]. It has also been claimed [8] that large flat direction VEV's can prevent non-perturbative

* Department of Physics and Astronomy, University of Aarhus, Ny Munkegade, DK-8000 Aarhus C, Denmark. E-mail: andersb@phys.au.dk.

parametric resonant decay (preheating) of the inflaton since the inflaton decay products become sufficiently massive preventing preheating from ever becoming efficient. These arguments hold so long as the flat direction VEV's do not rapidly decay - they must persist long enough so that they can delay thermalization and block inflaton preheating. In [9] it was claimed that non-perturbative decay can lead to a rapid depletion of the flat direction condensate and thus precludes the delay of thermalization after inflation. It was also concluded that in order for the flat direction to decay non-perturbatively the system requires more than one flat direction [9, 10]. In [10] it was stated that even in the presence of multiple flat directions, some degree of fine-tuning was necessary to achieve flat direction decay. We note that very recently [11] it has been claimed that even if non-perturbative particle production happen, the main decay mode will still be perturbative.

The presence of Nambu-Goldstone bosons (Goldstones) is a very important point in this discussion. The flat directions are charged under the gauge group of the MSSM. Therefore the flat direction VEV will break some or all of the gauge symmetries of the theory and therefore the presence of the associated Goldstones must be expected. [9] considers a gauged $U(1)$ model and constructs the mixing matrix for the excitations around the flat direction VEV. In [9] it was claimed that in the single flat direction case, non-perturbative decay proceeds solely via a massless Goldstone mode as only the Goldstone mode mixes with the Higgs and all other massless moduli remain decoupled. Since the Goldstone represents an unphysical gauge degree of freedom, it was concluded [9, 10] that no preheating occurs in the single flat direction case - a Goldstone can be gauged away. In order to determine if flat direction VEV's decay non-perturbatively into scalar degrees of freedom, one must remove the Goldstones ie. use the unitary gauge.

In an earlier paper [12] we and our colleagues considered toy models to demonstrate that, in the unitary gauge, the mixing matrix of the excitations around a flat direction VEV permits preheating. Moreover, we found that flat direction decay depends on the number of dynamical, physical phases appearing in the flat direction VEV. Specifically, a physical phase difference between two of the individual field VEV's making up the flat direction is needed.

In the present paper, we look at (some of) the actual SUSY flat directions. In section 7.2 we look at the LLE^c direction, in section 7.3 we review the particle production mechanism from rotating eigenvectors, in section 7.4 we conclude on the LLE^c case, and in section 7.5 we do the $U^cD^cD^c$. The mentioned directions are especially interesting, since they are mentioned as especially well suited inflaton candidates in [6]. We investigate $QLQLQLE^c$ in section 7.6. We conclude on one flat direction in section 7.7. Then we proceed to 2 directions, first the non-overlapping $LLE^c + U^cD^cD^c$ of the 2 inflaton candidates of [6] in section 7.8 and then the overlapping directions $QLD^c + LLE^c$ in section 7.9. Finally we look at the simpler approach of just counting the fields without any calculations in section 7.11 and conclude in section 7.12.

7.2 LLE^c

One flat direction often mentioned in the literature is LLE^c. Flatness demands the fields with VEV's to come from different generations, and the 2 L fields with VEV to have opposite SU(2)-charge. Also, the 3 VEV's must have the same absolute value. This leaves essentially only 1 choice (when masses are ignored).

We give these VEV's:

$$\begin{aligned} < \nu_e > &= \varphi e^{i\sigma_1} \\ < \mu > &= \varphi e^{i\sigma_2} \\ < \tau^c > &= \varphi e^{i\sigma_3}. \end{aligned} \tag{7.1}$$

Also, it is clear that 2 other fields will play a role.

$$\begin{aligned} < e > &= 0 \\ < \nu_\mu > &= 0. \end{aligned} \tag{7.2}$$

The Lagrangian reads

$$\mathcal{L} = \sum_{i=1}^{3} \frac{1}{2} |D_\mu \Phi_i|^2 - V - \frac{1}{4} F_{\mu\nu}^2 - \sum_i \frac{1}{4} W_{\mu\nu}^{i2} \tag{7.3}$$

where for field ϕ_i $D_i^\mu = \left[(\partial^\mu - i q_i A_0^\mu)\delta_{ij} - \sum_{a=1}^{3} i P_{ij}^a A_a^\mu \right] \phi_j$ denotes the covariant derivative. P^a is the a^{th} Pauli-matrix. The potential we consider arises from the supersymmetric D-terms and has the form

$$V = \frac{1}{2} \left(D_H^2 + \sum_a D_a^2 \right) \tag{7.4}$$

where

$$D_H = \frac{g_1}{2} \sum_i q_i |\phi_i|^2 \tag{7.5}$$

$$D_a = \frac{g_2}{2} \phi^\dagger P^a \phi \tag{7.6}$$

where q_i is the hypercharge, and g_1, g_2 are the hypercharge and SU2 gauge couplings.

The essential part is removing the Goldstones correctly. To do that we start by looking at the fields with the VEV's only (no excitations). We've written those earlier, and we get mixed kinetic terms

$$\mathcal{L} \supset -\varphi^2 A_0 (\dot{\sigma_1} + \dot{\sigma_2} - 2\dot{\sigma_3}) - \varphi^2 A_3 (\dot{\sigma_1} - \dot{\sigma_2}) \tag{7.7}$$

which has the form of a coupling between the gauge field and the background condensate. Terms of this type will feed into the equations of motion for the

gauge field which, in turn, will have an effect on the equations of motion for the scalar excitations. The remaining terms in $\mathcal{L}$ are

$$\frac{1}{2}\varphi^2\left[6A_0^2+2A_1^2+2A_2^2+2A_3^2+\dot{\sigma_1}^2+\dot{\sigma_2}^2+\dot{\sigma_3}^2\right] \tag{7.8}$$

- all desired terms. By making a $U(1)$ gauge transformation on the VEV,

$$\langle\Phi_i\rangle \rightarrow \left\langle\Phi_i'\right\rangle = e^{iq_i\lambda}\langle\Phi_i\rangle \tag{7.9}$$

with

$$\lambda = \frac{2\sigma_3-\sigma_1-\sigma_2}{3}, \tag{7.10}$$

and by making a $SU(2)$ gauge transformation on the VEV,

$$\langle\Phi_i\rangle \rightarrow \left\langle\Phi_i'\right\rangle = e^{iP^3\gamma}\langle\Phi_i\rangle \tag{7.11}$$

with

$$\gamma = \frac{\sigma_2-\sigma_1}{2}, \tag{7.12}$$

we can gauge the unwanted terms away and avoid a complicated analysis of the kinetic terms. The resulting form of the VEV reads,

$$\begin{aligned}\langle\nu_e\rangle &= \varphi e^{i\sigma}\\ \langle\mu\rangle &= \varphi e^{i\sigma}\\ \langle\tau^c\rangle &= \varphi e^{i\sigma}\end{aligned} \tag{7.13}$$

where $\sigma = (\sigma_1+\sigma_2+\sigma_3)/3$ represents the remaining independent physical phase. Following [13], we can write the fields in the unitary gauge as (including the other relevant fields),

$$\begin{aligned}\nu_e &= (\varphi+\xi_2)e^{i(\sigma+\frac{\xi_1}{\sqrt{3}\varphi})}\\ e &= (\xi_5+i\xi_6)e^{i\sigma}\\ \nu_\mu &= (\xi_7+i\xi_8)e^{i\sigma}\\ \mu &= (\varphi+\xi_3)e^{i(\sigma+\frac{\xi_1}{\sqrt{3}\varphi})}\\ \tau^c &= (\varphi+\xi_4)e^{i(\sigma+\frac{\xi_1}{\sqrt{3}\varphi})}\end{aligned} \tag{7.14}$$

where σ represents time dependent phase of the VEV (we have just showed the phase differences are gauged away), ξ_1 parameterises its excitation, $\xi_{2,3,4}$ parameterise the excitations around the VEV, and $\xi_{5,6,7,8}$ parameterise the 2 no-VEV fields (the phase on these fields is not necessary, but allowed, and will be convenient).

Again we will look at the kinetic term. First, the φ^2-term

$$\frac{1}{2}\varphi^2\left[6A_0^2+2A_1^2+2A_2^2+2A_3^2+3\dot{\sigma}^2\right] \tag{7.15}$$

- not surprisingly. This contains no goldstones, so we proceed to next order.

The terms indicating Goldstones should include $\dot{\xi}_i$. These terms are

$$\mathcal{L} \supset -\varphi\left(A_1(\dot{\xi}_6+\dot{\xi}_8)+A_2(\dot{\xi}_7-\dot{\xi}_5)\right). \tag{7.16}$$

The remaining terms are on the forms

$$\mathcal{L} \supset \varphi\left(C_{ijk}\xi_i A_j A_k + D_{ij}\xi_i A_j\dot{\sigma} + E_i\xi_i\dot{\sigma}^2 - \sqrt{3}\dot{\xi}_1.\dot{\sigma}\right) \tag{7.17}$$

Here it is clear, that the field excitation terms (excluding derivative terms) are suppressed compared to φ^2-terms in the potential. The only excitation is the last term. However, it is just a "mixing" between an excitation and its own VEV.

The Goldstones are removed by demanding $\dot{\xi}_6 = -\dot{\xi}_8$ and $\dot{\xi}_7 = \dot{\xi}_5$. Doing this, and renormalising, we take

$$\begin{aligned}
\nu_e &= (\varphi+\xi_2)e^{i(\sigma+\frac{\xi_1}{\sqrt{3}\varphi})} \\
e &= \frac{(\xi_5+i\xi_6)}{\sqrt{2}}e^{i\sigma} \\
\nu_\mu &= \frac{(\xi_5-i\xi_6)}{\sqrt{2}}e^{i\sigma} \\
\mu &= (\varphi+\xi_3)e^{i(\sigma+\frac{\xi_1}{\sqrt{3}\varphi})} \\
\tau^c &= (\varphi+\xi_4)e^{i(\sigma+\frac{\xi_1}{\sqrt{3}\varphi})}.
\end{aligned} \tag{7.18}$$

This does indeed kill the mixed derivative terms. The remaining terms stay as they are. But they are all VEV-suppressed, so it is justified to move to the coordinate derivative, rather than the covariant derivative.

The remaining kinetic term (to zero'th order in φ) are

$$\begin{aligned}
\mathcal{L} \supset \sum_{i=1}^{6}\left(\frac{1}{2}\dot{\xi_i}^2\right) + \sum_{i=2}^{6}\left(\frac{1}{2}\xi_i^2\dot{\sigma}^2\right) \\
+\sum_{i=2}^{4}\left(\varphi\xi_i\dot{\sigma}^2 + \frac{2}{\sqrt{3}}\xi_i\dot{\xi}_1\right) + \frac{3}{2}\varphi^2\dot{\sigma}^2 + \sqrt{3}\varphi\dot{\sigma}\dot{\xi}_1.
\end{aligned} \tag{7.19}$$

The first term are the kinetic terms that show we have correctly normalised kinetic fields - including that there are no cross terms. The second term is completely negligible compared to the φ^2-terms of V. The third term, though bigger than the prior one, is still suppressed. The fourth term is a rotation between the excitation states. These are very important and will give the U-matrix below. The fifth term is just a VEV-term, and the final term is the "mixing" between an excitation and its own VEV. So everything is fine.

On substituting the fields of eq.7.18 into the Lagrangian given in eq.7.3 and defining the vector $\Xi \equiv (\xi_1,\xi_2,\xi_3,\xi_4,\xi_5,\xi_6)^T$, we find the quadratic terms

$$\mathcal{L} \supset \frac{1}{2}|\partial_\mu\Xi|^2 - \frac{1}{2}\Xi^T\mathcal{M}^2\Xi - \dot{\Xi}^T U\Xi + ... \tag{7.20}$$

where the ellipses denote higher order terms and interactions. The matrix U given in the second part of the third term in eq.7.19 reads

$$U_{init} = \begin{pmatrix} 0 & -\frac{2\dot{\sigma}}{\sqrt{3}} & -\frac{2\dot{\sigma}}{\sqrt{3}} & -\frac{2\dot{\sigma}}{\sqrt{3}} & 0 & 0 \\ 0 & 0 & 0 & 0 & 0 & 0 \\ 0 & 0 & 0 & 0 & 0 & 0 \\ 0 & 0 & 0 & 0 & 0 & 0 \\ 0 & 0 & 0 & 0 & 0 & 0 \\ 0 & 0 & 0 & 0 & 0 & 0. \end{pmatrix} \tag{7.21}$$

However, we want an antisymmetric matrix for the procedure below. Using partial integration - and ignoring surface terms - we find

$$U = \begin{pmatrix} 0 & -\frac{\dot{\sigma}}{\sqrt{3}} & -\frac{\dot{\sigma}}{\sqrt{3}} & -\frac{\dot{\sigma}}{\sqrt{3}} & 0 & 0 \\ \frac{\dot{\sigma}}{\sqrt{3}} & 0 & 0 & 0 & 0 & 0 \\ \frac{\dot{\sigma}}{\sqrt{3}} & 0 & 0 & 0 & 0 & 0 \\ \frac{\dot{\sigma}}{\sqrt{3}} & 0 & 0 & 0 & 0 & 0 \\ 0 & 0 & 0 & 0 & 0 & 0 \\ 0 & 0 & 0 & 0 & 0 & 0 \end{pmatrix} \tag{7.22}$$

while the mass matrix for the physical excitations appears as

$$\mathcal{M}^2 = \varphi^2 \begin{pmatrix} 0 & 0 & 0 & 0 & 0 & 0 \\ 0 & g_1^2+g_2^2 & g_1^2-g_2^2 & -2g_1^2 & 0 & 0 \\ 0 & g_1^2-g_2^2 & g_1^2+g_2^2 & -2g_1^2 & 0 & 0 \\ 0 & -2g_1^2 & -2g_1^2 & 4g_1^2 & 0 & 0 \\ 0 & 0 & 0 & 0 & 2g_2^2 & 0 \\ 0 & 0 & 0 & 0 & 0 & 2g_2^2 \end{pmatrix} = B\mathcal{M}_d^2 B^T, \tag{7.23}$$

with eigenvalues $M_1^2 = 6g_1^2\varphi^2$, $M_2^2 = M_3^2 = M_4^2 = 2g_2^2\varphi^2$,$M_5^2 = M_6^2 = 0$ (the entries of the diagonal matrix $\mathcal{M}_d$). B is an orthogonal matrix which diagonalises $\mathcal{M}^2$ and M_{1-4}^2 corresponds to the mass of the physical eigenstates associated with the spontaneous breaking of the symmetries. $M_5^2 = M_6^2 = 0$ correspond to the massless excitations around the flat direction VEV.

The last term in eq.7.20 appears as a consequence of the time-dependence of the background – it represents a mixing between the fields $\xi_{1,2,3,4,5,6}$, and their time-derivatives. The effect of these terms on the system becomes clear if we make field redefinitions that remove the mixed derivative terms. The resulting transformation leaves the system in an inertial frame in field space and leads to a time-dependent mass matrix. Defining $\Xi' = A\Xi$ (A is orthogonal), we find the condition that A must satisfy in order for all the mixed derivative terms to cancel

$$\dot{A}^T A = U. \tag{7.24}$$

The Lagrangian for the Ξ' system now reads

$$\mathcal{L} \supset \frac{1}{2}|\partial_\mu \Xi'|^2 - \frac{1}{2}\Xi'^T \mathcal{M}'^2 \Xi' \tag{7.25}$$

where $\mathcal{M}'^2 = A\mathcal{M}^2A^T = AB\mathcal{M}_d^2B^TA^T = C\mathcal{M}_d^2C^T$, and $C = AB$. The matrix C is an orthogonal time-dependent matrix, with columns corresponding to the eigenvectors of $\mathcal{M}'^2$. We now have a system of scalar fields with canonically normalized kinetic terms and time dependent eigenvectors.

The central point of this discussion centers precisely on the appearance of the *time dependent* eigenvectors for the six scalar fields. This satisfies a necessary but not sufficient condition for preheating. In the next section, we briefly run through the details of the non-perturbative production of the light scalar fields following the analysis of [14]. This is a more brief summary than in [12] - which is otherwise followed here.

7.3 Non-perturbative production of particles

Including gravity, the dynamics of the re-scaled conformally coupled scalar fields, $\chi_i = a\Xi_i'$, where a denotes the scale factor and Ξ_i' the i-th component of the vector Ξ', are governed by the following equations of motion (sum over repeated indices is implied),

$$\ddot{\chi}_i + \Omega_{ij}^2(t)\chi_j = 0 \tag{7.26}$$

where dots represent derivatives with respect to conformal time t, and

$$\Omega_{ij}^2 = a^2\mathcal{M}'^2_{ij} + k^2\delta_{ij}, \tag{7.27}$$

where k labels the comoving momentum. Using an orthogonal time-dependent matrix $C(t)$, we can diagonalise Ω_{ij} via $C^T(t)\Omega^2(t)C(t) = \omega^2(t)$, giving the diagonal entries $\omega_j^2(t)$. Terms of the form $\sim \varphi\dot{\sigma}\dot{\chi}$ arising from the kinetic terms do not affect the evolution of the nonzero k quantum modes [15].

As the vacuum changes, a new set of creation/annihilation operators are required. We use Bogolyubov transformation with Bogolyubov coefficients α and β (which denote matrices in the multi-field case).

Initially $\alpha = \mathbb{I}$ and $\beta = 0$ while the coupled differential equations (matrix multiplication implied):

$$\begin{aligned} \dot{\alpha} &= -i\omega\alpha + \frac{\dot{\omega}}{2\omega}\beta - I\alpha - J\beta \\ \dot{\beta} &= \frac{\dot{\omega}}{2\omega}\alpha + i\omega\beta - J\alpha - I\beta, \end{aligned} \tag{7.28}$$

govern the system's time evolution with the matrices I and J given by

$$I = \frac{1}{2}\left(\sqrt{\omega}\,C^T\dot{C}\frac{1}{\sqrt{\omega}} + \frac{1}{\sqrt{\omega}}\,C^T\dot{C}\sqrt{\omega}\right) \tag{7.29}$$

$$J = \frac{1}{2}\left(\sqrt{\omega}\,C^T\dot{C}\frac{1}{\sqrt{\omega}} - \frac{1}{\sqrt{\omega}}\,C^T\dot{C}\sqrt{\omega}\right). \tag{7.30}$$

Similarly to the single-field case it can be shown [14] that at any generic time the occupation number of the ith bosonic eigenstate reads (no summation implied)

$$n_i(t) = (\beta^*\beta^T)_{ii}. \tag{7.31}$$

As pointed out in [9, 14], there exists two sources of non-adiabaticity in the multi-field scenario. The first source arises from the individual frequency time dependence and appears as the only source of non-adiabaticity in the single field case. The second source appears from the time dependence of the frequency matrix Ω_{ij} giving rise to terms in eq.7.28 proportional to I and J. This second source provides the most important contribution in our analysis and gives rise to non-perturbative particle production.

Since initially $\alpha = \mathbb{I}$ and $\beta = 0$, eq.7.28 shows that a non-vanishing matrix J is a necessary condition to obtain $\dot{\beta} \neq 0$ and hence $n_i(t) \neq 0$. In general, we have

$$C^T\dot{C} = B^T A^T \dot{A} B = -B^T U B \tag{7.32}$$

where A, B and U were defined in the previous section. The last equation only holds if B is constant in time. This is obviously the case in the LLE^c-case, since, B diagonalises a constant matrix.

7.4 LLE^c Conclusion

For the LLE^c example outlined above, J is a 6×6 zero matrix. Therefore there is no particle production and no preheating.

7.5 $U^cD^cD^c$

One would expect the $U^cD^cD^c$ case to be much the same - as indeed we shall see it is. We give VEV's to these fields (again from different generations to avoid F-terms)

$$\begin{aligned} < u^{c\bar{1}} > &= \varphi e^{i\sigma_1} \\ < s^{c\bar{2}} > &= \varphi e^{i\sigma_2} \\ < b^{c\bar{3}} > &= \varphi e^{i\sigma_3}. \end{aligned} \tag{7.33}$$

The Lagrangian reads

$$\mathcal{L} = \sum_{i=1}^{3} \frac{1}{2}|D_\mu \Phi_i|^2 - V - \sum_i \frac{1}{4} F_{\mu\nu}^{i2} - \sum_i \frac{1}{4} G_{\mu\nu}^{i2} \tag{7.34}$$

where for field ϕ_i $D_i^\mu = \left[(\partial^\mu - iq_i A_0^\mu)\delta_{ij} - \sum_{A=1}^{8} iGM_{ij}^A B_A^\mu\right]\phi_j$ denotes the covariant derivative. where GM^A is the A^{th} Gell-Mann-matrix. The potential now looks like

$$V = \frac{1}{2}\left(D_H^2 + \sum_A D_A^2\right) \tag{7.35}$$

where

$$D_A = \frac{g_3}{2}\phi^\dagger GM^A \phi \tag{7.36}$$

where g_3 is SU(3) gauge couplings. Removing mixed kinetic terms as before (in 2 tempi), we use

$$\begin{aligned}
u^{c\bar{1}} &= (\varphi+\xi_2)e^{i(\sigma+\frac{\xi_1}{\sqrt{3}\varphi})},\\
u^{c\bar{2}} &= \frac{(\xi_5+i\xi_6)}{\sqrt{2}}e^{i\sigma},\\
u^{c\bar{3}} &= \frac{(\xi_7+i\xi_8)}{\sqrt{2}}e^{i\sigma},\\
s^{c\bar{1}} &= \frac{(\xi_5-i\xi_6)}{\sqrt{2}}e^{i\sigma},\\
s^{c\bar{2}} &= (\varphi+\xi_3)e^{i(\sigma+\frac{\xi_1}{\sqrt{3}\varphi})}\\
s^{c\bar{3}} &= \frac{(\xi_9+i\xi_{10})}{\sqrt{2}}e^{i\sigma},\\
b^{c\bar{1}} &= \frac{(\xi_7-i\xi_8)}{\sqrt{2}}e^{i\sigma},\\
b^{c\bar{2}} &= \frac{(\xi_9-i\xi_{10})}{\sqrt{2}}e^{i\sigma},\\
b^{c\bar{3}} &= (\varphi+\xi_4)e^{i(\sigma+\frac{\xi_1}{\sqrt{3}\varphi})}.
\end{aligned} \tag{7.37}$$

The U-matrix is

$$U=\begin{pmatrix}
0 & -\frac{\dot\sigma}{\sqrt{3}} & -\frac{\dot\sigma}{\sqrt{3}} & -\frac{\dot\sigma}{\sqrt{3}} & 0 & 0 & 0 & 0 & 0 & 0\\
\frac{\dot\sigma}{\sqrt{3}} & 0 & 0 & 0 & 0 & 0 & 0 & 0 & 0 & 0\\
\frac{\dot\sigma}{\sqrt{3}} & 0 & 0 & 0 & 0 & 0 & 0 & 0 & 0 & 0\\
\frac{\dot\sigma}{\sqrt{3}} & 0 & 0 & 0 & 0 & 0 & 0 & 0 & 0 & 0\\
0 & 0 & 0 & 0 & 0 & 0 & 0 & 0 & 0 & 0\\
0 & 0 & 0 & 0 & 0 & 0 & 0 & 0 & 0 & 0\\
0 & 0 & 0 & 0 & 0 & 0 & 0 & 0 & 0 & 0\\
0 & 0 & 0 & 0 & 0 & 0 & 0 & 0 & 0 & 0\\
0 & 0 & 0 & 0 & 0 & 0 & 0 & 0 & 0 & 0\\
0 & 0 & 0 & 0 & 0 & 0 & 0 & 0 & 0 & 0
\end{pmatrix} \tag{7.38}$$

while the mass matrix for the physical excitations appears as

$$\begin{aligned}
\mathcal{M}^2 &= \varphi^2\\
&\begin{pmatrix}
0 & 0 & 0 & 0 & 0 & 0 & 0 & 0 & 0 & 0\\
0 & \frac{16}{9}g_1^2+\frac{4}{3}g_3^2 & \frac{-8}{9}g_1^2+\frac{-2}{3}g_3^2 & -\frac{-8}{9}g_1^2+\frac{-2}{3}g_3^2 & 0 & 0 & & & & \\
0 & \frac{-8}{9}g_1^2+\frac{-2}{3}g_3^2 & \frac{4}{9}g_1^2+\frac{4}{3}g_3^2 & \frac{4}{9}g_1^2+\frac{-2}{3}g_3^2 & 0 & 0 & 0 & 0 & 0 & 0\\
0 & \frac{-8}{9}g_1^2+\frac{-2}{3}g_3^2 & \frac{4}{9}g_1^2+\frac{-2}{3}g_3^2 & \frac{4}{9}g_1^2+\frac{4}{3}g_3^2 & 0 & 0 & 0 & 0 & 0 & 0\\
0 & 0 & 0 & 0 & 2g_3^2 & 0 & 0 & 0 & 0 & 0\\
0 & 0 & 0 & 0 & 0 & 2g_3^2 & 0 & 0 & 0 & 0\\
0 & 0 & 0 & 0 & 0 & 0 & 2g_3^2 & 0 & 0 & 0\\
0 & 0 & 0 & 0 & 0 & 0 & 0 & 2g_3^2 & 0 & 0\\
0 & 0 & 0 & 0 & 0 & 0 & 0 & 0 & 2g_3^2 & 0\\
0 & 0 & 0 & 0 & 0 & 0 & 0 & 0 & 0 & 2g_3^2
\end{pmatrix}\\
&= B\mathcal{M}_d^2B^T,
\end{aligned} \tag{7.39}$$

with eigenvalues $M_1^2 = \left(\frac{8}{3}g_1^2 + 2g_3^2\right)\varphi^2$, $M_2^2 = M_3^2 = M_4^2 = M_5^2 = M_6^2 = M_7^2 = M_8^2 = 2g_3^2\varphi^2$,$M_9^2 = M_{10}^2 = 0$. Also here, we end up with $J = 0$ and no particle production and therefore preheating.

7.6 $QLQLQLE^c$

$QLQLQLE^c$ case has so many fields with nonzero VEV, that all the phase differences cannot be gauged away. The starting point could be (notice that here, there are 2 essentially different possibilities - the squarks having identical $SU(2)$-charge - or not)

$$\begin{aligned} < u^{c1} > &= \varphi e^{i\sigma_1} \\ < c^{c2} > &= \varphi e^{i\sigma_2} \\ < t^{c3} > &= \varphi e^{i\sigma_3} \\ < e > &= \varphi e^{i\sigma_4} \\ < \mu > &= \varphi e^{i\sigma_5} \\ < \tau > &= \varphi e^{i\sigma_6} \\ < e^c > &= \varphi e^{i\sigma_7} \end{aligned} \tag{7.40}$$

The Lagrangian reads

$$\mathcal{L} = \sum_{i=1}^{3} \frac{1}{2}|D_\mu \Phi_i|^2 - V - \frac{1}{4}F_{\mu\nu}^2 - \frac{1}{4}\sum_i W_{\mu\nu}^{i2} - \frac{1}{4}\sum_i G_{\mu\nu}^{i2} \tag{7.41}$$

where for field ϕ_i $D_i^\mu = \left[(\partial^\mu - iq_i A_0^\mu)\delta_{ij} - \sum_{a=1}^{3} iP_{ij}^a A_a^\mu - \sum_{A=1}^{8} iGM_{ij}^A B_A^\mu\right]\phi_j$ denotes the covariant derivative. The potential now looks like

$$V = \frac{1}{2}\left(D_H^2 + \sum_a D_a^2 + \sum_A D_A^2\right). \tag{7.42}$$

Removing mixed kinetic terms as before (in 2 tempi), we use

$$
\begin{aligned}
u^{c1} &= (\varphi+\xi_4)e^{i(\sigma_1+\frac{\xi_1}{\sqrt{7}\varphi})} \\
c^{c2} &= (\varphi+\xi_5)e^{i(\sigma_1+\frac{\xi_1}{\sqrt{7}\varphi})} \\
t^{c3} &= (\varphi+\xi_6)e^{i(\sigma_1+\frac{\xi_1}{\sqrt{7}\varphi})} \\
e &= (\varphi+\xi_7)e^{i(\sigma_1+\frac{\xi_1}{\sqrt{7}\varphi}+\sigma_2+\frac{\xi_2}{\sqrt{2}\varphi}+\sigma_3+\frac{\xi_3}{\sqrt{6}\varphi})} \\
\mu &= (\varphi+\xi_8)e^{i(\sigma_1+\frac{\xi_1}{\sqrt{7}\varphi}-\sigma_2-\frac{\xi_2}{\sqrt{2}\varphi}+\sigma_3+\frac{\xi_3}{\sqrt{6}\varphi})} \\
\tau &= (\varphi+\xi_9)e^{i(\sigma_1+\frac{\xi_1}{\sqrt{7}\varphi}-2\sigma_3-\frac{2\xi_3}{\sqrt{6}\varphi})} \\
e^c &= (\varphi+\xi_{10})e^{i(\sigma_1+\frac{\xi_1}{\sqrt{7}\varphi})} \\
u^{c2} &= \frac{\xi_{11}+i\xi_{12}}{\sqrt{2}}e^{i\sigma_1} \\
u^{c3} &= \frac{\xi_{13}+i\xi_{14}}{\sqrt{2}}e^{i\sigma_1} \\
d^{c1} &= \left(\frac{\xi_{15}+i\xi_{16}}{\sqrt{2}}-\frac{\xi_{21}+i\xi_{22}}{\sqrt{6}}-\frac{\xi_{27}+i\xi_{28}}{2\sqrt{3}}+\frac{\xi_{29}-i\xi_{30}}{2\sqrt{5}}+\frac{\xi_{31}-i\xi_{32}}{\sqrt{30}}\right)e^{i\sigma_1} \quad (7.43) \\
c^{c1} &= \frac{\xi_{11}-i\xi_{12}}{\sqrt{2}}e^{i\sigma_1} \\
c^{c3} &= \frac{\xi_{19}+i\xi_{20}}{\sqrt{2}}e^{i\sigma_1} \\
s^{c2} &= \left(\frac{\xi_{21}+i\xi_{22}}{\sqrt{\frac{3}{2}}}-\frac{\xi_{27}+i\xi_{28}}{2\sqrt{3}}+\frac{\xi_{29}-i\xi_{30}}{2\sqrt{5}}+\frac{\xi_{31}-i\xi_{32}}{\sqrt{30}}\right)e^{i\sigma_1} \\
t^{c1} &= \frac{\xi_{13}-i\xi_{14}}{\sqrt{2}}e^{i\sigma_1} \\
t^{c2} &= \frac{\xi_{19}-i\xi_{20}}{\sqrt{2}}e^{i\sigma_1} \\
b^{c3} &= \left(\frac{\xi_{27}+i\xi_{28}}{2\sqrt{\frac{1}{3}}}+\frac{\xi_{29}-i\xi_{30}}{2\sqrt{5}}+\frac{\xi_{31}-i\xi_{32}}{\sqrt{30}}\right)e^{i\sigma_1} \\
\nu_e &= \left(\frac{\xi_{29}+i\xi_{30}}{2\sqrt{5}}-\frac{\xi_{31}+i\xi_{32}}{\sqrt{30}}\right)e^{i(\sigma_1+\sigma_2+\sigma_3)} \\
\nu_\mu &= \left(\frac{\xi_{31}+i\xi_{32}}{\sqrt{\frac{6}{5}}}\right)e^{i(\sigma_1-\sigma_2+\sigma_3)} \\
\nu_\tau &= \left(\frac{\xi_{15}-i\xi_{16}}{\sqrt{2}}+\frac{\xi_{21}-i\xi_{22}}{\sqrt{6}}+\frac{\xi_{27}-i\xi_{28}}{2\sqrt{3}}-\frac{\xi_{29}+i\xi_{30}}{2\sqrt{5}}-\frac{\xi_{31}+i\xi_{32}}{\sqrt{30}}\right)e^{i(\sigma_1-2\sigma_3)}.
\end{aligned}
$$

The non-zero elements of the U-matrix are

$$
\begin{aligned}
U_{4,1} &= U_{5,1} = U_{6,1} = U_{10,1} = \frac{\sigma'_1}{\sqrt{7}} \\
U_{7,1} &= = \frac{\sigma'_1 + \sigma'_2 + \sigma'_3}{\sqrt{7}} \\
U_{7,2} &= = \frac{\sigma'_1 + \sigma'_2 + \sigma'_3}{\sqrt{2}} \\
U_{7,3} &= = \frac{\sigma'_1 + \sigma'_2 + \sigma'_3}{\sqrt{6}} \\
U_{8,1} &= \frac{\sigma'_1 - \sigma'_2 + \sigma'_3}{\sqrt{7}} \\
U_{8,2} &= \frac{\sigma'_1 - \sigma'_2 + \sigma'_3}{\sqrt{2}} \\
U_{8,3} &= \frac{\sigma'_1 - \sigma'_2 + \sigma'_3}{\sqrt{6}} \\
U_{9,1} &= \frac{\sigma'_1 - 2\sigma'_3}{\sqrt{7}} \\
U_{3,9} &= \frac{\sigma'_1 - 2\sigma'_3}{\sqrt{\frac{3}{2}}} \\
U_{15,16} &= \sigma'_3 \\
U_{20,15} &= U_{16,19} = \frac{\sigma'_1 - \sigma'_3}{\sqrt{3}} \\
U_{22,15} &= U_{16,21} = \frac{\sigma'_1 - \sigma'_3}{\sqrt{6}} \\
U_{24,15} &= U_{23,16} = \frac{\sigma'_1 - \sigma'_3}{\sqrt{10}} \\
U_{26,15} &= U_{25,16} = \frac{\sigma'_1 - \sigma'_3}{\sqrt{15}} \\
U_{19,20} &= \frac{2\sigma'_1 + \sigma'_3}{3} \\
U_{22,19} &= U_{20,21} = \frac{\sigma'_1 - \sigma'_3}{3\sqrt{2}} \\
U_{24,19} &= U_{23,20} = \frac{\sigma'_1 - \sigma'_3}{\sqrt{30}} \\
U_{26,19} &= U_{25,20} = \frac{\sigma'_1 - \sigma'_3}{3\sqrt{5}} \\
U_{21,22} &= \frac{5\sigma'_1 + \sigma'_3}{6} \\
U_{24,21} &= U_{23,22} = \frac{\sigma'_1 - \sigma'_3}{2\sqrt{15}} \\
U_{26,21} &= U_{25,22} = \frac{\sigma'_1 - \sigma'_3}{3\sqrt{10}} \\
U_{23,24} &= \frac{7\sigma'_1 + 8\sigma'_2 + 7\sigma'_3}{10} \\
U_{26,23} &= U_{24,25} = \frac{3\sigma'_1 + 2\sigma'_2 + 3\sigma'_3}{5\sqrt{6}} \\
U_{25,26} &= \frac{4\sigma'_1 - 4\sigma'_2 + 4\sigma'_3}{5}
\end{aligned}
\tag{7.44}
$$

and their antisymmetric counterparts.

The mass matrix for the physical excitations appears as (in units of φ^2)

$$
\begin{aligned}
M_{4,4} &= M_{5,5} = M_{6,6} = \frac{g_1^2}{9} + g_2^2 + \frac{4g_3^2}{3} \\
M_{4,5} &= M_{4,6} = M_{5,6} = \frac{g_1^2}{9} + g_2^2 - \frac{2g_3^2}{3} \\
M_{4,7} &= M_{4,8} = M_{4,9} = M_{5,7} = M_{5,8} = M_{5,9} = M_{6,7} = M_{6,8} = M_{6,9} = \frac{-g_1^2}{3} - g_2^2 \\
M_{4,10} &= M_{5,10} = \frac{2g_1^2}{3} \\
M_{7,7} &= M_{7,8} = M_{7,9} = M_{8,8} = M_{8,9} = M_{9,9} = g_1^2 + g_2^2 \\
M_{7,10} &= = M_{8,10} = M_{9,10} = -2g_1^2 \\
M_{10,10} &= 4g_1^2 \\
M_{11,11} &= M_{12,12} = M_{13,13} = M_{14,14} = M_{17,17} = M_{18,18} = 2g_3^2 \\
M_{15,15} &= M_{16,16} = 2g_2^2 \\
M_{15,19} &= M_{16,20} = \frac{2g_2^2}{\sqrt{3}} \\
M_{15,21} &= M_{16,22} = \frac{\sqrt{2}g_2^2}{\sqrt{3}} \\
M_{15,23} &= -M_{16,24} = \frac{3\sqrt{2}g_2^2}{\sqrt{5}} \\
M_{15,25} &= -M_{16,26} = \frac{2\sqrt{3}g_2^2}{\sqrt{5}} \\
M_{19,19} &= M_{20,20} = \frac{2g_2^2}{3} \\
M_{19,21} &= M_{20,22} = \frac{\sqrt{2}g_2^2}{3} \\
M_{19,23} &= -M_{20,24} = \frac{\sqrt{6}g_2^2}{\sqrt{5}} \\
M_{19,25} &= -M_{20,26} = \frac{2g_2^2}{\sqrt{5}} \\
M_{21,21} &= M_{22,22} = \frac{g_2^2}{3} \\
M_{21,23} &= -M_{22,24} = \frac{\sqrt{3}g_2^2}{\sqrt{5}} \\
M_{21,25} &= -M_{22,26} = \frac{\sqrt{2}g_2^2}{\sqrt{5}} \\
M_{23,23} &= M_{24,24} = \frac{9g_2^2}{5} \\
M_{23,25} &= M_{24,26} = \frac{3\sqrt{6}g_2^2}{5} \\
M_{25,25} &= M_{26,26} = \frac{6g_2^2}{5}
\end{aligned}
\tag{7.45}
$$

and their symmetric counterparts. The eigenvalues are $M_1^2 = \frac{11g_1^2+9g_2^2+\sqrt{121g_1^4-54g_1^2g_2^2+81g_2^4}}{3}\varphi^2$, $M_2^2 = \frac{11g_1^2+9g_2^2-\sqrt{121g_1^4-54g_1^2g_2^2+81g_2^4}}{3}\varphi^2$,$M_3^2 = M_4^2 = 6g_2^2\varphi^2, M_5^2 = M_6^2 = M_7^2 = M_8^2 = M_9^2 = M_{10}^2 = M_{11}^2 = M_{12}^2 = 2g_3^2\varphi^2$,$M_{13}^2 = ... = M_{26}^2 = 0$.

The J-matrix is (really:The J-matrix can be - the splitting of eigenspaces of higher dimensions into subspaces is arbitrary)

$$J_{4,13} = -J_{3,14} = \frac{-\sqrt{k}+\sqrt{k+\frac{6g_2^2\varphi^2}{k}}}{4\sqrt{2}(k^2+6g_2^2\varphi^2)^{\frac{1}{4}}}\left(\sigma_2' - 2\sigma_3'\right)$$

$$J_{3,16} = -J_{4,15} = \frac{-\sqrt{k}+\sqrt{k+\frac{6g_2^2\varphi^2}{k}}}{4\sqrt{30}(k^2+6g_2^2\varphi^2)^{\frac{1}{4}}}\left(5\sigma_2' + 6\sigma_3'\right)$$

$$J_{4,17} = J_{3,18} = -\frac{\sqrt{3}(-\sqrt{k}+\sqrt{k+\frac{6g_2^2\varphi^2}{k}})}{4\sqrt{10}(k^2+6g_2^2\varphi^2)^{\frac{1}{4}}}\sigma_3'$$

$$J_{4,19} = J_{3,20} = -\frac{-\sqrt{k}+\sqrt{k+\frac{6g_2^2\varphi^2}{k}}}{4\sqrt{2}(k^2+6g_2^2\varphi^2)^{\frac{1}{4}}}\sigma_3'$$

$$J_{1,24} = \frac{\left(g_1^2+9g_2^2+\sqrt{121g_1^4-54g_1^2g_2^2+81g_2^4}\right)\left(-3\sqrt{k}+\sqrt{\frac{9k^2+3(11g_1^2+9g_2^2+\sqrt{121g_1^4-54g_1^2g_2^2+81g_2^4})\varphi^2}{k}}\right)}{3^{\frac{3}{4}}8\sqrt{14}g_1^2\sqrt{\frac{\sqrt{121g_1^4-54g_1^2g_2^2+81g_2^4}}{3g_1^2-9g_2^2+\sqrt{121g_1^4-54g_1^2g_2^2+81g_2^4}}}\left(3k^2+\left(11g_1^2+9g_2^2+\sqrt{121g_1^4-54g_1^2g_2^2+81g_2^4}\right)\varphi^2\right)^{\frac{1}{4}}}\sigma_3' \tag{7.46}$$

$$J_{1,25} = \frac{\left(g_1^2+9g_2^2+\sqrt{121g_1^4-54g_1^2g_2^2+81g_2^4}\right)\left(-3\sqrt{k}+\sqrt{\frac{3k^2+3(11g_1^2+9g_2^2+\sqrt{121g_1^4-54g_1^2g_2^2+81g_2^4})\varphi^2}{k}}\right)}{3^{\frac{3}{4}}8\sqrt{14}g_1^2\sqrt{\frac{\sqrt{121g_1^4-54g_1^2g_2^2+81g_2^4}}{3g_1^2-9g_2^2+\sqrt{121g_1^4-54g_1^2g_2^2+81g_2^4}}}\left(3k^2+\left(11g_1^2+9g_2^2+\sqrt{121g_1^4-54g_1^2g_2^2+81g_2^4}\right)\varphi^2\right)^{\frac{1}{4}}}\sigma_2'$$

$$J_{2,24} = \frac{\left(g_1^2+9g_2^2-\sqrt{121g_1^4-54g_1^2g_2^2+81g_2^4}\right)\left(-3\sqrt{k}+\sqrt{\frac{9k^2+3(11g_1^2+9g_2^2-\sqrt{121g_1^4-54g_1^2g_2^2+81g_2^4})\varphi^2}{k}}\right)}{3^{\frac{3}{4}}8\sqrt{14}g_1^2\sqrt{\frac{\sqrt{121g_1^4-54g_1^2g_2^2+81g_2^4}}{-3g_1^2+9g_2^2+\sqrt{121g_1^4-54g_1^2g_2^2+81g_2^4}}}\left(3k^2+\left(11g_1^2+9g_2^2-\sqrt{121g_1^4-54g_1^2g_2^2+81g_2^4}\right)\varphi^2\right)^{\frac{1}{4}}}\sigma_3'$$

$$J_{2,25} = \frac{\left(g_1^2+9g_2^2-\sqrt{121g_1^4-54g_1^2g_2^2+81g_2^4}\right)\left(-3\sqrt{k}+\sqrt{\frac{3k^2+3(11g_1^2+9g_2^2-\sqrt{121g_1^4-54g_1^2g_2^2+81g_2^4})\varphi^2}{k}}\right)}{3^{\frac{3}{4}}8\sqrt{14}g_1^2\sqrt{\frac{\sqrt{121g_1^4-54g_1^2g_2^2+81g_2^4}}{-3g_1^2+9g_2^2+\sqrt{121g_1^4-54g_1^2g_2^2+81g_2^4}}}\left(3k^2+\left(11g_1^2+9g_2^2-\sqrt{121g_1^4-54g_1^2g_2^2+81g_2^4}\right)\varphi^2\right)^{\frac{1}{4}}}\sigma_2'$$

and their symmetric counterparts.

Here the J matrix show rotation between states 1-4 and the light states, giving particle production and possible preheating. The reason that the SU(3) states do not rotate is that the 3 Q's have the same SU(2)-charge, and the 2

diagonal SU(3) generators have removed the phases between them.

In fact, changing the assignments such that the quarks have split SU(2)-charges will change something, even the eigenvalues, but it will not change that J is nonzero and preheating is possible.

7.7 One Flat direction - summary

For the 2 flat directions mentioned as the most obvious candidate to be the inflaton in [6], QLD^c and LLE^c, we find no preheating. The reason [12] found differently with a toy model direction of 3 superfields was that it was rather special to have 3 VEV-fields and only 1 broken generator. When only 1 generator was broken, only one phase difference was removed, and the second phase difference gave the preheating. However, for LLE^c and $U^cD^cD^c$ 2 diagonal generators are broken and there is no preheating due to the diagonal generators. We think, inspired by [9], it makes sense to split the involved fields in those connected to VEV's by the diagonal generators (from here: Sector 1), and those connected to the VEV by the off-diagonal generators (from here: Sector 2). In this case, and we suspect in most others, the structure of Sector 2, is that the massive states are Higgses, and they all have the same eigenvalue. Therefore rotation does not have an effect (in fact, rotation does not make sense, since one cannot distinguish the eigenstates). In QLD^c though, they have different eigenvalues - some fields connected to the VEV through $SU(2)$, others through $SU(3)_c$. However, for each field it is either or. Any difference from this, should be if a field is connected to 2 VEV's, one by a $SU(2)$ and one by a $SU(3)_c$ generator. For Sector 1, it would take more than 3 fields (or less than 2 broken generators). This is what happens in $QLQLQLE^c$. We can gauge away 4 phase differences, but this leaves 2 phase differences that can give the preheating. There could also be a mixing between sectors, if a field was connected to 1 VEV by a diagonal generator and to another by an off-diagonal one. However, this seems impossible for a single flat direction.

7.8 $U^cD^cD^c$, LLE^c simultaniously

The 2 directions first presented can co-exist. In fact, there is no reason why they should not both get large VEV's [9]. It is not so easy to argue why there should be no preheating - since now we have 6 Sector 1 fields, and only 4 diagonal generators to break.

$$\begin{aligned} < u^{c\bar{1}} > &= \varphi e^{i\sigma_1} \\ < s^{c\bar{2}} > &= \varphi e^{i\sigma_2} \\ < b^{c\bar{3}} > &= \varphi e^{i\sigma_3} \\ < \nu_e > &= A\varphi e^{i\sigma_4} \\ < \mu > &= A\varphi e^{i\sigma_5} \\ < \tau^c > &= A\varphi e^{i\sigma_6} \end{aligned} \tag{7.47}$$

where A is the relation between the absolute value of the VEV's involved. The Lagrangian reads

$$\mathcal{L} = \sum_{i=1}^{3} \frac{1}{2}|D_\mu \Phi_i|^2 - V - \frac{1}{4}F_{\mu\nu}^2 - \frac{1}{4}\sum_i W_{\mu\nu}^{i2} - \frac{1}{4}\sum_i G_{\mu\nu}^{i2} \tag{7.48}$$

where for field ϕ_i $D_i^\mu = \left[(\partial^\mu - iq_i A_0^\mu)\delta_{ij} - \sum_{a=1}^{3} iP_{ij}^a A_a^\mu - \sum_{A=1}^{8} iGM_{ij}^A B_A^\mu\right]\phi_j$ denotes the covariant derivative. The potential now looks like

$$V = \frac{1}{2}\left(D_H^2 + \sum_a D_a^2 + \sum_A D_A^2\right). \tag{7.49}$$

To remove mixed kinetic terms we must reparametrise

$$\begin{aligned}
u^{c\bar{1}} &= (\varphi + \xi_2)e^{i(\sigma_1 + \frac{\xi_1}{\sqrt{3}\varphi})}, \\
u^{c\bar{2}} &= \frac{\xi_5 + i\xi_6}{\sqrt{2}}e^{i\sigma_1}, \\
u^{c\bar{3}} &= \frac{\xi_7 + i\xi_8}{\sqrt{2}}e^{i\sigma_1}, \\
s^{c\bar{1}} &= \frac{\xi_5 - i\xi_6}{\sqrt{2}}e^{i\sigma_1}, \\
s^{c\bar{2}} &= (\varphi + \xi_3)e^{i(\sigma_1 + \frac{\xi_1}{\sqrt{3}\varphi})} \\
s^{c\bar{3}} &= \frac{\xi_9 + i\xi_{10}}{\sqrt{2}}e^{i\sigma_1}, \\
b^{c\bar{1}} &= \frac{\xi_7 - i\xi_8}{\sqrt{2}}e^{i\sigma_1}, \\
b^{c\bar{2}} &= \frac{\xi_9 - i\xi_{10}}{\sqrt{2}}e^{i\sigma_1}, \\
b^{c\bar{3}} &= (\varphi + \xi_4)e^{i(\sigma_1 + \frac{\xi_1}{\sqrt{3}\varphi})} \\
\nu_e &= (A\varphi + \xi_{12})e^{i(\sigma_2 + \frac{\xi_{11}}{\sqrt{3}A\varphi})}, \\
e &= \frac{\xi_{15} + i\xi_{16}}{\sqrt{2}}e^{i\sigma_2}, \\
\nu_\mu &= \frac{\xi_{15} - i\xi_{16}}{\sqrt{2}}e^{i\sigma_2}, \\
\mu &= (A\varphi + \xi_{13})e^{i(\sigma_2 + \frac{\xi_{11}}{\sqrt{3}A\varphi})} \\
\tau^c &= (A\varphi + \xi_{14})e^{i(\sigma_2 + \frac{\xi_{11}}{\sqrt{3}A\varphi})}
\end{aligned} \tag{7.50}$$

After verifying that the mixed derivatives have indeed been removed, we use coordinate derivatives, and find the remaining kinetic terms (those not to second

order) to be: (to zero'th order in φ)

$$\begin{aligned}\mathcal{L} \;\supset\; & \sum_{i=1}^{16}\left(\frac{1}{2}\dot{\xi_i}^2\right)+\sum_{i=2}^{10}\left(\frac{1}{2}\xi_i^2\dot{\sigma_1}^2\right)+\sum_{i=12}^{16}\left(\frac{1}{2}\xi_i^2\dot{\sigma_2}^2\right)\\ & +\sum_{i=2}^{4}\left(\varphi\xi_i\dot{\sigma_1}^2+\frac{2}{\sqrt{3}}\xi_i\dot{\xi_1}\right)+\sum_{i=12}^{14}\left(A\varphi\xi_i\dot{\sigma_2}^2+\frac{2}{\sqrt{3}}\xi_i\dot{\xi_{11}}\right) \qquad (7.51)\\ & +\frac{3}{2}\varphi^2\dot{\sigma_1}^2+\frac{3}{2}A^2\varphi^2\dot{\sigma_2}^2+\sqrt{3}\varphi\dot{\sigma_1}\dot{\xi_1}+\sqrt{3}A\varphi\dot{\sigma_2}\dot{\xi_{11}}.\end{aligned}$$

It seems the 2 directions do not "see" each other. We find (after antisymmetrising)

$$U=\begin{pmatrix}
0 & -\frac{\dot{\sigma_1}}{\sqrt{3}} & -\frac{\dot{\sigma_1}}{\sqrt{3}} & -\frac{\dot{\sigma_1}}{\sqrt{3}} & 0 & 0 & 0 & 0 & 0 & 0 & 0 & 0 & 0 & 0 & 0 & 0\\
\frac{\dot{\sigma_1}}{\sqrt{3}} & 0 & 0 & 0 & 0 & 0 & 0 & 0 & 0 & 0 & 0 & 0 & 0 & 0 & 0 & 0\\
\frac{\dot{\sigma_1}}{\sqrt{3}} & 0 & 0 & 0 & 0 & 0 & 0 & 0 & 0 & 0 & 0 & 0 & 0 & 0 & 0 & 0\\
\frac{\dot{\sigma_1}}{\sqrt{3}} & 0 & 0 & 0 & 0 & 0 & 0 & 0 & 0 & 0 & 0 & 0 & 0 & 0 & 0 & 0\\
0 & 0 & 0 & 0 & 0 & 0 & 0 & 0 & 0 & 0 & 0 & 0 & 0 & 0 & 0 & 0\\
0 & 0 & 0 & 0 & 0 & 0 & 0 & 0 & 0 & 0 & 0 & 0 & 0 & 0 & 0 & 0\\
0 & 0 & 0 & 0 & 0 & 0 & 0 & 0 & 0 & 0 & 0 & 0 & 0 & 0 & 0 & 0\\
0 & 0 & 0 & 0 & 0 & 0 & 0 & 0 & 0 & 0 & 0 & 0 & 0 & 0 & 0 & 0\\
0 & 0 & 0 & 0 & 0 & 0 & 0 & 0 & 0 & 0 & 0 & 0 & 0 & 0 & 0 & 0\\
0 & 0 & 0 & 0 & 0 & 0 & 0 & 0 & 0 & 0 & 0 & 0 & 0 & 0 & 0 & 0\\
0 & 0 & 0 & 0 & 0 & 0 & 0 & 0 & 0 & 0 & 0 & -\frac{\dot{\sigma_2}}{\sqrt{3}} & -\frac{\dot{\sigma_2}}{\sqrt{3}} & -\frac{\dot{\sigma_2}}{\sqrt{3}} & 0 & 0\\
0 & 0 & 0 & 0 & 0 & 0 & 0 & 0 & 0 & 0 & \frac{\dot{\sigma_2}}{\sqrt{3}} & 0 & 0 & 0 & 0 & 0\\
0 & 0 & 0 & 0 & 0 & 0 & 0 & 0 & 0 & 0 & \frac{\dot{\sigma_2}}{\sqrt{3}} & 0 & 0 & 0 & 0 & 0\\
0 & 0 & 0 & 0 & 0 & 0 & 0 & 0 & 0 & 0 & \frac{\dot{\sigma_2}}{\sqrt{3}} & 0 & 0 & 0 & 0 & 0\\
0 & 0 & 0 & 0 & 0 & 0 & 0 & 0 & 0 & 0 & 0 & 0 & 0 & 0 & 0 & 0\\
0 & 0 & 0 & 0 & 0 & 0 & 0 & 0 & 0 & 0 & 0 & 0 & 0 & 0 & 0 & 0
\end{pmatrix}$$

This looks as if the 2 parts are completely separated. The mass matrix for the physical excitations appears as

$$\mathcal{M}^2=\varphi^2 \qquad (7.52)$$

$$\begin{pmatrix}
0 & 0 & 0 & 0 & 0 & 0 & 0 & 0 & 0 & 0 & 0 & 0 & 0 & 0 & 0 & 0\\
0 & \frac{16g_1^2+12g_3^2}{9} & \frac{-8g_1^2-6g_3^2}{9} & \frac{8g_1^2+6g_3^2}{9} & 0 & 0 & 0 & 0 & 0 & 0 & 0 & \frac{4Ag_1^2}{3} & \frac{4Ag_1^2}{3} & \frac{-8Ag_1^2}{3} & 0 & 0\\
0 & \frac{-8g_1^2-6g_3^2}{9} & \frac{4g_1^2+12g_3^2}{9} & \frac{4g_1^2-6g_3^2}{9} & 0 & 0 & 0 & 0 & 0 & 0 & 0 & \frac{-2Ag_1^2}{3} & \frac{-2Ag_1^2}{3} & \frac{4Ag_1^2}{3} & 0 & 0\\
0 & \frac{-8g_1^2-6g_3^2}{9} & \frac{4g_1^2-6g_3^2}{9} & \frac{4g_1^2+12g_3^2}{9} & 0 & 0 & 0 & 0 & 0 & 0 & 0 & \frac{-2Ag_1^2}{3} & \frac{-2Ag_1^2}{3} & \frac{4Ag_1^2}{3} & 0 & 0\\
0 & 0 & 0 & 0 & 2g_3^2 & 0 & 0 & 0 & 0 & 0 & 0 & 0 & 0 & 0 & 0 & 0\\
0 & 0 & 0 & 0 & 0 & 2g_3^2 & 0 & 0 & 0 & 0 & 0 & 0 & 0 & 0 & 0 & 0\\
0 & 0 & 0 & 0 & 0 & 0 & 2g_3^2 & 0 & 0 & 0 & 0 & 0 & 0 & 0 & 0 & 0\\
0 & 0 & 0 & 0 & 0 & 0 & 0 & 2g_3^2 & 0 & 0 & 0 & 0 & 0 & 0 & 0 & 0\\
0 & 0 & 0 & 0 & 0 & 0 & 0 & 0 & 2g_3^2 & 0 & 0 & 0 & 0 & 0 & 0 & 0\\
0 & 0 & 0 & 0 & 0 & 0 & 0 & 0 & 0 & 2g_3^2 & 0 & 0 & 0 & 0 & 0 & 0\\
0 & 0 & 0 & 0 & 0 & 0 & 0 & 0 & 0 & 0 & 0 & 0 & 0 & 0 & 0 & 0\\
0 & \frac{4Ag_1^2}{3} & \frac{-2Ag_1^2}{3} & \frac{-2Ag_1^2}{3} & 0 & 0 & 0 & 0 & 0 & 0 & 0 & A^2g_1^2+A^2g_2^2 & A^2g_1^2-A^2g_2^2 & -2A^2g_1^2 & 0 & 0\\
0 & \frac{4Ag_1^2}{3} & \frac{-2Ag_1^2}{3} & \frac{-2Ag_1^2}{3} & 0 & 0 & 0 & 0 & 0 & 0 & 0 & A^2g_1^2-A^2g_2^2 & A^2g_1^2+A^2g_2^2 & -2A^2g_1^2 & 0 & 0\\
0 & \frac{-8Ag_1^2}{3} & \frac{4Ag_1^2}{3} & \frac{4Ag_1^2}{3} & 0 & 0 & 0 & 0 & 0 & 0 & 0 & -2A^2g_1^2 & -2A^2g_1^2 & 4A^2g_1^2 & 0 & 0\\
0 & 0 & 0 & 0 & 0 & 0 & 0 & 0 & 0 & 0 & 0 & 0 & 0 & 0 & 2A^2g_2^2 & 0\\
0 & 0 & 0 & 0 & 0 & 0 & 0 & 0 & 0 & 0 & 0 & 0 & 0 & 0 & 0 & 2A^2g_3^2
\end{pmatrix}$$

(7.53)

with eigenvalues

$$\begin{aligned}
M_1^2 &= \left(\frac{4+9A^2}{3}g_1^2+g_3^2+\frac{1}{3}\sqrt{(4+9A^2)^2g_1^4-6(-4+9A^2)g_1^2g_3^2+9g_3^4}\right)\varphi^2 \\
M_2^2 &= \left(\frac{4+9A^2}{3}g_1^2+g_3^2-\frac{1}{3}\sqrt{(4+9A^2)^2g_1^4-6(-4+9A^2)g_1^2g_3^2+9g_3^4}\right)\varphi^2 \\
M_3^2 &= M_4^2=M_5^2=M_6^2=M_7^2=M_8^2=M_9^2=2g_3^2\varphi^2 \\
M_{10}^2 &= M_{11}^2=M_{12}^2=2A^2g_2^2\varphi^2 \\
M_{13}^2 &= M_{14}^2=M_{15}^2=M_{16}^2=0.
\end{aligned} \tag{7.54}$$

Even though this indeed looks like a mixing between the two directions, again $J = 0$ (16 by 16 matrix) and there is no particle production and therefore no preheating.

7.9 $QLD^c + LLE^c$ - an overlapping direction

While $U^cD^cD^+LLE^c$ shows that more than 1 phase is not enough to secure preheating, it is clear that the 2 directions did not overlap. There are flat directions more intimately connected. One example of this is $QLD^c + LLE^c$ - with one L-field in common. This is exiting, since here the flat directions cannot just have one phase each. Q and D^c must be from different generations and have the same (or opposite, if you like) colour charge. It is easy to show that flatness is independent of phase, and that the common field shall have a VEV that is the square root of the sum of squares of the VEV's from the 2 directions.

$$\begin{aligned}
< d^{c^1} > &= A\varphi e^{i\sigma_4} \\
< s^{c^{\bar{1}}} > &= A\varphi e^{i\sigma_5} \\
< \nu_e > &= \sqrt{1+A^2}\varphi e^{i\sigma_3} \\
< \mu > &= \varphi e^{i\sigma_2} \\
< \tau^c > &= \varphi e^{i\sigma_1}
\end{aligned} \tag{7.55}$$

where A is the relation between the absolute values of the VEV's. The Lagrangian, covariant derivatives and the potential looks as before.

To remove mixed kinetic terms, we must re-parameterise

$$
\begin{aligned}
u^{c^1} &= \left(\frac{\xi_8 + i\xi_9}{\sqrt{1+A^2}} + \frac{A(\xi_{14} - i\xi_{15})}{\sqrt{2(1+A^2)}}\right) e^{i\left(\sigma + \left(-1 - \frac{1-A^2}{5(1+A^2)}\right)\gamma\right)} \\
d^{c^1} &= (A\varphi + \xi_4) e^{i\left((\sigma + \frac{1}{\sqrt{5}}\xi_6) + \left(-1 - \frac{1-A^2}{5(1+A^2)}\right)\left(\gamma + \frac{\sqrt{5}(1+A^2)}{2\sqrt{6+8A^2+6A^4}}\xi_7\right)\right)} \\
d^{c^2} &= \frac{\xi_{10} + i\xi_{11}}{\sqrt{2}} e^{i\left(\sigma + \left(-1 - \frac{1-A^2}{5(1+A^2)}\right)\gamma\right)} \\
d^{c^3} &= \frac{\xi_{12} + i\xi_{13}}{\sqrt{2}} e^{i\left(\sigma + \left(-1 - \frac{1-A^2}{5(1+A^2)}\right)\gamma\right)} \\
s^{c\bar{1}} &= (A\varphi + \xi_5) e^{i\left((\sigma + \frac{1}{\sqrt{5}}\xi_6) + \left(-1 - \frac{1-A^2}{5(1+A^2)}\right)\left(\gamma + \frac{\sqrt{5}(1+A^2)}{2\sqrt{6+8A^2+6A^4}}\xi_7\right)\right)} \\
s^{c\bar{2}} &= \frac{-\xi_{10} + i\xi_{11}}{\sqrt{2}} e^{i\left(\sigma + \left(-1 - \frac{1-A^2}{5(1+A^2)}\right)\gamma\right)} \\
s^{c\bar{3}} &= \frac{-\xi_{12} + i\xi_{13}}{\sqrt{2}} e^{i\left(\sigma + \left(-1 - \frac{1-A^2}{5(1+A^2)}\right)\gamma\right)} \\
\nu_e &= (\sqrt{1+A^2}\varphi + \xi_3) e^{i\left((\sigma + \frac{1}{\sqrt{5}}\xi_6) + \frac{4(1-A^2)}{5(1+A^2)}\left(\gamma + \frac{\sqrt{5}(1+A^2)}{2\sqrt{6+8A^2+6A^4}}\xi_7\right)\right)} \\
e &= \frac{\xi_{14} + i\xi_{15}}{\sqrt{2}} e^{i\left(\sigma + \frac{4(1-A^2)}{5(1+A^2)}\gamma\right)} \\
\nu_\mu &= \left(\frac{-A(\xi_8 + i\xi_9)}{\sqrt{1+A^2}} + \frac{\xi_{14} - i\xi_{15}}{\sqrt{2(1+A^2)}}\right) e^{i\left(\sigma + \left(1 - \frac{1-A^2}{5(1+A^2)}\right)\gamma\right)} \\
\mu &= (\varphi + \xi_2) e^{i\left((\sigma + \frac{1}{\sqrt{5}}\xi_6) + \left(1 - \frac{1-A^2}{5(1+A^2)}\right)\left(\gamma + \frac{\sqrt{5}(1+A^2)}{2\sqrt{6+8A^2+6A^4}}\xi_7\right)\right)} \\
\tau^c &= (\varphi + \xi_1) e^{i\left((\sigma + \frac{1}{\sqrt{5}}\xi_6) + \left(1 - \frac{1-A^2}{5(1+A^2)}\right)\left(\gamma + \frac{\sqrt{5}(1+A^2)}{2\sqrt{6+8A^2+6A^4}}\xi_7\right)\right)}
\end{aligned}
\tag{7.56}
$$

There are quite many kinetic terms now, but they include

$$
\mathcal{L} \supset \sum_{i=1}^{15} \left(\frac{1}{2}\dot{\xi_i}^2\right) \tag{7.57}
$$

and no cross terms. The U-matrix is (after antisymmetrising)

$$\begin{aligned}
U_{1,6} &= -U_{6,1} = U_{2,6} = -U_{6,2} = \frac{(4+6A^2)\dot{\gamma} + 5(1+A^2)\dot{\sigma}}{5\sqrt{5}(1+A^2)} \\
U_{1,7} &= -U_{7,1} = U_{2,7} = -U_{7,2} = \frac{(2+3A^2)((4+6A^2)\dot{\gamma} + 5(1+A^2)\dot{\sigma})}{5\sqrt{10}(1+A^2)\sqrt{3+4A^2+3A^4}} \\
U_{3,6} &= -U_{6,3} = \frac{4(1-A^2)\dot{\gamma} + 5(1+A^2)\dot{\sigma}}{5\sqrt{5}(1+A^2)} \\
U_{3,7} &= -U_{7,3} = \frac{\sqrt{2}(-1+A^2)(4(-1+A^2)\dot{\gamma} - 5(1+A^2)\dot{\sigma})}{5\sqrt{5}(1+A^2)\sqrt{3+4A^2+3A^4}} \\
U_{4,6} &= -U_{6,4} = U_{5,6} = -U_{6,5} = \frac{-(6+4A^2)\dot{\gamma} + 5(1+A^2)\dot{\sigma}}{5\sqrt{5}(1+A^2)} \\
U_{4,7} &= -U_{7,4} = U_{5,7} = -U_{7,5} = \frac{(3+2A^2)((6+4A^2)\dot{\gamma} - 5(1+A^2)\dot{\sigma})}{5\sqrt{10}(1+A^2)\sqrt{3+4A^2+3A^4}} \\
U_{8,9} &= -U_{9,8} = \frac{6(-1+A^2)\dot{\gamma}}{5(1+A^2)} + \dot{\sigma} \\
U_{8,15} &= -U_{15,8} = U_{9,14} = -U_{14,9} = \frac{\sqrt{2}A\dot{\gamma}}{(1+A^2)} \\
U_{remaining} &= 0.
\end{aligned} \tag{7.58}$$

This looks as if everything mixes - certainly it does not look as if there are 2 separable parts. The mass matrix is quite complicated, but the structure is like this

$$\mathcal{M}^2 = \varphi^2 \begin{pmatrix} M_{7\times 7} & 0_{7\times 8} \\ 0_{8\times 7} & D_{8\times 8} \end{pmatrix} \tag{7.59}$$

where M is the mass matrix (with no 0-entries) for the previously mentioned sector 1, while D is a diagonal matrix which is for the previously mentioned sector 2. So, the sectors are clearly separated. The sector 1 part, has 3 very complicated eigenvalues, and zero is eigenvalue with multiplicity of 4. The sector 2 part has eigenvalues (entries) ordered after the ξ-fields:
$(0, 0, 2A^2 g_3^2, 2A^2 g_3^2, 2A^2 g_3^2, 2A^2 g_3^2, 2(1+A^2) g_2^2, 2(1+A^2) g_2^2)\varphi^2$. Also, it is important to notice that M is time-dependant. All the elements involving 6 or 7 are time dependent.

The elements (symmetry implied) are

$$
\begin{aligned}
M_{1,1} &= 4g_1^2, M_{1,2} = -2g_1^2, M_{1,3} = -2\sqrt{1+A^2}g_1^2, M_{1,4} = \frac{2Ag_1^2}{3}, M_{1,5} = \frac{4Ag_1^2}{3} \\
M_{2,2} &= g_1^2 + g_2^2, M_{2,3} = \sqrt{1+A^2}(g_1^2 - g_2^2), M_{2,4} = A((-g_1^2/3) + g_2^2), M_{2,5} = \frac{-2Ag_1^2}{3} \\
M_{3,3} &= (1+A^2)(g_1^2+g_2^2), M_{3,4} = -\tfrac{1}{3}A\sqrt{1+A^2}(g_1^2+3g_2^2), M_{3,5} = -\tfrac{2}{3}A\sqrt{1+A^2}g_1^2 \\
M_{4,4} &= \frac{A^2(g_1^2+9g_2^2+12g_3^2)}{9}, M_{4,5} = \frac{2(g_1^2-6g_3^2)A^2}{9}, M_{5,5} = \frac{4A^2(g_1^2+3g_3^2)}{9} \\
M_{1,6} &= \frac{2g_1^2\left((1+A^2)\sin[\frac{8(-1+A^2)\gamma}{5(1+A^2)} - 2\sigma] + \sqrt{1+A^2}\left(-A\sin[\frac{4((3+2A^2)\gamma)}{5(1+A^2)} - 2\sigma] + \sin[\frac{4(2+3A^2)\gamma}{5(1+A^2)} + 2\sigma]\right)\right)}{\sqrt{5}\sqrt{1+A^2}} \\
M_{1,7} &= \frac{\sqrt{\frac{2}{5}}g_1^2\left(2(1-A^4)\sin[\frac{8(-1+A^2)\gamma}{5(1+A^2)} - 2\sigma] + \sqrt{1+A^2}\left(A(3+2A^2)\sin[\frac{4(3+2A^2)\gamma}{5(1+A^2)} - 2\sigma] + (2+3A^2)\sin[\frac{4(2+3A^2)\gamma}{5(1+A^2)} + 2\sigma]\right)\right)}{\sqrt{3+7A^2+7A^4+3A^6}} \\
M_{2,6} &= -\frac{(g_1^2-g_2^2)\left((1+A^2)\sin[\frac{8(-1+A^2)\gamma}{5(1+A^2)} - 2\sigma] + \sqrt{1+A^2}\left(-A\sin[\frac{4(3+2A^2)\gamma}{5(1+A^2)} - 2\sigma] + \sin[\frac{4(2+3A^2)\gamma}{5(1+A^2)} + 2\sigma]\right)\right)}{\sqrt{5}\sqrt{1+A^2}} \\
M_{2,7} &= \frac{(g_1^2-g_2^2)\left(2(A^4-1)\sin[\frac{8(-1+A^2)\gamma}{5(1+A^2)} - 2\sigma] - \sqrt{1+A^2}\left(A(3+2A^2)\sin[\frac{4(3+2A^2)\gamma}{5(1+A^2)} - 2\sigma] + (2+3A^2)\sin[\frac{4(2+3A^2)\gamma}{5(1+A^2)} + 2\sigma]\right)\right)}{\sqrt{10}\sqrt{3+7A^2+7A^4+3A^6}} \\
M_{3,6} &= -\frac{(g_1^2+g_2^2)\left((1+A^2)\sin[\frac{8(-1+A^2)\gamma}{5(1+A^2)} - 2\sigma] + \sqrt{1+A^2}((-A\sin[\frac{4((3+2A^2))\gamma}{5(1+A^2)} - 2\sigma] + \sin[\frac{4(2+3A^2)\gamma}{5(1+A^2)} + 2\sigma]))\right)}{\sqrt{5}} \\
M_{3,7} &= -\frac{(g_1^2+g_2^2)\left(2(1-A^4)\sin[\frac{8(-1+A^2)\gamma}{5(1+A^2)} - 2\sigma] + \sqrt{1+A^2}\left(A(3+2A^2)\sin[\frac{4(3+2A^2)\gamma}{5(1+A^2)} - 2\sigma] + (2+3A^2)\sin[\frac{4((2+3A^2))\gamma}{5(1+A^2)} + 2\sigma)\right)\right)}{\sqrt{10}\sqrt{3+4A^2+3A^4}} \\
M_{4,6} &= \frac{A(g_1^2+3g_2^2)\left((1+A^2)\sin[\frac{8(-1+A^2)\gamma}{5(1+A^2)} - 2\sigma] + \sqrt{1+A^2}\left(-A\sin[\frac{4(3+2A^2)\gamma}{5(1+A^2)} - 2\sigma] + \sin[\frac{4(2+3A^2)\gamma}{5(1+A^2)} + 2\sigma]\right)\right)}{3\sqrt{5}\sqrt{1+A^2}} \\
M_{4,7} &= \frac{A(g_1^2+3g_2^2)\left(2(1-A^4)\sin[\frac{8(-1+A^2)\gamma}{5(1+A^2)} - 2\sigma] + \sqrt{1+A^2}\left(A(3+2A^2)\sin[\frac{4(3+2A^2)\gamma}{5(1+A^2)} - 2\sigma] + (2+3A^2)\sin[\frac{4(2+3A^2)\gamma}{5(1+A^2)} + 2\sigma]\right)\right)}{3\sqrt{10}\sqrt{3+7A^2+7A^4+3A^6}} \\
M_{5,6} &= \frac{2Ag_1^2\left((1+A^2)\sin[\frac{8(-1+A^2)\gamma}{5(1+A^2)} - 2\sigma] + \sqrt{1+A^2}\left(-A\sin[\frac{4(3+2A^2)\gamma}{5(1+A^2)} - 2\sigma] + \sin[\frac{4(2+3A^2)\gamma}{5(1+A^2)} + 2\sigma]\right)\right)}{3\sqrt{5}\sqrt{1+A^2}} \\
M_{5,7} &= \frac{\sqrt{\frac{2}{5}}Ag_1^2\left(-2(-1+A^4)\sin[\frac{8(-1+A^2)\gamma}{5(1+A^2)} - 2\sigma] + \sqrt{1+A^2}\left(A(3+2A^2)\sin[\frac{4(3+2A^2)\gamma}{5(1+A^2)} - 2\sigma] + (2+3A^2)\sin[\frac{4(2+3A^2)\gamma}{5(1+A^2)} + 2\sigma]\right)\right)}{3\sqrt{3+7A^2+7A^4+3A^6}}
\end{aligned}
$$

$M_{6,6}, M_{6,7}, M_{7,7}$ are much more complicated and are omitted here.

7.10 $QLD^c + LLE^c$ - preheating

In this case, where the mass matrix is time dependent, we must redo eq.7.32 and we find

$$C^T\dot{C} = B^TA^T(\dot{A}B + A\dot{B}) = -B^TUB + B^T\dot{B} \tag{7.60}$$

and therefore

$$
\begin{aligned}
J &= \frac{1}{2}\left(\sqrt{\omega}\,C^T\dot{C}\frac{1}{\sqrt{\omega}} - \frac{1}{\sqrt{\omega}}\,C^T\dot{C}\sqrt{\omega}\right) \qquad (7.61)\\
&= \frac{1}{2}\left(\sqrt{\omega}\,(-B^TUB)\frac{1}{\sqrt{\omega}} - \frac{1}{\sqrt{\omega}}\,(-B^TUB)\sqrt{\omega}\right) + \frac{1}{2}\left(\sqrt{\omega}\,B^T\dot{B}\frac{1}{\sqrt{\omega}} - \frac{1}{\sqrt{\omega}}\,B^T\dot{B}\sqrt{\omega}\right) \\
&= J_1 + J_2(\textbf{with the obvious definition}).
\end{aligned}
$$

It has been shown numerically that J_1 has the following structure - treating

everything but ξ_i, σ, γ as constants -

$$J_1 = \begin{pmatrix} 0 & 0 & 0 & NZ & NZ & NZ & NZ & 0 & 0 & 0 & 0 & 0 & 0 & 0 & 0 \\ 0 & 0 & 0 & NZ & NZ & NZ & NZ & 0 & 0 & 0 & 0 & 0 & 0 & 0 & 0 \\ 0 & 0 & 0 & NZ & NZ & NZ & NZ & 0 & 0 & 0 & 0 & 0 & 0 & 0 & 0 \\ NZ & NZ & NZ & 0 & 0 & 0 & 0 & 0 & 0 & 0 & 0 & 0 & 0 & 0 & 0 \\ NZ & NZ & NZ & 0 & 0 & 0 & 0 & 0 & 0 & 0 & 0 & 0 & 0 & 0 & 0 \\ NZ & NZ & NZ & 0 & 0 & 0 & 0 & 0 & 0 & 0 & 0 & 0 & 0 & 0 & 0 \\ NZ & NZ & NZ & 0 & 0 & 0 & 0 & 0 & 0 & 0 & 0 & 0 & 0 & 0 & 0 \\ 0 & 0 & 0 & 0 & 0 & 0 & 0 & 0 & 0 & 0 & 0 & 0 & 0 & 0 & NZ \\ 0 & 0 & 0 & 0 & 0 & 0 & 0 & 0 & 0 & 0 & 0 & 0 & 0 & NZ & 0 \\ 0 & 0 & 0 & 0 & 0 & 0 & 0 & 0 & 0 & 0 & 0 & 0 & 0 & 0 & 0 \\ 0 & 0 & 0 & 0 & 0 & 0 & 0 & 0 & 0 & 0 & 0 & 0 & 0 & 0 & 0 \\ 0 & 0 & 0 & 0 & 0 & 0 & 0 & 0 & 0 & 0 & 0 & 0 & 0 & 0 & 0 \\ 0 & 0 & 0 & 0 & 0 & 0 & 0 & 0 & 0 & 0 & 0 & 0 & 0 & 0 & 0 \\ 0 & 0 & 0 & 0 & 0 & 0 & 0 & 0 & NZ & 0 & 0 & 0 & 0 & 0 & 0 \\ 0 & 0 & 0 & 0 & 0 & 0 & 0 & NZ & 0 & 0 & 0 & 0 & 0 & 0 & 0 \end{pmatrix} \tag{7.62}$$

where NZ stands for a nonzero element. Since the columns of B were chosen such that the first 3 columns represent the massive states of sector 1, the next 4 the massless states in sector 1, and the last 8 columns represent the states of sector 2 - in the order in which the eigenvalues were mentioned, this represents particle production from the rotation between the 3 massive states and the massless states of sector 1, and particle production from the rotation between 2 of the massive and the massless states of sector 2. Reassuringly, there is no particle producing rotations between (indistinguishable) states of the same mass. Also it is easy to see that J_2 will not alter this picture, since the last 8 columns of B are constant. This make the last 8 columns of $\dot{B}$ (and therefore of $B^T\dot{B}$) zero and since multiplying by diagonal matrices cannot chance zero entries, it is clear that at least the last 8 columns of J are identical to the last 8 columns of J_1. Therefore the J-matrix is definitely nonzero, and there is particle production from the rotating eigenstates. It was shown in [12] that in general all phases will have nontrivial dynamics, which is necessary for the conclusion that J is nonzero.

7.11 The method of field counting - and its limits

A simpler approach for determining if preheating is possible is to count the fields, establishing the number of broken generators and thus the number of Goldstones and the number of Higgses and by subtraction finding the number of remaining, physical light degrees of freedom [9]. This can be done sector by sector.

LLE^c breaks $SU(2) \times U(1)$ completely. It has 6 fields (real) in sector 1, it breaks 2 diagonal generators and thus have 2 Higgses and 2 Goldstones. This leaves 2 light degrees of freedom, which corresponds to the flat direction. (It is clear that the sum of the phases cannot be gauged away.) However, one needs

to argue why the 2 Higgses cannot rotate between each other - since they have different eigenvalues a possible rotation would be physical, and why the flat direction stays out of this rotation. In this case the flat direction - understood as 2 real fields, that is the direction itself, and the field combination that is orthogonal to it in all superfields individually - stays constant. So it is clearly not rotating. Sector 2 is very easy. There are 4 fields, and 2 broken off-diagonal generators and therefore 2 Higgses and 2 Goldstones. Since the 2 Higgses have the same eigenvalue, there will surely not be particle production in this sector.

$U^cD^cD^c$ breaks $SU(3)_c \times U(1)$ to $U(1)_{NEW}$. It has 6 fields in sector 1, it breaks 2 diagonal generators and thus have 2 Higgses and 2 Goldstones. This leaves 2 light degrees of freedom, which corresponds to the flat direction. However, as before, one needs to argue why the 2 Higgses cannot rotate between each other. The flat directions stay out of this rotation. Sector 2 is again very easy. There are 12 fields, and 6 broken off-diagonal generators and therefore 6 Higgses and 6 Goldstones. Since the 2 Higgses have the same eigenvalue, there will surely not be particle production in this sector.

$QLQLQLE^c$ breaks $SU(3)_c \times SU(2) \times U(1)$ completely. It has 14 fields in sector 1, it breaks 4 diagonal generators and thus have 4 Higgses and 4 Goldstones. This leaves 6 light degrees of freedom, corresponding to the 1 flat direction and 4 additional light degrees of freedom to which there can be rotations which give preheating. In Sector 2 there are 38 fields, and 8 broken off-diagonal generators and therefore 8 Higgses and 8 Goldstones. Since each field is exclusively connected to the VEV by $SU(3)$ or $SU(2)$ the Higgses cannot rotate between each other. 12 fields are completely decoupled (those of Q, differing in both $SU(3)_c$ and $SU(2)$-charge from the VEV).Indeed there is rotation to some of the remaining 10 states, but it is hard to argue exactly why and to how many, without doing the full investigation.

$LLE^c + U^cD^cD^c$ breaks $SU(3)_c \times SU(2) \times U(1)$ completely. It has 12 fields in sector 1, it breaks 4 diagonal generators and thus have 4 Higgses and 4 Goldstones. This leaves 4 light degrees of freedom, corresponding to the 2 flat directions. Again one needs to argue why the 4 Higgses cannot rotate between each other. The flat direction clearly stays out of the rotation. In Sector 2 there are 16 fields, and 8 broken off-diagonal generators and therefore 8 Higgses and 8 Goldstones. Since each field is exclusively connected to the VEV by $SU(3)$ or $SU(2)$ the Higgses cannot rotate between each other.

$QLD^c + LLE^c$ breaks $SU(3)_c \times SU(2) \times U(1)$ to $SU(2)_c$. It has 10 fields in sector 1 (one complex field in common), it breaks 3 diagonal generators and thus have 3 Higgses and 3 Goldstones. This leaves 4 light degrees of freedom, corresponding to the 2 flat directions. Again one needs to argue why the 3 Higgses cannot rotate between each other and why in this case the light fields corresponding to the flat directions *does rotate* with the Higgses. In Sector 2 there are 18 fields and 6 broken off-diagonal generators and therefore 6 Higgses and 6 Goldstones and 4 are completely decoupled. This leaves 2 light fields that can rotate. One can also argue, that the 4 down fields in Q and 4 strange fields in D^c must represent the 4 color Higgses and 4 color Goldstones with no particle production.

It seems clear, that while this counting is a nice tool to look for opportunities

for preheating and to exclude preheating especially in sector 2, it is still necessary to do the full analysis in the unitary gauge to draw firm conclusions - at least when it comes to the role of the fields corresponding to the flat directions themselves.

7.12 Summary and conclusion

For the conclusions on one flat direction, see section 7.7. For 2 flat directions, we have found that particle production is possible in $QLD^c + LLE^c$ but not in $U^cD^cD^c + LLE^c$. The difference seems to be the presence of a common field in the former case, but not in the latter. We have also found that it is necessary to transform to the unitary gauge after identifying the Goldstones, in order to make correct conclusions. Counting fields and broken generators can give hints to whether there is particle production or not, but it is not sufficient for firm conclusions.

Finally, we shall stress that what we have shown is that there will be particle production in the $QLD^c + LLE^c$ case. However, the statement that both directions are likely to get large VEV's [9] has not been investigated in this paper. Neither has the very recent claim that even if non-perturbative particle production happen, the main decay mode will still be perturbative [11]. Also, whether the rotation of the flat directions are fast enough for this particle production to lead to preheating and thus not giving the effect of delayed thermalisation is outside the scope of the present paper. We presume that the situation is close to the situation in [12] - and that there will be very significant particle production. However, as stated in [12], the effect of SUSY breaking terms in the Lagrangian has not been taken into account.

But we can conclude that in order to determine the role of SUSY flat directions in (p)reheating, it is absolutely necessary to determine which flat directions get the large VEVs (only a limited number of the countless flat directions can get large VEVs at the same time) and if many directions get a large VEV a numerical study will probably be necessary to determine if the role of some additional flat directions can be ignored.

7.13 Acknowledgements

I would like to thank David Maybury, Francesco Riva and Stephen M West for the collaboration that led to the formalism used in the present paper. I would also like to thank Steen Hannestad and Martin S Sloth for useful discussions.

BIBLIOGRAPHY

[1] T. Gherghetta, C. F. Kolda and S. P. Martin, Nucl. Phys. B **468**, 37 (1996).

[2] For a review, see K. Enqvist and A. Mazumdar, Phys. Rept. **380**, 99 (2003).

[3] I. Affleck and M. Dine, Nucl. Phys. B **249**, 361 (1985).

[4] A. D. Linde, Phys. Lett. B **160**, 243 (1985).

[5] M. Dine, L. Randall and S. D. Thomas, Phys. Rev. Lett. **75**, 398 (1995).

[6] See eg., R. Allahverdi, K. Enqvist, J. Garcia-Bellido and A. Mazumdar, Phys. Rev. Lett. **97** (2006) 191304.

[7] R. Allahverdi and A. Mazumdar, JCAP **0610**, 008 (2006). [arXiv:hep-ph/0512227v2].

[8] R. Allahverdi and A. Mazumdar, Phys. Rev. D **76**, 103526 (2007).

[9] K. A. Olive and M. Peloso, Phys. Rev. D **74**, 103514 (2006).

[10] R. Allahverdi and A. Mazumdar, J. Cosmol. Astropart. Phys. 08 (2007) 023.

[11] R. Allahverdi and A. Mazumdar, [arXiv:hep-ph/0802.4430v1].

[12] A. Basboll, D. Maybury, Francesco Riva and S. M. West, Phys. Rev. D **76**, 065005 (2007).

[13] T. W. B. Kibble Phys. Rev. **155** (1967) 1554.

[14] H. P. Nilles, M. Peloso and L. Sorbo, JHEP **0104** (2001) 004.

[15] R. Casadio, P. L. Iafelice and G. P. Vacca, Nucl. Phys. **B783**,1 (2007).

8

Are cosmological neutrinos free–streaming?

The paper *Are cosmological neutrinos free–streaming?* presented in this chapter has been submitted to Phys. Rev. D [26].

[26] A. Basbøll, O. E. Bjælde, S. Hannestad and G. Raffelt: Are cosmological neutrinos free–streaming?, arXiv:astro-ph/0806.1735.

Except for minor typographical changes the content of this chapter is the version published on arXiv.org.

Are cosmological neutrinos free–streaming?

Anders Basbøll* Ole Eggers Bjælde† Steen Hannestad ‡
Georg Raffelt §

Abstract

Precision data from cosmology suggest neutrinos stream freely and hence interact very weakly around the epoch of recombination. We study this issue in a simple framework where neutrinos recouple instantaneously and stop streaming freely at a redshift z_i. The latest cosmological data imply $z_i \lesssim 1500$, the exact constraint depending somewhat on the assumed prior on z_i. This bound translates into a limit on the coupling strength between neutrinos and majoron-like particles ϕ, implying $\tau \gtrsim 1 \times 10^{10}\,\mathrm{s}\,(m_2/50\,\mathrm{meV})^3$ for the decay $\nu_2 \to \nu_1 + \phi$.

8.1 Introduction

With the advent of high-precision cosmology it has become feasible to probe progressively more detailed aspects of the cosmic neutrino background radiation [1, 2]. In the standard model, neutrinos provide relativistic energy density which influences the cosmic microwave background (CMB) radiation mainly via the early Integrated Sachs–Wolfe (ISW) effect and the matter fluctuation spectrum via the relation between neutrino energy density and the epoch of matter–radiation equality. The existence of a cosmological background of relativistic energy density has been unambiguously detected in the WMAP-5 data [3] and was already previously detected using the combination of CMB and Large Scale Structure (LSS) data [4–8]. Furthermore, cosmological data provide a restrictive upper bound on the sum of neutrino masses of 0.2–1 eV, depending on the specific choice of data sets and model space [1, 9–16].

The present level of precision allows us to turn to more subtle issues. For example, it is timely to probe the possibility that neutrinos have non-standard interactions where one case in point is an interaction with the Nambu-Goldstone boson of a new, broken $U(1)$ symmetry as in majoron models [17–19]. Such an interaction would recouple the neutrinos to each other at some "interaction

[1] Department of Physics and Astronomy, University of Aarhus, Ny Munkegade, DK-8000 Aarhus C, Denmark.
[2] Department of Physics and Astronomy, University of Aarhus, Ny Munkegade, DK-8000 Aarhus C, Denmark.
[3] Department of Physics and Astronomy, University of Aarhus, Ny Munkegade, DK-8000 Aarhus C, Denmark.
[4] Max-Planck-Institut für Physik (Werner-Heisenberg-Institut), Föhringer Ring 6, 80805 München, Germany.

redshift" z_i, whereas at earlier epochs they would behave in the same way as standard-model neutrinos. For the cases of interest, this recoupling occurs much later than the electroweak decoupling. Therefore, in the limit of relativistic neutrinos the total energy density in the combined fluid of neutrinos and majorons is conserved, preventing any direct impact on cosmological observables.

However, neutrinos lose their free-streaming property if the interaction is sufficiently strong. As a consequence, any anisotropic stress components in the Boltzmann hierarchy are suppressed, effectively truncating the Boltzmann hierarchy at first order, equivalent to the equations for a perfect fluid [20–28]. (See Ref. [29] for a detailed description of the Boltzmann hierarchy.)

The impact of neutrino free streaming on cosmological observables was recently studied in Ref. [28]. The fit parameter was the effective viscosity $c^2_{\rm vis}$, taken to be independent of redshift. Our study is complementary in that we assume that $c^2_{\rm vis}$ drops instantaneously at z_i from the free-streaming value 1/3 to the perfect-fluid value 0. Our conclusion that neutrinos should stream freely around the epoch of recombination is perfectly consistent with Ref. [28]. However, our approach lends itself more directly to an interpretation in terms of a specific interaction model where the recoupling redshift is related to a dimensionless coupling constant g. Therefore, we can translate our limits on z_i into limits on g.

From flavor oscillation experiments we know that neutrinos have masses which therefore are unavoidable cosmological fit parameters. The usual cosmological limits on the sum of neutrino masses imply that any single mass eigenstate should obey $m \lesssim 0.2$–0.3 eV so that all neutrinos would be relativistic around the recombination epoch. Treating them as massless is therefore a reasonable approximation for the simple problem addressed here. On the other hand, a strong majoron-type interaction can lead to the annihilation of "heavy" neutrinos into majorons ("neutrinoless universe" [22]). Such scenarios lead to a complicated evolution of the neutrino-majoron fluid that we are not investigating, although it would have a strong impact on cosmological observables. In any event, our constraint on the free-streaming nature of the relevant radiation at recombination does not depend on the physical nature of the radiation.

Eventually the KATRIN experiment, unless it detects a significant neutrino mass, will constrain the neutrino mass scale to $m \lesssim 0.2$ eV [30]. Such a bound would imply that neutrinos can not have disappeared at the recombination epoch and our constraint indeed applies to neutrinos. In this sense the anticipated KATRIN limit will strengthen the case for translating our limit on z_i into a limit on exotic neutrino interactions.

We begin in Sec. 8.2 with a description of our model space, data sets, and statistical methodology. In Sec. 8.3 we provide our bounds on z_i that are translated, in Sec. 8.4, into limits on a neutrino-majoron coupling strength g. We conclude in Sec. 8.5.

8.2 Models, data, and methodology

Our parameter constraints will be based on a reasonably general 10-parameter model consisting of

$$\Theta = (\omega_{\rm CDM}, \omega_{\rm B}, H_0, n_s, \alpha_s, \tau, A_s, N_\nu, z_i), \tag{8.1}$$

where $h = H_0/(100\ {\rm km\ s^{-1}\ Mpc^{-1}})$, and the cold dark matter and baryon contents are given by $\omega_{\rm CDM} = \Omega_{\rm CDM}h^2$ and $\omega_{\rm B} = \Omega_{\rm B}h^2$ respectively. We assume spatial flatness, i.e. the dark energy density is given by $\Omega_{\rm DE} = 1 - \Omega_{\rm CDM} - \Omega_{\rm B}$. For the dark energy we assume a constant equation of state parameter w. The primordial fluctuations are assumed to be adiabatic and described by the scalar amplitude A_s, the spectral index n_s, and the running α_s. We do not consider the presence of tensor modes or an isocurvature component. Finally, we include the present Hubble parameter, H_0, and the optical depth to reionization, τ. As discussed in the previous section we assume massless neutrinos.

In order to keep our study on the properties of the radiation as general as possible, we will sometimes use the effective number of neutrino flavors, N_ν, as a fit parameter to express the radiation content in the usual way. The standard value is $N_\nu = 3.046$ [31].

Neutrino interactions are assumed to recouple instantaneously at a redshift z_i. Here our standard prior is linear (i.e. uniform) in z_i, but we will also test an alternative case where a linear prior is used on $\log(z_i + 1)$.

The priors on our model parameters are listed in Table 8.1, including the alternatives that we use in some cases.

We use CMB data from WMAP-5 [3,32–34] and measurements of the matter power spectrum based on the Sloan Digital Sky Survey–Luminous Redshift Galaxies (SDSS–LRG) [36] and 2–degree–Field (2dF) galaxy samples [35]. In addition we include the Supernova Type Ia (SN–Ia) data from Ref. [39], the SDSS–LRG Baryon Acoustic Oscillation measurement (SDSS–LRG BAO) from Ref. [38], and the Hubble Space Telescope (HST) key project measurement of H_0 [40].

Our treatment of non-linear corrections to the LSS power spectra follows the prescription given in Ref. [41], i.e., we include data up to $k = 0.2\,h\,{\rm Mpc}^{-1}$ and correct for non-linearity using the shot-noise term $P_{\rm shot}$.

In order to derive constraints on our model parameters we have modified the publicly available CAMB code [45] to allow for neutrino interactions and combined it with the Markov Chain Monte Carlo software COSMOMC [46]. Credible intervals are calculated using Bayesian inference as implemented in the GetDist routine of COSMOMC.

8.3 Limit on Recoupling Redshift

Following the approach described in the previous section we have calculated 68% and 95% credible regions in the 2D parameter space of N_ν and z_i that we show in Fig. 8.1. In the upper panel we have used the linear prior on z_i described in Table 8.1. The cosmological precision data show (i) strong evidence for the

existence of relativistic energy density and (ii) that it must be freely streaming at a redshift around recombination ($z_r \approx 1100$). Marginalizing over N_ν we find $z_i < 1500$ at 95% C.L.

We have repeated the same exercise for a logarithmic prior on z_i, i.e., one that is uniform in $\log(z_i + 1)$. The corresponding credible regions are shown in the lower panel of Fig. 8.1. Marginalizing once more over N_ν we find $z_i < 795$ at 95% C.L. The difference arises because the effective volume at low z_i becomes larger for the logarithmic prior and therefore integration favors slightly lower values of z_i. This effect is well known for parameters with a highly non-Gaussian likelihood, other notable examples being neutrino mass, m_ν [16], and the tensor to scalar ratio, r [43, 44].

While the exact redshift at which neutrinos can become strongly interacting depends on assumptions about priors, we find that neutrinos which were strongly interacting significantly before recombination are excluded by data at much more than 95% C.L., a conclusion which is fully consistent with Ref. [28].

Our results pertain to any form of radiation present around recombination. However, we ultimately want to test the interactions of ordinary neutrinos. The cosmic standard radiation content is given by $N_\nu = 3.046$. Repeating the above exercises with this fixed prior we find $z_i < 1520$ for the linear z_i prior and $z_i < 790$ for the logarithmic prior. These limits are almost identical to those where we marginalized over N_ν. This is hardly surprising since $N_\nu \sim 3$ allows the largest values of z_i.

In order to test more quantitatively how disfavored strongly coupled neutrinos are we have performed a high-precision run with $N_\nu = 3.046$ and the more conservative linear z_i prior to calculate a sequence of progressively higher confidence limits. We find $z_i < 1910$ at 99% C.L. and 2230 at 99.7% C.L. At even higher confidence limits the Markov chains show signs of incomplete convergence and we refrain from quoting bounds.

We also show 2D credible regions in the plane spanned by the matter density $\Omega_{\rm M} = \Omega_{\rm CDM} + \Omega_{\rm B}$ and z_i in Fig. 8.2 where the conservative linear z_i prior was used and N_ν kept as a fit parameter. In the top panel we have used the full data set as in Fig. 8.1 and find consistent results. In the bottom panel have used only WMAP-5 data and thus confirm with our method that WMAP-5 data alone do not significantly constrain z_i [28].

8.4 Limit on Coupling Strength

Our approach of neutrinos recoupling at some redshift z_i was motivated by a majoron-type interaction model where neutrinos interact with a new massless pseudoscalar by virtue of a dimensionless Yukawa coupling g. In the framework of such a model we can translate our limit on z_i into a limit on g in analogy to a previous paper by two of us [24]. When considering the scattering process the bound applies to any component of g_{ij}, the indices referring to the different neutrino flavors. The off-diagonal parts, however, are much more tightly constrained by the decay process $\nu_i \to \nu_j \phi$ [24].

At $z \sim 1500$ the universe is matter dominated and to a good approximation $H \propto T^{3/2}$. Since for scattering the rate is $\Gamma \sim g^4 T$, we can translate the

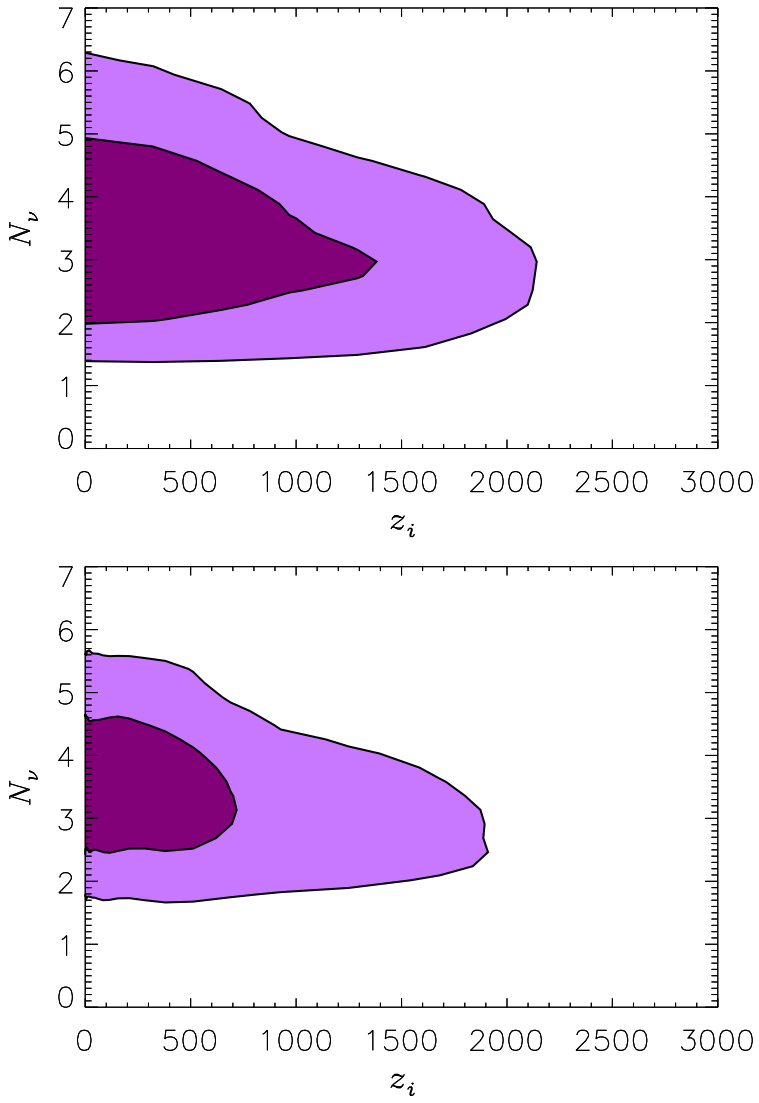

Fig. 8.1: 2D marginal 68% and 95% contours for z_i and N_ν. Top: Linear prior for z_i. Bottom: Logarithmic prior, i.e., linear in $\log(1 + z_i)$.

condition for strong interaction, $\Gamma/H \gtrsim 1$, to a bound on g [24]. Since $\Gamma/H \propto g^4 T^{-1/2}$, and in the previous paper we effectively used $z_i = 1088$ to obtain $g < 10^{-7}$ we now get $g < 10^{-7}(1500/1088)^{1/8} \sim 1.05 \times 10^{-7}$, i.e. a negligible 5% difference compared with our previous result.

It should be noted that for masses below the recombination temperature, $m \lesssim T_R \sim 0.3$ eV, our bound applies equally well to the case of neutrino decay and inverse decay [24]. In fact, we can now make the bound more quantitative by adding that at 95% C.L. the interaction cannot be very strong before $z_i \sim 1500$. Roughly this translates to a bound on the lifetime (again scaling from our previous limit derived using $z_i = 1088$) of

$$\tau > 1.0 \times 10^{10}\,\mathrm{s}\,\left(\frac{m}{50\,\mathrm{meV}}\right)^3. \tag{8.2}$$

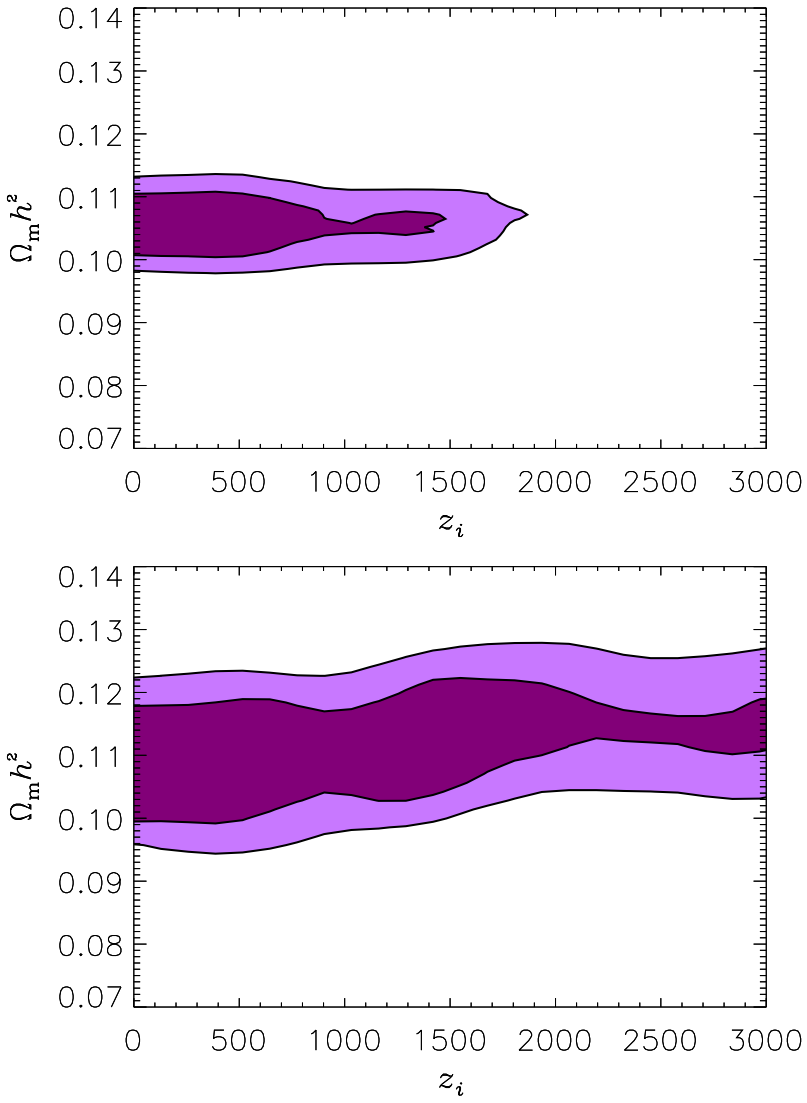

Fig. 8.2: 2D marginal 68% and 95% contours for z_i and $\Omega_M h^2$, using the linear prior for z_i and using N_ν as a fit parameter. Top: Full data set. Bottom: WMAP-5 data only.

This limit is slightly weaker than before [24] because of the slightly more conservative assumption about z_i, but it remains by far the most restrictive bound on invisible decays of low-mass neutrinos.

8.5 Discussion

We have updated bounds on the coupling strength between neutrinos and a new, light pseudo-scalar, ϕ, using the latest cosmological data. Performing a slightly more refined calculation than in an earlier paper by two of us [24] we find essentially unchanged constraints.

One way to improve this limit in future is by actually detecting neutrino

hot dark matter in cosmological precision data. In decay scenarios involving massless pseudoscalars and for a mass of 50 meV, the lifetime limit would improve by some six orders of magnitude [42].

Our more general conclusion is that neutrinos which are strongly interacting around recombination are strongly disfavored by data. The present data strongly support the conclusion that the cosmic neutrino background (i) exists around the epoch of recombination and (ii) its fluctuations do have an anisotropic stress component. In future CMB data alone will likely suffice to reach the same or better sensitivity so that the bound on g can be expected to improve significantly [25, 28].

Acknowledgments

We acknowledge use of computing resources from the Danish Center for Scientific Computing (DCSC). GGR acknowledges partial support by the Deutsche Forschungsgemeinschaft (grant TR-27) and by the Cluster of Excellence "Origin and Structure of the Universe."

Tab. 8.1: Priors on the model parameters. Note that for N_ν we use the prior $0 \leq N_\nu \leq 50$ for Figs. 8.1 and 8.2, and $N_\nu = 3.046$ everywhere else.

Parameter	Standard (linear) prior	Alternative (log) prior
$\omega_{\rm CDM}$	0.01–0.9	0.01–0.9
$\omega_{\rm B}$	0.005–0.1	0.005–0.1
H_0	40–100	40–100
w	−2–0	−2–0
n_s	0.5–1.5	0.5–1.5
α_s	−0.2–0.2	−0.2–0.2
$\log[10^{10} A_s]$	2.5–4	2.5–4
τ	0–1	0–1
N_ν	3.046 / 0–50	3.046 / 0–50
z_i	0–10^4	—
$\log(1 + z_i)$	—	0–4

BIBLIOGRAPHY

[1] S. Hannestad, Ann. Rev. Nucl. Part. Sci. **56**, 137 (2006) [arXiv:hep-ph/0602058].

[2] J. Lesgourgues and S. Pastor, Phys. Rept. **429**, 307 (2006) [arXiv:astro-ph/0603494].

[3] E. Komatsu *et al.*, arXiv:0803.0547 [astro-ph].

[4] S. Hannestad, Phys. Rev. D **64**, 083002 (2001) [arXiv:astro-ph/0105220].

[5] S. Hannestad, JCAP **0601**, 001 (2006) [arXiv:astro-ph/0510582].

[6] K. Ichikawa, M. Kawasaki and F. Takahashi, JCAP **0705**, 007 (2007) [arXiv:astro-ph/0611784].

[7] G. Mangano, A. Melchiorri, O. Mena, G. Miele and A. Slosar, JCAP **0703**, 006 (2007) [arXiv:astro-ph/0612150].

[8] J. Hamann, S. Hannestad, G. G. Raffelt and Y. Y. Y. Wong, JCAP **0708**, 021 (2007) [arXiv:0705.0440].

[9] C. Zunckel and P. G. Ferreira, JCAP **0708**, 004 (2007) [arXiv:astro-ph/0610597].

[10] M. Cirelli and A. Strumia, JCAP **0612**, 013 (2006) [arXiv:astro-ph/0607086].

[11] A. Goobar, S. Hannestad, E. Mörtsell and H. Tu, JCAP **0606**, 019 (2006) [arXiv:astro-ph/0602155].

[12] J. R. Kristiansen, H. K. Eriksen and O. Elgaroy, Phys. Rev. D **74**, 123005 (2006).

[13] U. Seljak, A. Slosar and P. McDonald, JCAP **0610**, 014 (2006) [arXiv:astro-ph/0604335].

[14] G. L. Fogli *et al.*, Phys. Rev. D **75**, 053001 (2007) [arXiv:hep-ph/0608060].

[15] S. Hannestad, JCAP **0305**, 004 (2003) [arXiv:astro-ph/0303076].

[16] S. Hannestad, arXiv:0710.1952 [hep-ph].

[17] G. B. Gelmini and M. Roncadelli, Phys. Lett. B **99**, 411 (1981).

[18] Y. Chikashige, R. N. Mohapatra and R. D. Peccei, Phys. Lett. B **98**, 265 (1981).

[19] J. Schechter and J. W. F. Valle, Phys. Rev. D **25**, 774 (1982).

[20] G. Raffelt and J. Silk, Phys. Lett. B **192**, 65 (1987).

[21] F. Atrio-Barandela and S. Davidson, Phys. Rev. D **55**, 5886 (1997) [arXiv:astro-ph/9702236].

[22] J. F. Beacom, N. F. Bell and S. Dodelson, Phys. Rev. Lett. **93**, 121302 (2004) [arXiv:astro-ph/0404585].

[23] S. Hannestad, JCAP **0502**, 011 (2005) [arXiv:astro-ph/0411475].

[24] S. Hannestad and G. Raffelt, Phys. Rev. D **72**, 103514 (2005) [arXiv:hep-ph/0509278].

[25] A. Friedland, K. M. Zurek and S. Bashinsky, arXiv:0704.3271 [astro-ph].

[26] R. F. Sawyer, Phys. Rev. D **74**, 043527 (2006) [arXiv:astro-ph/0601525].

[27] N. F. Bell, E. Pierpaoli and K. Sigurdson, Phys. Rev. D **73**, 063523 (2006) [arXiv:astro-ph/0511410].

[28] F. De Bernardis, L. Pagano, P. Serra, A. Melchiorri and A. Cooray, arXiv:0804.1925 [astro-ph].

[29] C. P. Ma and E. Bertschinger, Astrophys. J. **455**, 7 (1995) [arXiv:astro-ph/9506072].

[30] G. Drexlin [KATRIN Collaboration], Nucl. Phys. Proc. Suppl. **145**, 263 (2005).

[31] G. Mangano, G. Miele, S. Pastor, T. Pinto, O. Pisanti and P. D. Serpico, Nucl. Phys. B **729**, 221 (2005) [arXiv:hep-ph/0506164].

[32] Legacy Archive for Microwave Background Data Analysis (LAMBDA), `http://lambda.gsfc.nasa.gov`

[33] M. R. Nolta *et al.*, arXiv:0803.0593 [astro-ph].

[34] J. Dunkley *et al.* [WMAP Collaboration], arXiv: 0803.0586 [astro-ph].

[35] S. Cole *et al.* [The 2dFGRS Collaboration], Mon. Not. Roy. Astron. Soc. **362**, 505 (2005) [arXiv:astro-ph/0501174].

[36] M. Tegmark *et al.*, Phys. Rev. D **74**, 123507 (2006) [arXiv:astro-ph/0608632].

[37] W. J. Percival *et al.*, Astrophys. J. **657**, 645 (2007) [arXiv:astro-ph/0608636].

[38] D. J. Eisenstein *et al.* [SDSS Collaboration], Astrophys. J. **633** (2005) 560 [arXiv:astro-ph/0501171]; see also `http://cmb.as.arizona.edu/~eisenste/acousticpeak`

[39] T. M. Davis *et al.*, arXiv:astro-ph/0701510.

[40] W. L. Freedman *et al.*, Astrophys. J. **553**, 47 (2001) [arXiv:astro-ph/0012376].

[41] J. Hamann, S. Hannestad, A. Melchiorri and Y. Y. Y. Wong, arXiv:0804.1789 [astro-ph].

[42] P. D. Serpico, Phys. Rev. Lett. **98**, 171301 (2007) [arXiv:astro-ph/0701699].

[43] W. Valkenburg, L. M. Krauss and J. Hamann, arXiv:0804.3390 [astro-ph].

[44] H. Peiris and R. Easther, JCAP **0607**, 002 (2006) [arXiv:astro-ph/0603587].

[45] `http://www.cosmologist.info`

[46] A. Lewis and S. Bridle, Phys. Rev. D **66**, 103511 (2002) [arXiv:astro-ph/0205436].

9

Thermalisation of a neutrino gas

The paper *Thermalisation of a neutrino gas by decays and inverse decays* is not finished for publication. I have made the major part of the analytical and numerical work presented in this version. This I have written with the agreement of Ole E. Bjælde and Steen Hannested – the other persons who have, so far, contributed to this project.

Thermalisation of a neutrino gas by decays and inverse decays

Anders Basbøll* Ole Eggers Bjælde† Steen Hannestad ‡
Georg Raffelt §

Abstract

[**To be included**]

9.1 Introduction

The possibility for neutrino interactions beyond the standard model have been studied in many contexts over the years. One particularly simple possibility is that neutrinos couple to a new pseudoscalar degree of freedom, as is for example the case in majoron models.

Astrophysics provides fairly stringent constraints on such couplings. For example SN1987A provides an upper bound on the dimensionless coupling constant of order [**To be included**] by requiring that the neutrino signal should not be significantly shortened.

In the same way there are two cosmological bounds on g. First, the value of g should not be large enough that pseudoscalars are fully thermalised before BBN. This leads to $g \lesssim 10^{-5}$. Second, a significant value of g will make neutrinos self-interacting in the late universe and prevent neutrino free-streaming. This possibility has been discussed a number of times in the literature (see [**To be included**]).

The effect on cosmological observables such as the CMB spectrum were studied in [**To be included**], particularly it was found that although models with no neutrino free streaming can mimic the matter power spectrum of ΛCDM models they produce a distinct signature in the CMB spectrum which is much harder to reproduce. The feature arises because neutrinos act as a source term for photon perturbations. If there is no free-streaming the source term is stronger and consequently the CMB anisotropy is increased for all scales inside

[1] Department of Physics and Astronomy, University of Aarhus, Ny Munkegade, DK-8000 Aarhus C, Denmark.
[2] Department of Physics and Astronomy, University of Aarhus, Ny Munkegade, DK-8000 Aarhus C, Denmark.
[3] Department of Physics and Astronomy, University of Aarhus, Ny Munkegade, DK-8000 Aarhus C, Denmark.
[4] Max-Planck-Institut für Physik (Werner-Heisenberg-Institut), Föhringer Ring 6, 80805 München, Germany.

the particle horizon at recombination. On the other hand there is no effect on larger scales.

This dinstinct signature was used in [**To be included**] to constrain models without neutrino free-streaming and in [**To be included**] it was used to constrain the correponding neutrino-pseudoscalar coupling parameters.

However, for decays and inverse decays the interaction was treated in a somewhat simplified manner in the sense that the momentum equilibration rate was assumed to be roughly $\Gamma^* \sim 1/(\gamma^2\tau)$, where τ is the rest-frame lifetime and $\gamma \sim E_\nu/m_\nu$ is the boost factor.

9.2 Thermalisation of a gas with only decays and inverse decays

Thermalisation of a gas by decay and inverse decay is a non-trivial process because of phase space limitation. As long as one of the involved particles can interact with an external heat bath it is in principle possible to thermalise the gas provided that the interaction rate is sufficiently fast. This is for instance the case with thermal leptogenesis in which the decay products are thermalised by SM gauge interactions.

However, for the case studied here this is not true. The weak interactions are far too weak to maintain equilibrium at the eV temperatures considered here. In this case full thermal equilibrium can never be achieved.

The standard case usually studied, for example in the case of thermal leptogenesis is a spatially homogeneous gas in which interactions drive the ditribution towards thermal equilibrium. [**More to be included**]

However, from the point of view of structure formation and more specifically free-streaming the important point is the rate of directional momentum transfer between species. For example, Thompson scattering is inefficient for maintaining energy equilibration between electrons and photons, but very efficient for exchanging momentum between the two species. This can be seen from the simple relations $|\Delta E_\gamma/E_\gamma| \sim E_\gamma/m_e$ and $|\Delta\vec{p}/p| \sim 1$ in a single scattering event. Therefore Thompson scattering is very efficient for driving the acoustic baryon-photon oscillations prior to recombination.

However, for a gas with only decays and inverse decays momentum transfer is even more inefficient than energy transfer. Roughly the energy transfer timescale is given by the decay rate $\Gamma = 1/(\gamma\tau)$, i.e. the usual Lorentz suppressed rest-frame decay rate. However, in the lab frame the decay products are emitted in a cone of opening angle $1/\gamma$ relative to the direction of momentum of the parent particle. Therefore, in a single decay the momentum direction is changed by only $|\Delta\vec{p}/p| \sim 1/\gamma$. This finally means that the rate of momentum change in the gas is roughly $1/(\gamma^2\tau)$, i.e. for relativistic decays it is highly suppressed, and even suppressed relative to the energy exchange rate.

In the following section we derive the specific Boltzmann collision integrals relevant for decays and inverse decays in an inhomogeneous gas.

The variation of any over all quantity Q can be calculated from the distribution functions:

$$\frac{(\frac{\partial Q_{tot}}{dt})}{\text{Volume}} = \sum_i \int \frac{d^3p_1}{(2\pi)^3 2E_1}\frac{d^3p_2}{(2\pi)^3 2E_2}\frac{d^3p_\varphi}{(2\pi)^3 2E_\varphi}(2\pi)^4\delta^4(p_1-p_2-p_\varphi)|M|^2 \\ [f_2 f_\varphi(1-f_1)-f_1(1-f_2)(1+f_\varphi)]Q_i S_i \tag{9.1}$$

where $S_1 = 1$ and $S_2 = S_\varphi = -1$.

9.3 Total transverse momentum - with no background

We want to calculate the initial transverse momentum when we start with a standing wave of 1's. The distribution functions are

$$f_1 = \frac{n_1}{2}\left(\delta^3(\vec{p_1}-\vec{p_0})+\delta^3(\vec{p_1}+\vec{p_0})\right) \\ f_2 = f_\varphi = 0 \tag{9.2}$$

Since the 2 terms obviously contribute equally, we are free to change to one beam instead

$$f_1 = n_1\delta^3(\vec{p_1}-\vec{p_0}) \\ f_2 = f_\varphi = 0 \tag{9.3}$$

This will give the same result.

We calculate the matrix element. From tracing, and averaging over incoming and summing over outgoing spins (here 4-vector notation at first, scalar notation later)

$$|M|^2 = 4g^2(p_1\cdot p_2 - m_1m_2) = 4g^2(E_1E_2 - p_1p_2C_{12}) \\ = 4g^2\left(E_1p_2 - p_1p_2\frac{p_1^2-E_1^2+2E_1p_2}{2p_1p_2}\right) = 2g^2m^2 \tag{9.4}$$

So we find

$$\frac{(\frac{\partial Q_{tot}}{dt})}{\text{Volume}} = -\sum_i \int \frac{d^3p_1}{(2\pi)^3 2E_1}\frac{d^3p_2}{(2\pi)^3 2E_2}\frac{d^3p_\varphi}{(2\pi)^3 2E_\varphi}(2\pi)^4\delta^4(p_1-p_2-p_\varphi) \\ 2g^2m^2n_1\delta^3(\vec{p_1}-\vec{p_0})Q_iS_i \\ = \frac{-g^2m^2n_1}{4(2\pi)^5}\sum_i\int\frac{d^3p_1d^3p_2d^3p_\varphi}{E_1E_2E_\varphi}\delta^4(p_1-p_2-p_\varphi)\delta^3(\vec{p_1}-\vec{p_0})Q_iS_i$$

What we want to find is a measure of the transverse momentum created in the transverse direction. Obviously, there is no momentum if we just sum over the transverse momentum vectors, so we sum the magnitudes of created

transverse momenta instead. This means putting $-Q_i S_i = |\vec{p_i} \times \hat{\vec{p_0}}|$. Thus we have

$$\frac{\frac{\partial |P_\perp|}{dt}}{\text{Volume}} = \frac{g^2 m^2 n_1}{4(2\pi)^5} \int \frac{d^3p_1 d^3p_2 d^3p_\varphi}{E_1 E_2 E_\varphi} \delta^4(p_1 - p_2 - p_\varphi) \delta^3(\vec{p_1} - \vec{p_0}) \left(|\vec{p_1} \times \hat{\vec{p_0}}| + |\vec{p_2} \times \hat{\vec{p_0}}| + |\vec{p_\varphi} \times \hat{\vec{p_0}}| \right) \tag{9.5}$$

The 1-integration is straight forward

$$\frac{\frac{\partial |P_\perp|}{dt}}{\text{Volume}} = \frac{g^2 m^2 n_1}{4(2\pi)^5} \int \frac{d^3p_2 d^3p_\varphi}{E_0 E_2 E_\varphi} \delta^4(p_0 - p_2 - p_\varphi) \left(|\vec{p_0} \times \hat{\vec{p_0}}| + |\vec{p_2} \times \hat{\vec{p_0}}| + |\vec{p_\varphi} \times \hat{\vec{p_0}}| \right) \tag{9.6}$$

Of the 3 terms, the first is clearly 0 and the last 2 will contribute the same when all the integrations have been done. Therefore

$$\frac{\frac{\partial |P_\perp|}{dt}}{\text{Volume}} = \frac{g^2 m^2 n_1}{2(2\pi)^5} \int \frac{d^3p_2 d^3p_\varphi}{E_0 E_2 E_\varphi} \delta^4(p_0 - p_2 - p_\varphi) |\vec{p_2} \times \hat{\vec{p_0}}| \tag{9.7}$$

We integrate φ out.

$$\frac{\frac{\partial |P_\perp|}{dt}}{\text{Volume}} = \frac{g^2 m^2 n_1}{2(2\pi)^5} \int \frac{d^3p_2}{E_0 E_2 E_{\varphi *}} \delta(p_0 - p_2 - p_{\varphi *}) |\vec{p_2} \times \hat{\vec{p_0}}| \tag{9.8}$$

where $*$ means that it is a function of the remaining variables. From the cosine relation: (C_{02} means cosine to angle between sides 0 and 2):

$$C_{02} = \frac{p_0^2 + p_2^2 - p_\varphi^2}{2p_0 p_2} = \frac{p_0^2 - E_0^2 + 2E_0 p_2}{2p_0 p_2} \tag{9.9}$$

we find

$$p_\varphi = \sqrt{p_0^2 + p_2^2 - 2p_0 p_2 C_{02}} \tag{9.10}$$

which can be inserted in the energy delta function. This and energy conservation $E_\varphi = E_0 - E_2$ gives

$$\begin{aligned} \frac{\frac{\partial |P_\perp|}{dt}}{\text{Volume}} &= \frac{g^2 m^2 n_1}{2(2\pi)^5} \int \frac{d^3p_2}{E_0 E_2 (E_0 - E_2)} \\ &\delta\left(p_0 - p_2 - \sqrt{p_0^2 + p_2^2 - 2p_0 p_2 C_{02}} \right) |\vec{p_2} \times \hat{\vec{p_0}}| \\ &= \frac{g^2 m^2 n_1}{2(2\pi)^5} \int \frac{d^3p_2}{E_0 E_2 (E_0 - E_2)} \\ &\delta\left(p_0 - p_2 - \sqrt{p_0^2 + p_2^2 - 2p_0 p_2 C_{02}} \right) |p_2| |S_{02}| \end{aligned} \tag{9.11}$$

where S_{02} is the sine between 0 and 2. Now we align the coordinate system for the p_2 such that the $z-axis$ is aligned with p_0 and use $d^3p_2 = p_2^2 dC_{02} dp_2$

$$\frac{\frac{\partial |P_\perp|}{dt}}{\text{Volume}} = \frac{g^2 m^2 n_1}{2(2\pi)^5} \int \frac{dp_2 dC_{02} p_2^2}{E_0 p_2 (E_0 - p_2)} \delta\left(p_0 - p_2 - \sqrt{p_0^2 + p_2^2 - 2p_0 p_2 C_{02}}\right) p_2 \sqrt{1 - C_{02}^2}$$

$$= \frac{g^2 m^2 n_1}{2(2\pi)^5} \int \frac{dp_2 dC_{02} p_2^2}{E_0 (E_0 - p_2)} \delta\left(p_0 - p_2 - \sqrt{p_0^2 + p_2^2 - 2p_0 p_2 C_{02}}\right) \sqrt{1 - C_{02}^2} \tag{9.12}$$

To eliminate the delta function we use $g(C_{02}) = E_0 - p_2 - \sqrt{p_0^2 + p_2^2 - 2p_0 p_2 C_{02}}$. The root of g is given by $E_0 - p_2 = \sqrt{p_0^2 + p_2^2 - 2p_0 p_2 C_{02*}}$. This defines C_{02*}. Therefore

$$g'(C_{02*}) = \frac{-(-2p_0 p_2)}{2\sqrt{p_0^2 + p_2^2 - 2p_0 p_2 C_{02*}}} = \frac{p_0 p_2}{E_0 - p_2} \tag{9.13}$$

This gives

$$\begin{aligned} \frac{\frac{\partial |P_\perp|}{dt}}{\text{Volume}} &= \frac{g^2 m^2 n_1}{2(2\pi)^5} \int \frac{dp_2 p_2^2}{E_0 (E_0 - p_2)} \frac{E_0 - p_2}{p_0 p_2} \sqrt{1 - C_{02*}^2} \\ &= \frac{g^2 m^2 n_1}{2(2\pi)^5 E_0 p_0} \int dp_2 p_2 \sqrt{1 - C_{02*}^2} \end{aligned} \tag{9.14}$$

We need to find the cosine to insert

$$E_0 - p_2 = \sqrt{p_0^2 + p_2^2 - 2p_0 p_2 C_{02*}} \Rightarrow \tag{9.15}$$

$$C_{02*}^2 = \frac{E_0^2 p_2^2 - E_0 p_2 m^2 + \frac{m^4}{4}}{p_0^2 p_2^2} \tag{9.16}$$

where $E^2 = p^2 + m^2$ has been used. This shall be inserted

$$\frac{\frac{\partial |P_\perp|}{dt}}{\text{Volume}} = \frac{g^2 m^2 n_1}{2(2\pi)^5 E_0 p_0} \int dp_2 p_2 \sqrt{1 - \frac{E_0^2 p_2^2 - E_0 p_2 m^2 + \frac{m^4}{4}}{p_0^2 p_2^2}} \tag{9.17}$$

$$= \frac{g^2 m^3 n_1}{32(2\pi)^4 E_0} \tag{9.18}$$

Inserting $g^2 m = \frac{16\pi}{\tau}$ where τ is the 1-lifetime, and $\frac{m}{E_0} = \frac{1}{\gamma}$ our final result is

$$\frac{\frac{d|P_\perp|}{dt}}{\text{Volume}} = \frac{n_1 E_0}{4(2\pi)^3 \tau \gamma^2} \propto \frac{1}{\tau \gamma^2} \tag{9.19}$$

as expected.

9.4 A more general case

In more complicated cases we will have to use

$$\begin{aligned} \Lambda &\equiv f_2 f_\varphi (1-f_1) - f_1(1-f_2)(1-f_\varphi) && (9.20)\\ &= f_2 f_\varphi - f_1(1+f_\varphi - f_2) && (9.21)\end{aligned}$$

This complicates things a bit. But if we again take only the initial time it is solvable.

Now we have to take the $|f_2 f_\varphi - f_1(1+f_\varphi - f_2)||\vec{p_i}\times\hat{\vec{p_0}}|$ In general, taking the absolute value would mean that you can not just split the integral in the f_1-part and the other part. However you we can split the integral over a vanishingly small volume around p_0 and the rest. In the small volume, the non-f_1 part will not contribute since we are integrating a finite function over a vanishing volume. On the other hand, f_1 only contributes in the vanishing volume, and therefore it gives the same result as before (at least if one says $f_\varphi = f_2$).

In the case of initial equilibrium densities of 2 and φ this will be the case. Here we can use $f_2 f_\varphi = \mathrm{e}^{-E_1/T}$. Thus the extra part will be

$$\begin{aligned} \frac{\frac{\partial |P_\perp|}{dt}}{\mathrm{Volume}_{\mathrm{extra}}} &= \int \frac{d^3p_1}{(2\pi)^3 2E_1}\frac{d^3p_2}{(2\pi)^3 2E_2}\frac{d^3p_\varphi}{(2\pi)^3 2E_\varphi}(2\pi)^4\delta^4(p_1-p_2-p_\varphi) \\ &\quad 2g^2m^2\mathrm{e}^{-E_1/T}\left(|\vec{p_1}\times\hat{\vec{p_0}}| + |\vec{p_2}\times\hat{\vec{p_0}}| + |\vec{p_\varphi}\times\hat{\vec{p_0}}|\right) \quad (9.22)\end{aligned}$$

This integral can be integrated (over all space) as 3 independent terms. Since the 2 last are identical (over all space) we can write

$$\begin{aligned} \frac{\frac{\partial |P_\perp|}{dt}}{\mathrm{Volume}_{\mathrm{extra}}} &= \int \frac{d^3p_1}{(2\pi)^3 2E_1}\frac{d^3p_2}{(2\pi)^3 2E_2}\frac{d^3p_\varphi}{(2\pi)^3 2E_\varphi}(2\pi)^4\delta^4(p_1-p_2-p_\varphi) \\ &\quad 2g^2m^2\mathrm{e}^{-E_1/T}\left(|\vec{p_1}\times\hat{\vec{p_0}}| + 2|\vec{p_2}\times\hat{\vec{p_0}}|\right) \quad (9.23)\end{aligned}$$

Now we do the integration over φ as before

$$\begin{aligned}
\frac{\frac{\partial|P_\perp|}{dt}|}{\text{Volume}_{\text{extra}}} &= 2g^2m^2\int\frac{d^3p_1}{(2\pi)^3 2E_1}\frac{d^3p_2}{(2\pi)^3 2p_2}\frac{1}{(2\pi)^3 2(E_1-p_2)}(2\pi)^4 \\
&\quad \delta\left(E_1-p_2-\sqrt{p_1^2+p_2^2-2p_1p_2C_{12}}\right)\mathrm{e}^{-E_1/T} \\
&\quad \left(|\vec{p_1}\times\hat{\vec{p_0}}|+2|\vec{p_2}\times\hat{\vec{p_0}}|\right) \\
&= 2g^2m^2\int\frac{d^3p_1}{(2\pi)^3 2E_1}\frac{d^3p_2}{(2\pi)^3 2p_2}\frac{1}{(2\pi)^3 2(E_1-p_2)}(2\pi)^4 \\
&\quad \delta\left(E_1-p_2-\sqrt{p_1^2+p_2^2-2p_1p_2C_{12}}\right)\mathrm{e}^{-E_1/T} \\
&\quad (p_1|C_{10}|+2p_2|C_{20}|) \\
&= \frac{g^2m^2}{4(2\pi)^3}\int\frac{dp_1p_1^2}{E_1}\frac{dp_2p_2^2}{p_2}\frac{\mathrm{e}^{-E_1/T}}{(E_1-p_2)} \\
&\quad \int dC_2dC_1\delta\left(E_1-p_2-\sqrt{p_1^2+p_2^2-2p_1p_2C_{12}}\right) \\
&\quad (p_1|C_{10}|+2p_2|C_{20}|)
\end{aligned}$$

where the lack of index in the integration highlights the fact that we integrate over all directions.

We split the inner integral in two. For

$$\int dC_1dC_2\delta\left(E_1-p_2-\sqrt{p_1^2+p_2^2-2p_1p_2C_{12}}\right)p_1|C_{10}| \tag{9.24}$$

we choose to make the 2-integration the innermost, and align the coordinate system for 2 after particle 1. The coordinate system for 1, we align after the beam direction 0. So we calculate

$$\int dC_{10}\left(\int dC_{12}\delta\left(E_1-p_2-\sqrt{p_1^2+p_2^2-2p_1p_2C_{12}}\right)\right)p_1|C_{10}| \tag{9.25}$$

The elimination of the delta function goes exactly as the part between 9.12 og 9.13 so we get

$$=\int dC_{10}\frac{E_1-p_2}{p_1p_2}p_1|C_{10}| = \frac{E_1-p_2}{p_2} \tag{9.26}$$

by analogy

$$\begin{aligned}
&\int dC_2dC_{12}\delta\left(E_1-p_2-\sqrt{p_1^2+p_2^2-2p_1p_2C_{12}}\right)(2p_2|C_{20}|) \\
&\qquad = \frac{2(E_1-p_2)}{p_1}
\end{aligned} \tag{9.27}$$

such that

$$\begin{aligned}&\int dC_2 dC_1 \delta\left(E_1 - p_2 - \sqrt{p_1^2 + p_2^2 - 2p_1 p_2 C_{12}}\right)(p_1|C_{10}| + 2p_2|C_{20}|)\\ =\ & \frac{(E_1 - p_2)(2p_2 + p_1)}{p_1 p_2}\end{aligned} \tag{9.28}$$

and

$$\begin{aligned}\frac{\frac{\partial|P_\perp|}{dt}|}{\text{Volume}_{\text{extra}}} &= \frac{g^2 m^2}{4(2\pi)^3}\int \frac{dp_1 p_1^2}{E_1}\frac{dp_2 p_2^2}{p_2}\frac{\mathrm{e}^{-E_1/T}}{(E_1 - p_2)}\frac{(E_1 - p_2)(2p_2 + p_1)}{p_1 p_2}\\ &= \frac{g^2 m^2}{4(2\pi)^3}\int \frac{dp_1 p_1}{E_1} dp_2 \mathrm{e}^{-E_1/T}(2p_2 + p_1)\end{aligned} \tag{9.29}$$

We know $dp_i p_i = dE_i E_i$ so we have

$$\frac{\frac{\partial|P_\perp|}{dt}|}{\text{Volume}_{\text{extra}}} = \frac{g^2 m^2}{4(2\pi)^3}\int dE_1 dp_2 \mathrm{e}^{-E_1/T}(2p_2 + p_1) \tag{9.30}$$

The limit on p_2 will be the usual, whereas the E_1 can be anything, except less than the mass.

$$\begin{aligned}\frac{\frac{\partial|P_\perp|}{dt}|}{\text{Volume}_{\text{extra}}} &= \frac{g^2 m^2}{4(2\pi)^3}\int_m^\infty dE_1 \mathrm{e}^{-E_1/T}\left[\left(\int_{\frac{m^2}{2(E_0+p_0)}}^{\frac{m^2}{2(E_0-p_0)}} dp_2(2p_2 + p_1)\right)\right]\\ &= \frac{g^2 m^2 p_0}{4(2\pi)^3}\int_m^\infty dE_1 \mathrm{e}^{-E_1/T}\left[p_1 + E_0\right]\end{aligned} \tag{9.31}$$

Since

$$\int_m^\infty dE_1 \mathrm{e}^{-E_1/T} = T\mathrm{e}^{-m/T} \tag{9.32}$$

we have

$$\frac{\frac{\partial|P_\perp|}{dt}|}{\text{Volume}_{\text{extra}}} = \frac{E_0 p_0}{2\pi^2 \tau\gamma}\left(E_0 T\mathrm{e}^{-m/T} + \int_m^\infty dE_1 \mathrm{e}^{-E_1/T} p_1\right) \tag{9.33}$$

Since

$$\int_0^\infty dE_1 \mathrm{e}^{-E_1/T} E_1 = 2T^2 \tag{9.34}$$

the relativistic limit is

$$\frac{\frac{\partial|P_\perp}{dt}}{\text{Volume}_{\text{extra}}} = \frac{E_0 p_0}{2\pi^2\tau\gamma}\left(E_0 T \mathrm{e}^{-m/T} + 2T^2\right). \tag{9.35}$$

Thus the total thing is

$$\begin{aligned}\frac{\frac{\partial|P_\perp|}{dt}}{\text{Volume}_{\text{extra}}} &= \frac{E_0 n_1}{4(2\pi)^3\tau\gamma^2} \\ &+\frac{E_0 p_0}{2\pi^2\tau\gamma}\left(E_0 T \mathrm{e}^{-m/T} + \int_m^\infty dE_1 \mathrm{e}^{-E_1/T} p_1\right)\end{aligned} \tag{9.36}$$

with relativistic limit

$$\frac{\frac{\partial|P_\perp|}{dt}}{\text{Volume}_{\text{extra}}} = \frac{E_0 n_1}{4(2\pi)^3\tau\gamma^2} + \frac{E_0 p_0}{2\pi^2\tau\gamma}\left(E_0 T \mathrm{e}^{-m/T} + 2T^2\right) \tag{9.37}$$

9.5 Numerical results

In the numerical implementation we had to change the setup a little. Due to problems with the bins, it was impossible to get the heavy neutrino to have vanishing momentum in the transverse direction. This could not be helped by increasing the number of bins. Therefore we made a thermal distribution of 1's around an average momentum. Specifically we chose a standard scenario with $m = 2T, < p_x >= \pm 3T$ and made a thermal distribution around this. We checked that the code did end up with equilibrium both under the initial condition of no light neutrinos from the beginning and under the assumption of an initial thermal distribution of light neutrinos. More on the numerics in appendix 9.7. This means that the calculated formulas cannot be verified explicitly, since we have no well-defined gamma factor. However, the factor of $\frac{1}{\tau\gamma^2}$ can almost be found. First, the $\frac{1}{\tau}$ is, of course, trivial. If the coupling is weakened the lifetime is correspondingly longer. We checked that our code yielded this result. The $\frac{1}{\gamma}$ for the time dilation of the neutrino lifetime is also quite trivial. We found this as well - by noticing the decreased numbers of 2's produced in the very first step when we used an alternative scenario: $m = 2T, < p_x >= \pm 4T$. Since we had thermal distributions rather than sharply defined momenta, we could not expect to find the exact relation between average gammas to be the same as the relation between the created particles.

However, the most interesting second $\frac{1}{\gamma}$ can be illustrated by numerical plots. Figure 9.1 shows the first distributions after the very first step, whereas figure 9.2 shows the distributions after the first step in the alternative scenario with a larger gamma factor. Two things are very important to notice. First, the created 2's are indeed anisotropic. This is the effect of taking their isotropic distribution in the frame of the decaying particle 1 and make a Lorentz transformation to the (cosmic) laboratory frame. Secondly, the fact that the alternative scenario give more anisotropy among the 2's should make it clear that it must be a gamma factor.

For completeness, figure 9.3 shows the development in the standard scenario at a later time, and figure 9.4 shows the standard scenario at an even later time, where equilibrium is almost there.

One should note that distribution functions are defined according to the cylinder coordinates used in the code – see the appendix 9.7 for details. Also, one should note that p_y in the plots are in fact the transverse momentum - not the momentum in one of the transverse directions.

[**More to be included - including specifying the relevant times of the plots**]

9.6 Discussion

[**To be included**]

Acknowledgements

[**To be included**]

9.7 Appendix: Numerics

In order to follow this numerically we notice that we have 3 particles in 3 momentum coordinates - that is 9 dimensions (no isotropy). We notice that when we assume Maxwell-Boltzmann statistics particles 2 and φ behave alike. This means that if starting conditions are the same, we only have to track one of them. Eventhough there is not isotropy, azimuthal angles are arbitrary. So we end up with 4 dimensions. 2 particles, with a momentum in the initial beam direction and momentum in a transverse direction. So we want to integrate the remaining coordinates out. We start with

$$\begin{aligned} C[1] &= \frac{1}{2E_1}\int \frac{d^3p_2}{(2\pi)^3 2E_2}\frac{d^3p_\varphi}{(2\pi)^3 2E_\varphi}(2\pi)^4\delta^4(p_1-p_2-p_\varphi)2g^2m^2(f_1-f_2f_\varphi) \\ &= \frac{dp_{\varphi x}dp_{\varphi R}dp_{2x}dp_{2R}p_{2R}p_{\varphi R}}{(2\pi)^2E_1E_2E_\varphi}\delta(E_1-p_2-p_\varphi)\delta(p_{1x}-p_{2x}-p_{\varphi x}) \\ &\quad 2g^2m^2\int dp_\psi dp_\theta \delta(p_y)\delta(p_z)(f_1-f_2f_\varphi) \end{aligned} \tag{9.38}$$

where we have defined (including aligning the coordinate system with particle 1) momenta
$p_1 = (p_{1x}, p_{R1}, 0), p_2 = (p_{2x}, p_{2R}Cos(\psi), p_{2R}Sin(\psi)), p_\varphi = (p_{\varphi x}, p_{\varphi R}Cos(\theta), p_{\varphi R}Sin(\theta))$
The key integral is:

$$\begin{aligned} I &= \int_0^{2\pi}\int_0^{2\pi}\delta(p_{2R}Sin(\psi)+p_{\varphi R}Sin(\theta))\delta(p_{R1} \\ &\quad +p_{2R}Cos(\psi)+p_{\varphi R}Cos(\theta))d\psi d\theta \end{aligned} \tag{9.39}$$

with explicit symmetry between 2 and φ.

$$g(\psi) = p_{2R}Sin(\psi) + p_{\varphi R}Sin(\theta) \Rightarrow \tag{9.40}$$

$$g'(\psi) = -p_{2R}Cos(\psi) \Rightarrow |g'(\psi)| = p_{2R}|Cos(\psi)| \tag{9.41}$$

$$g(\psi_i) = 0 \Rightarrow \tag{9.42}$$

$$p_{2R}|Cos(\psi_i)| = \sqrt{p_{2R}^2 - {p_{\varphi R}}^2 Sin^2(\theta)} \tag{9.43}$$

with the condition

$$p_{\varphi R}|Sin(\theta)| < p_{2R} \tag{9.44}$$

so what is left

$$\begin{aligned} I &= \int_0^{2\pi} \frac{1}{\sqrt{p_{2R}^2 - {p_{\varphi R}}^2 Sin^2(\theta)}} \\ &\quad \sum_i \delta\left(p_{1R} + p_{2R}Cos(\psi_i) + p_{\varphi R}Cos(\theta)\right) d\theta \\ &= \sum_{sign} \int_0^{2\pi} \frac{1}{\sqrt{p_{2R}^2 - {p_{\varphi R}}^2 Sin^2(\theta)}} \\ &\quad \delta\left(p_{1R} \pm \sqrt{p_{2R}^2 - {p_{\varphi R}}^2 Sin^2(\theta)} + p_{\varphi R}Cos(\theta)\right) d\theta \end{aligned} \tag{9.45}$$

defining

$$\begin{aligned} h \pm (\theta) = p_{1R} \pm \sqrt{p_{2R}^2 - {p_{\varphi R}}^2 Sin^2(\theta)} + p_{\varphi R}Cos(\theta) \Rightarrow \\ |h \pm (\theta)'| = \left| \pm \frac{p_{\varphi R}^2 Sin(\theta)Cos(\theta)}{\sqrt{p_{2R}^2 - {p_{\varphi R}}^2 Sin^2(\theta)}} + p_{\varphi R}Sin(\theta) \right| \end{aligned} \tag{9.46}$$

$$h \pm (\theta_i) = 0 \Rightarrow \tag{9.47}$$

$$p_{2R}^2 - {p_{\varphi R}}^2 Sin^2(\theta_i) = (p_{1R} + p_{\varphi R}Cos(\theta_i))^2 \Rightarrow \tag{9.48}$$

Here it is important to remember, it is only an implication. Only one of the signs will give a correct solution. The solutions found must be checked against the non-squared equation

$$p_{2R}^2 - {p_{\varphi R}}^2 Sin^2(\theta_i) = p_{1R}^2 + p_{\varphi R}^2 Cos(\theta_i)^2 + 2p_{1R}p_{\varphi R}Cos(\theta_i) \Rightarrow \tag{9.49}$$

$$Cos(\theta_i) = \frac{p_{2R}^2 - p_{\varphi R}^2 - p_{1R}^2}{2p_{1R}p_{\varphi R}} \Rightarrow \tag{9.50}$$

$$p_{\varphi R}Sin(\theta_i) = \pm\sqrt{p_{\varphi R}^2 - \left(\frac{p_{2R}^2 - p_{\varphi R}^2 - p_{1R}^2}{2p_{1R}}\right)^2} \Rightarrow \tag{9.51}$$

Now it is easy to see, that (9.44) is trivially fulfilled. We also have a now condition, from (9.44). It goes

$$|Cos(\theta_i)| = |\frac{p_{2R}^2 - p_{\varphi R}^2 - p_{1R}^2}{2p_{1R}p_{\varphi R}}| \leq 1 \Rightarrow \tag{9.52}$$

$$|p_{2R}^2 - p_{\varphi R}^2 - p_{1R}^2| < 2p_{1R}p_{\varphi R} \Rightarrow \tag{9.53}$$

$$\pm(p_{2R}^2 - p_{\varphi R}^2 - p_{1R}^2) < 2p_{1R}p_{\varphi R} \Rightarrow \tag{9.54}$$

$$(p_{\varphi R} - p_{1R})^2 < p_{2R}^2 < (p_{\varphi R} + p_{1R})^2 \Rightarrow \tag{9.55}$$

$$|p_{\varphi R} - p_{1R}| < p_{2R} < |p_{\varphi R} + p_{1R}| \tag{9.56}$$

This is not only the welcomed triangle equation, it is also the only condition, and this condition is symmetrical for 2 and φ. It is easy to show, that a triangle condition is symmetrical between all 3 terms. This solves the sign question. Since $p_{\varphi R} < p_{2R} + p_{1R} \Rightarrow p_{\varphi R}^2 < p_{2R}^2 + p_{1R}^2$ and from (9.50) we get $p_{\varphi R}Cos(\theta_i) = \frac{p_{2R}^2 - p_{\varphi R}^2 - p_{1R}^2}{2p_{1R}} \Rightarrow p_{1R} + p_{\varphi R}Cos(\theta_i) = \frac{p_{2R}^2 - p_{\varphi R}^2 + p_{1R}^2}{2p_{1R}}$ we find that $p_{1R} + p_{\varphi R}Cos(\theta_i) > 0$ and therefore (9.46) shows that only the negative sign should be used.

Now we insert [together with the cosine expression]ignoring the sign here, because it's an overall factor in an expression, of which the numerical value will be taken

$$\begin{aligned}
|h(\theta_i)'| &= \Bigg| - \frac{\frac{p_{2R}^2 - p_{\varphi R}^2 - p_{1R}^2}{2p_{1R}} \sqrt{p_{\varphi R}^2 - \left(\frac{p_{2R}^2 - p_{\varphi R}^2 - p_{1R}^2}{2p_{1R}}\right)^2}}{\sqrt{p_{2R}^2 - \left(p_{\varphi R}^2 - \left(\frac{p_{2R}^2 - p_{\varphi R}^2 - p_{1R}^2}{2p_{1R}}\right)^2\right)}} \\
&\quad + \sqrt{p_{\varphi R}^2 - \left(\frac{p_{2R}^2 - p_{\varphi R}^2 - p_{1R}^2}{2p_{1R}}\right)^2} \Bigg| \\
&= \frac{1}{2p_{1R}} \Bigg| - \frac{(p_{2R}^2 - p_{\varphi R}^2 - p_{1R}^2)\sqrt{4p_{1R}^2 p_{\varphi R}^2 - \left(p_{2R}^2 - p_{\varphi R}^2 - p_{1R}^2\right)^2}}{\sqrt{4p_{1R}^2 p_{2R}^2 - 4p_{1R}^2 p_{\varphi R}^2 + \left(p_{2R}^2 - p_{\varphi R}^2 - p_{1R}^2\right)^2}} \\
&\quad + \sqrt{4p_{1R}^2 p_{\varphi R}^2 - \left(p_{2R}^2 - p_{\varphi R}^2 - p_{1R}^2\right)^2} \Bigg| \Rightarrow
\end{aligned} \tag{9.57}$$

Not only is this expression the same for both $\theta_i's$, the front factor outside the delta function is also the same. Therefore

$$I = 2\frac{1}{\sqrt{p_{2R}^2 - \left(p_{\varphi R}^2 - \left(\frac{p_{2R}^2 - p_{\varphi R}^2 - p_{1R}^2}{2p_{1R}}\right)^2\right)}}$$

$$\frac{2p_{1R}}{\left|-\frac{(p_{2R}^2 - p_{\varphi R}^2 - p_{1R}^2)\sqrt{4p_{1R}^2 p_{\varphi R}^2 - \left(p_{2R}^2 - p_{\varphi R}^2 - p_{1R}^2\right)^2}}{\sqrt{4p_{1R}^2 p_{2R}^2 - 4p_{1R}^2 p_{\varphi R}^2 + \left(p_{2R}^2 - p_{\varphi R}^2 - p_{1R}^2\right)^2}} + \sqrt{4p_{1R}^2 p_{\varphi R}^2 - \left(p_{2R}^2 - p_{\varphi R}^2 - p_{1R}^2\right)^2}\right|}$$

$$= \frac{2(2p_{1R})^2}{\sqrt{4p_{1R}^2 p_{2R}^2 - \left(4p_{1R}^2 p_{\varphi R}^2 - \left(p_{2R}^2 - p_{\varphi R}^2 - p_{1R}^2\right)^2\right)}} \tag{9.58}$$

$$\frac{1}{\left|-\frac{(p_{2R}^2 - p_{\varphi R}^2 - p_{1R}^2)\sqrt{4p_{1R}^2 p_{\varphi R}^2 - \left(p_{2R}^2 - p_{\varphi R}^2 - p_{1R}^2\right)^2}}{\sqrt{4p_{1R}^2 p_{2R}^2 - 4p_{1R}^2 p_{\varphi R}^2 + \left(p_{2R}^2 - p_{\varphi R}^2 - p_{1R}^2\right)^2}} + \sqrt{4p_{1R}^2 p_{\varphi R}^2 - \left(p_{2R}^2 - p_{\varphi R}^2 - p_{1R}^2\right)^2}\right|}$$

so all together

$$C[1] = \frac{dp_{\varphi x} dp_{\varphi R} dp_{2x} dp_{2R} p_{2R} p_{\varphi R}}{(2\pi)^2 E_1 E_2 E_\varphi} \delta(E_1 - p_2 - p_\varphi)\delta(p_{1x} - p_{2x} - p_{\varphi x})$$

$$2g^2 m^2 (f_1 - f_2 f_\varphi) \frac{2 * (2p_{1R})^2}{\sqrt{4p_{1R}^2 p_{2R}^2 - \left(4p_{1R}^2 p_{\varphi R}^2 - \left(p_{2R}^2 - p_{\varphi R}^2 - p_{1R}^2\right)^2\right)}}$$

$$\frac{1}{\left|-\frac{(p_{2R}^2 - p_{\varphi R}^2 - p_{1R}^2)\sqrt{4p_{1R}^2 p_{\varphi R}^2 - \left(p_{2R}^2 - p_{\varphi R}^2 - p_{1R}^2\right)^2}}{\sqrt{4p_{1R}^2 p_{2R}^2 - 4p_{1R}^2 p_{\varphi R}^2 + \left(p_{2R}^2 - p_{\varphi R}^2 - p_{1R}^2\right)^2}} + \sqrt{4p_{1R}^2 p_{\varphi R}^2 - \left(p_{2R}^2 - p_{\varphi R}^2 - p_{1R}^2\right)^2}\right|}$$

$$= \frac{dp_{\varphi x} dp_{\varphi R} dp_{2x} dp_{2R} p_{2R} p_{\varphi R}}{\pi^2 E_1 E_2 E_\varphi} \delta(E_1 - p_2 - p_\varphi)\delta(p_{1x} - p_{2x} - p_{\varphi x})$$

$$g^2 m^2 (f_1 - f_2 f_\varphi) \frac{(2p_{1R})^2}{\sqrt{4p_{1R}^2 p_{2R}^2 - 4p_{1R}^2 p_{\varphi R}^2 + \left(p_{2R}^2 - p_{\varphi R}^2 - p_{1R}^2\right)^2}} \tag{9.59}$$

$$\frac{1}{\left|-\frac{(p_{2R}^2 - p_{\varphi R}^2 - p_{1R}^2)\sqrt{4p_{1R}^2 p_{\varphi R}^2 - \left(p_{2R}^2 - p_{\varphi R}^2 - p_{1R}^2\right)^2}}{\sqrt{4p_{1R}^2 p_{2R}^2 - 4p_{1R}^2 p_{\varphi R}^2 + \left(p_{2R}^2 - p_{\varphi R}^2 - p_{1R}^2\right)^2}} + \sqrt{4p_{1R}^2 p_{\varphi R}^2 - \left(p_{2R}^2 - p_{\varphi R}^2 - p_{1R}^2\right)^2}\right|}$$

Using

$$\begin{aligned} &4p_{1R}^2 p_{\varphi R}^2 - \left(p_{2R}^2 - p_{\varphi R}^2 - p_{1R}^2\right)^2 \\ &= -p_{2R}^4 - p_{\varphi R}^4 - p_{1R}^4 + 2(p_{2R}^2 p_{\varphi R}^2 + p_{1R}^2 p_{\varphi R}^2 + p_{2R}^2 p_{\varphi 1}^2) \equiv S \end{aligned} \tag{9.60}$$

and therefore

$$4p_{1R}^2p_{2R}^2 - 4p_{1R}^2p_{\varphi R}^2 + \left(p_{2R}^2 - p_{\varphi R}^2 - p_{1R}^2\right)^2 = 4p_{1R}^2p_{2R}^2 - S \tag{9.61}$$

(where S is clearly symmetrical between 2 and φ)

$$\begin{aligned} C[1] &= \frac{dp_{\varphi x}dp_{\varphi R}dp_{2x}dp_{2R}p_{2R}p_{\varphi R}}{\pi^2 E_1E_2E_\varphi}\delta(E_1 - p_2 - p_\varphi)\delta(p_{1x} - p_{2x} - p_{\varphi x}) \\ &\quad g^2m^2(f_1 - f_2f_\varphi)\frac{(2p_{1R})^2}{\sqrt{4p_{1R}^2p_{2R}^2 - S}}\frac{1}{\left|-\frac{(p_{2R}^2 - p_{\varphi R}^2 - p_{1R}^2)\sqrt{S}}{\sqrt{4p_{1R}^2p_{2R}^2 - S}} + \sqrt{S}\right|} \\ &= \frac{dp_{\varphi x}dp_{\varphi R}dp_{2x}dp_{2R}p_{2R}p_{\varphi R}}{\pi^2 E_1E_2E_\varphi}\delta(E_1 - p_2 - p_\varphi)\delta(p_{1x} - p_{2x} - p_{\varphi x}) \\ &\quad g^2m^2(f_1 - f_2f_\varphi)\frac{(2p_{1R})^2}{\sqrt{S}}\frac{1}{\left|-(p_{2R}^2 - p_{\varphi R}^2 - p_{1R}^2) + \sqrt{4p_{1R}^2p_{2R}^2 - S}\right|} \end{aligned} \tag{9.62}$$

where the last step is allowed, since both roots are positive. We find

$$(p_{2R}^2 - p_{\varphi R}^2 - p_{1R}^2)^2 = -S + 4p_{1R}^2p_{\varphi R}^2 \tag{9.63}$$

and conclude that since the term in the bracket is surely negative by the triangle condition, we have

$$-(p_{2R}^2 - p_{\varphi R}^2 - p_{1R}^2) = \sqrt{4p_{1R}^2p_{\varphi R}^2 - S} \tag{9.64}$$

so we finally have

$$\begin{aligned} C[1] = \frac{dp_{\varphi x}dp_{\varphi R}dp_{2x}dp_{2R}p_{2R}p_{\varphi R}}{\pi^2 E_1E_2E_\varphi}\delta(E_1 - p_2 - p_\varphi)\delta(p_{1x} - p_{2x} - p_{\varphi x})g^2m^2 \\ (f_1 - f_2f_\varphi)\frac{(2p_{1R})^2}{\sqrt{S}}\frac{1}{\sqrt{4p_{1R}^2p_{\varphi R}^2 - S} + \sqrt{4p_{1R}^2p_{2R}^2 - S}} \end{aligned} \tag{9.65}$$

For numerical purposes, let us underline the formula in the way it should be implemented.

$$\frac{df(\vec{p_i})}{dt} = C[i](\vec{p_i}) \tag{9.66}$$

however the vectors will not be introduced. Rather we use

$$\begin{aligned} \int_\theta f(\vec{p_i})dp_\theta &= \int_\theta f(p_{ix}, p_{iR}, p_\theta)p_{iR}dp_\theta \\ &= 2\pi p_{iR} * f(p_{ix}, p_{iR}, p_\theta) \equiv 2\pi p_{iR}\tilde{f}(p_{ix}, p_{iR}) \end{aligned} \tag{9.67}$$

and likewise for $C[i]$. This means that the function $\tilde{f}$ that we implement is of dimension E^{-1} and its derivative dimensionless. The equation implemented is thus

$$\begin{aligned} d\tilde{f}(p_{ix}, p_{iR}) = \tilde{C}[1] = \frac{dp_{\varphi x} dp_{\varphi R} dp_{2x} dp_{2R} p_{2R} p_{\varphi R}}{\pi^3 E_1 E_2 E_\varphi} \delta(E_1 - p_2 - p_\varphi) \\ \delta(p_{1x} - p_{2x} - p_{\varphi x}) g^2 m^2 (f_1 - f_2 f_\varphi) \frac{2p_{1R}}{\sqrt{S}} \\ \frac{1}{\sqrt{4p_{1R}^2 p_{\varphi R}^2 - S} + \sqrt{4p_{1R}^2 p_{2R}^2 - S}} \end{aligned} \tag{9.68}$$

where still $S = -p_{2R}^4 - p_{\varphi R}^4 - p_{1R}^4 + 2(p_{2R}^2 p_{\varphi R}^2 + p_{1R}^2 p_{\varphi R}^2 + p_{2R}^2 p_{\varphi 1}^2)$. The implementation of 2 is quite easy since for fixed momenta $\vec{p_1}, \vec{p_2}, \vec{p_\varphi}$

$$C[1] = -C[2] \tag{9.69}$$

or

$$2\pi p_{1R} \tilde{C}[1] = -2\pi p_{2R} \tilde{C}[2] \tag{9.70}$$

References

[**To be included**]

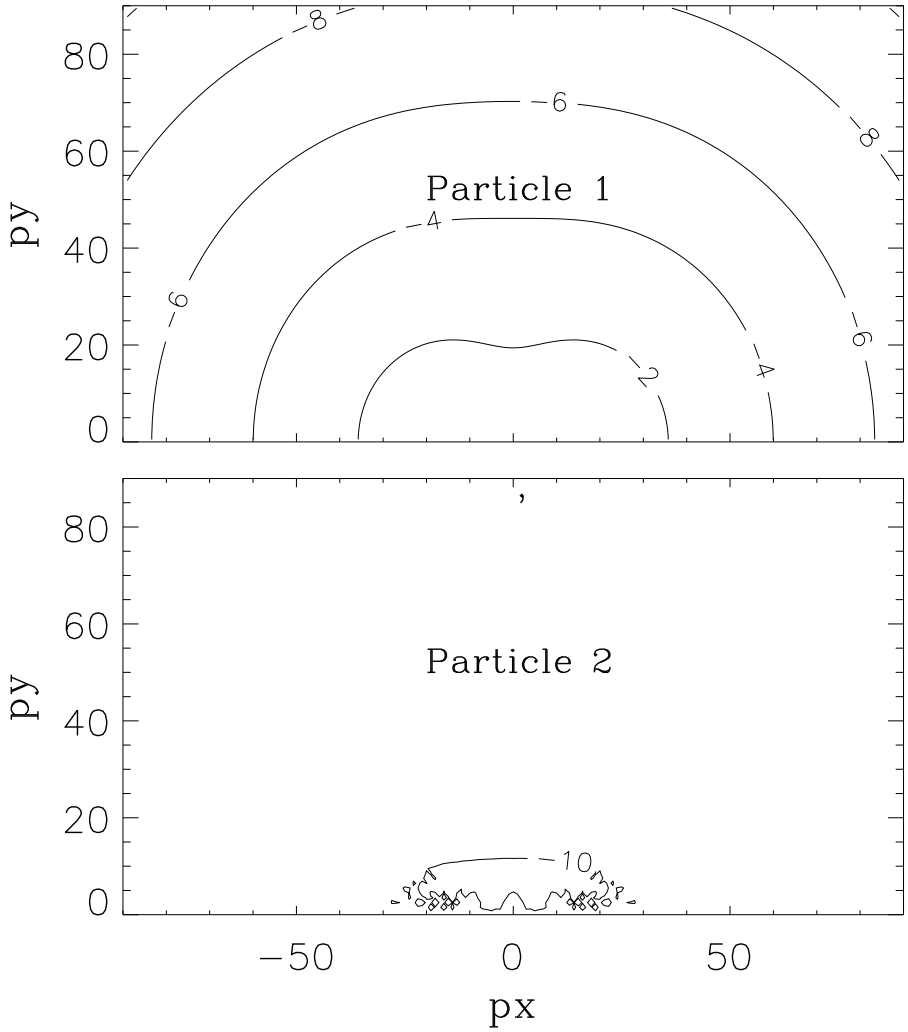

Fig. 9.1: The situation just after the first step in the standard scenario. The lines are contour plots of the distribution function - as defined in the appendix. p_y means transverse momentum

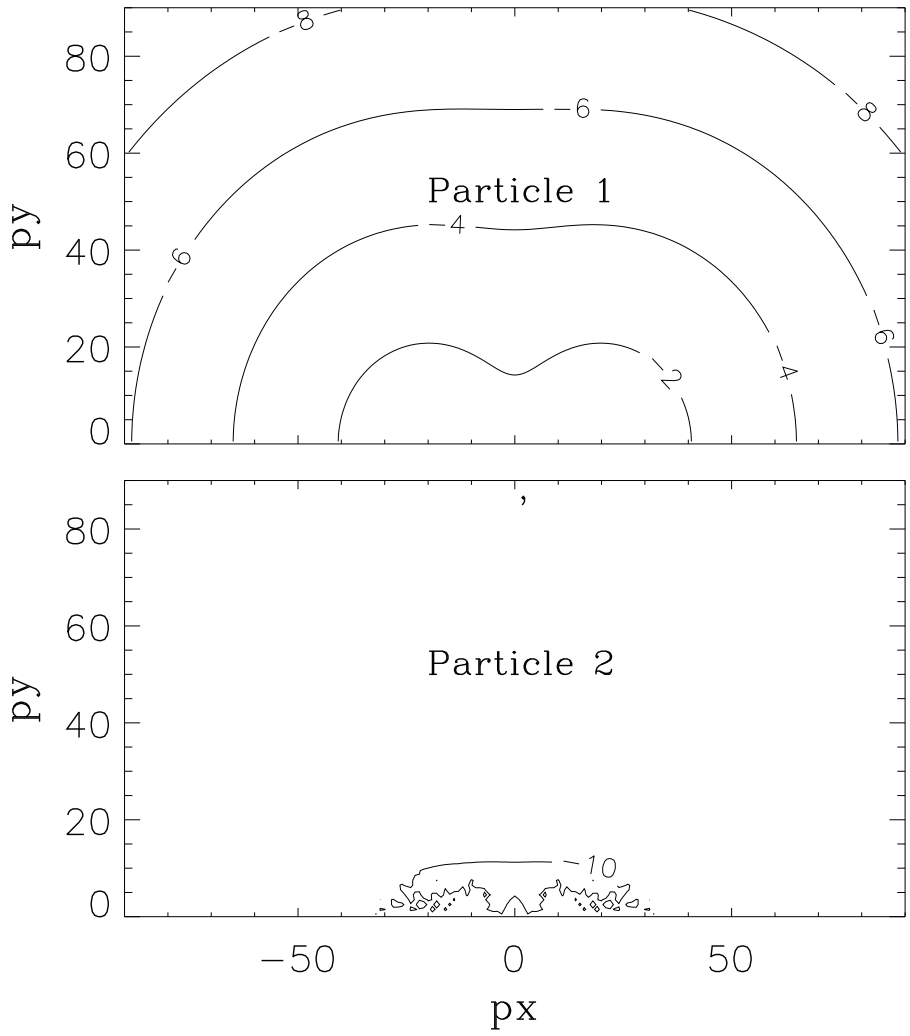

Fig. 9.2: The situation just after the first step in the alternative scenario. The lines are contour plots of the distribution function - as defined in the appendix. p_y means transverse momentum

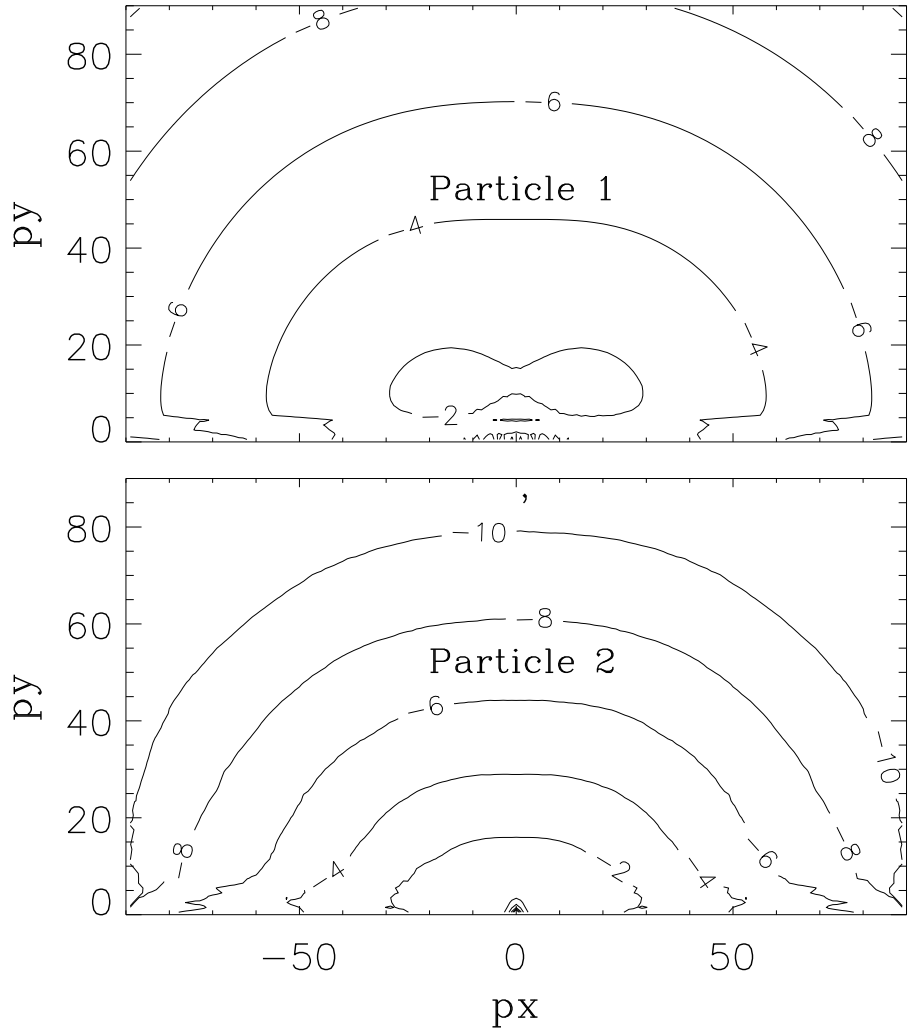

Fig. 9.3: The situation later in the standard scenario.

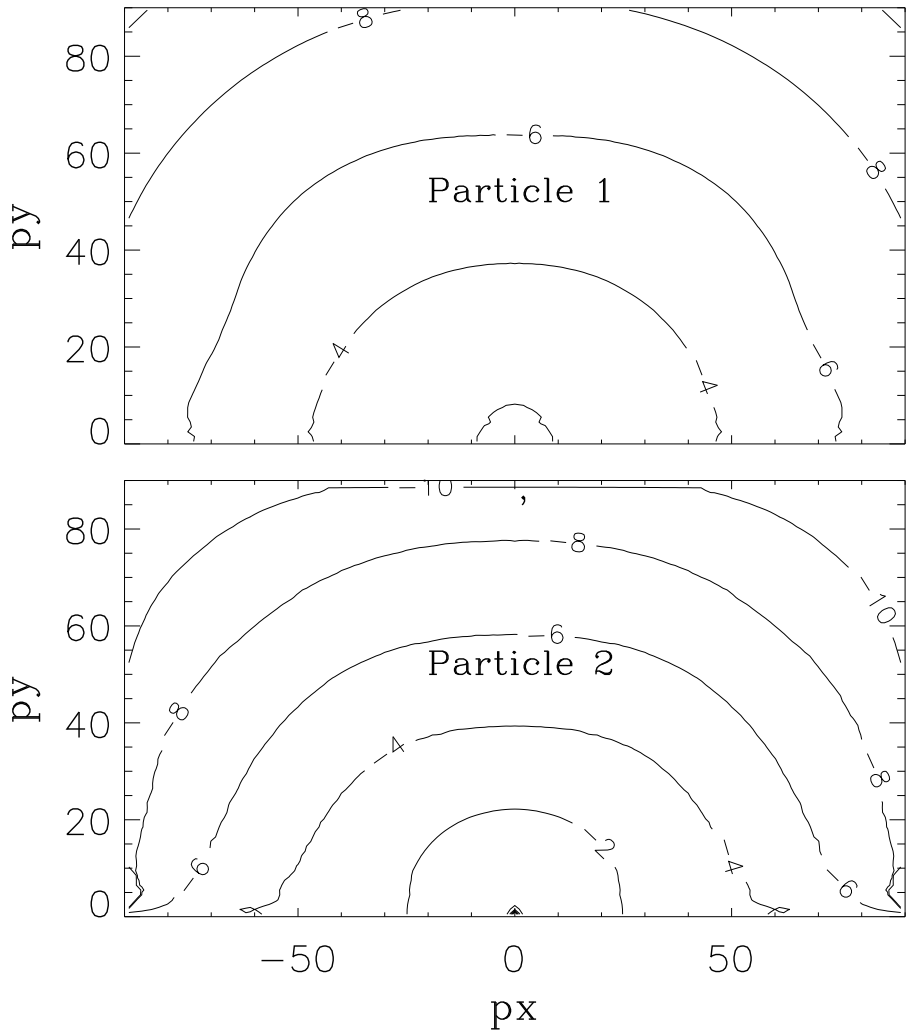

Fig. 9.4: The situation even later in the standard scenario.

BIBLIOGRAPHY

[1] D. Perkins, "Particle Astrophysics" Oxford University Press, 2003

[2] L. Kofman, A. Linde and A. A. Starobinsky, Phys. Rev. D **56**, 1997.

[3] L. Kofman, A. Linde and A. A. Starobinsky, Phys. Rev. Lett. **73**, 1994.

[4] H. P. Nilles, M. Peloso and L. Sorbo, JHEP 0104 (2001) 004.

[5] D. N. Spergel et al., astro-ph/0603449.

[6] Paolo S. Coppi, SLAC Summer Institute of Particle Physics, Aug 2-13 2004 www.slac.stanford.edu/econf/C040802/papers/L017.PDF

[7] A. D. Sakharov, JETP Lett. 5, 24, 1967.

[8] V. Kuzmin, V.A. Rubakov and M.E. Shaposhnikov, Phys. Lett. **155B**, 36-42 (1985).

[9] A. Jokinen, Ph.D. Thesis, University of Helsinki 2002.

[10] I. J. R. Aitchison, arXiv:hep-ph/0505105v1.

[11] T. Gherghetta, C. Kolda and S. P. Martin, Nucl. Phys. B **468**, (1995).

[12] M. Dine, L. Randall and S. D. Thomas, Phys. Rev. Lett. **75**, 398 (1995).

[13] R. Allahverdi and A. Mazumdar, Phys. Rev. D **76**, 103526(2007).

[14] K. A.Olive and M. Peloso, Phys. Rev. D **474** (2006).

[15] R. Allahverdi and A. Mazumdar, hep-ph/0608296v3

[16] See eg., R. Allahverdi, K. Enqvist, J. Garcia-Bellido and A. Mazumdar, Phys. Rev. Lett. **97** (2006) 191304.

[17] See eg., R. Allahverdi, K. Enqvist, J. Garcia-Bellido, A. Jokinen and A. Mazumdar, JCAP **06** (2007) 019.

[18] R. Allahverdi and A. Mazumdar, Phys. Rev. D **78**, 043511(2008).

[19] A. E. Gümrümçüoğlu, K. A. Olive, M. Peloso and M. Sexton, Phys. Rev. D **78**, 063512(2008).

[20] S. Hannestad, JCAP **0502**, 011 (2005).

[21] J. F. Beacom, N. F. Bell and S. Dodelson, Phys. Rev. Lett. **93**, 121302 (2004).

[22] S. Hannestad and G. Raffelt, Phys. Rev. D **72**, 103514 (2005).

[23] A. Basbøll and S. Hannestad, JCAP01(2007)003.

[24] A. Basbøll, D. Maybury, F. Riva and S. M. West, Phys. Rev. D **76**, 065005 (2007).

[25] A . Basbøll, Phys. Rev. D **78**, 023528 (2008).

[26] A. Basbøll, O. E. Bjælde, S. Hannestad and G. Raffelt: Are cosmological neutrinos free–streaming?, arXiv:astro-ph/0806.1735.